Nano-scale Surface Modification and Functionalization for Textile Materials

TSOI Wing Yu Iris

Master of Philosophy

The Hong Kong Polytechnic University

2012

The Hong Kong Polytechnic University

Institute of Textiles & Clothing

Nano-scale Surface Modification and Functionalization for Textile Materials

TSOI Wing Yu Iris

A thesis submitted in partial fulfilment of the requirements for the degree of Master of Philosophy

February

2011

CERTIFICATE OF ORIGINALITY

I hereby declare that this thesis is my own work and that, to the best of my knowledge and belief, it reproduces no material previously published or written, nor material that has been accepted for the award of any other degree or diploma, except where due acknowledgement has been made in the text.

_____ (Signed)

_____Tsoi Wing Yu Iris_____ (Name of student)

Abstract

The thesis is concerned with the study of the development of a nano-scale surface modification and funcationalisation of different textile materials, included polyester, wool and cotton, utilising the atmospheric pressure plasma technique. Based on the experimental results, it was found that the nano-scale surface modifications of textile materials was achievable under the appropriate control of the treatment parameters namely the ignition power of plasma, treatment duration, concentration of reactive plasma gas, and jet distance between the plasma nozzle and the textile substrates. These four parameters were the major attributes of the surface texturisation and funcationilsation of the substrates. The optimum conditions of the nano-scale plasma modification of each fabric substrates were developed to hydrophilise or hydrophobise the textile substrates. Surface wetting behaviour of the substrates was reverted using the appropriate kind of reactive gases. Oxygen (O_2) was utilised for hydrophilisation of polyester and wool while tetrafluoromethane (CF_4) was utilised for hydrophobisation of cotton. In significance, oxygen was also found to be capable of hydrophobisation of cotton taking the ageing property of the plasma-modified substrate into account.

Nano-scale plasma etching-hydrophilisation of hydrophobic textile substrates, both polyester and wool, was found to be achievable by He-O_2 atmospheric pressure plasma with the appropriate tuning of the plasma operation parameters. Nano-scale plasma etching-hydrophobisation of hydrophilic textile substrate, cotton, was found to be achievable by He-O_2 and He-CF_4 atmospheric pressure plasma with the appropriate manipulation of the plasma operation parameters. Though plasma was capable of modifying a wide scope of textile substrates, plasma modification showed substrate dependence. The optimum condition for plasma functionalisation deviated for each textile materials. Good knowledge of the substrate was essential for the manipulation of the plasma processing of different textile materials. Nature of the fibres needed to be taking into consideration prior to the modification. This study offers a deeper understanding of the physicochemical interaction between plasma and the textile materials.

List of publications

Book chapter

1. Tsoi, W.Y.I., Kan, C.W., Tang, T.B. and Yuen, C.W.M., (2010) "Nano-scale Plasma Etching-Hydrophilisation of Keratin Fibres", Méndez-Vilas, A., Díaz, J., (Eds.) *Microscopy: Science, Technology, Applications and Education*, Formatex Research Center, Spain, Volume 3, pp. 1793-1799

Referred journals

1. Cheng, S.Y., Yuen, C.W.M., Kan, C.W., Cheuk, K.K.L., Daoud, W.A., Lam, P.L. and Tsoi, W.Y.I. (2010) "Influence of Atmospheric Pressure Plasma Treatment on Various Fibrous Materials: Performance Properties and Surface Adhesion Analysis", *Vacuum*, Vol. 84, pp.1466–1470

2. Kan, C.W., Yuen, C.W.M. and Tsoi, W.Y.I., (2011) "Using Atmospheric Pressure Plasma for Enhancing the Deposition of Printing Paste on Cotton Fabric for Digital Ink-jet Printing", *Cellulose*, Volume 18, Number 3, pp.827-839

3. Tsoi, W.Y.I., Kan, C.W., Tang, T.B. and Yuen, C.W.M., (2011) "Nano-scale Hydrophobic Modification of Cotton Fabric with the use of Atmospheric Pressure Plasma", *International Journal of Arts & Sciences,* Volume. 4, number. 2, pp.48-66, ISSN:1944-6934 in CD-ROM format

4. Tsoi, W.Y.I., Kan, C.W., Yuen, C.W.M., Choi, T.M. and Tang, T.B., "Achieving Nano-scale Surface Structure on Wool Fibre by Atmospheric Pressure Plasma Treatment", *Journal of Adhesion Science and Technology* (submitted).

5. Tsoi, W.Y.I., Kan, C.W., Yuen, C.W.M. and Tang T.B., "Achieving Nano-scale Surface Structure on Polyester Film by Atmospheric Pressure Plasma Treatment", *Journal of Adhesion Science and Technology* (under review).

Conference presentations

1. Kan, C.W., Yuen, C.W.M., Tang, T.B. and Tsoi, W.Y., "X-ray and Birefringence Analysis of Plasma Treated Wool", *Proceedings of 2009* International Conference on Advanced Fibers and Polymer Materials, Donghua University, Shanghai, China, October 21-24, 2009, pp.6-9

2. Kan, C.W., Yuen, C.W.M., Tang, T.B. and Tsoi, W.Y., "Effect of Low Temperature Plasma Pretreatment on the Wettability and Dryability of Polyester and Nylon Fibres", P*roceedings of 2009 International Conference on Advanced Fibers and Polymer Materials*, Donghua University, Shanghai, China, October 21-24, 2009, pp.14-17.

3. Tsoi, W.Y.I., Kan, C.W., Tang, T.B. and Yuen, C.W.M., "Nano-scale Atmospheric Pressure Plasma Treatment on Polyester Film", *Proceedings of TACT 2009 International Thin Films Conference*, National Taipei University of Technology, Taipei, Taiwan, December 14-16, 2009, pp.211

4. Tsoi, W.Y.I., Kan, C.W., Tang, T.B. and Yuen, C.W.M., "Nano-scale Hydrophobic Modification of Cotton Fabric with the use of Atmospheric Pressure Plasma", *Proceedings of Conference of the International Journal of Arts & Sciences Semi-Annual Conference*, Gottenheim, Germany, November 28 – December 3, 2010, ISSN:1943-6114 in CD-ROM format (2011)

Acknowledgements

I would like to express my deepest gratitude to my chief supervisor, Dr. C. W. Kan, Assistant Professor of Institute of Textiles and Clothing at The Hong Kong Polytechnic University, for providing the opportunity of undertaking this project, and for his constant guidance, encouragement, and invaluable advice throughout the study.

I would like to express my sincere thanks to my co-supervisors, Prof. T. B. Tang, Professor of Department of physics at Hong Kong Baptist University, and Prof. C. W. M. Yuen, Professor of Institute of Textiles and Clothing at The Hong Kong Polytechnic University, for providing his invaluable advice and consecutive support in carrying out this research.

My thanks are also extended to all the staff members and technicians in the textile laboratories and Materials Research Centre at the Hong Kong Polytechnic University. I would also like to express my thanks to members in the Centre for Surface Analysis and Research of Hong Kong Baptist University for the assistance of the X-ray photoelectron spectrometric analysis.

Table of contents

List of figures

List of tables

Chapter 1   Introduction

1.1   Background

Plasma nanotechnology

Nanostructures exhibit distinctive properties with respect to a high area-to-volume ratio (Champion & Fecht, 2004). Plasma, in general, is competent to alter the surface layer of a substrate while leaving the desirable bulk properties unaffected under the controlled operation conditions. It induces a milder surface modification as compared to the other dry surface treatments such as electromagnetic irradiations, e.g. UV-laser, and electrical discharges, e.g. ion sputtering (Wong et al., 2000). Plasma is capable of achieving nano-scale surface modification compared to other conventional treatments. In addition to physical ablation, plasma is able to functionalise a substrate simultaneously in a single-step treatment using various reactive non-polymerising and polymerising gases and precursors at low temperature. In this aspect, the development of plasma nano-fabrication has attracted considerable attention (Matthew et al., 2004; Ren et al., 2008; Zhang & Fang, 2008).

Atmospheric pressure plasma (APP) recently has drawn growing interest owing to its outstanding properties when compared with its counterpart operated under the reduced pressure (Ren et al., 2008; Zhang & Fang, 2008; Kan & Yuen, 2008; Šimor et al., 2003, Wang et al., 2008a, b). APP generates low temperature plasma flux which is suitable to modify heat fragile materials. This category of plasma is a potential technique to achieve a nano-scale surface modification. With the continual development in various industrial sectors,

----

----

there is likely an expansion of the application of APP which is important to control the degree of modification up to an appropriate extent. Hitherto, plasma treatment is short of quantitative, dimensional investigation of the formation of topographical structures in relation to the operation parameters. A quantitative dimensional analysis of the plasma-induced structures on a substrate is essential to assist in manipulating the topographical development and to design desirable surface properties.

In recent years, there are increasing interests in the application of low temperature plasma in the textile industry. The plasma technique has a lot of benefits like flexibility, cleanliness, eco-friendliness and versatility (Matthew et al., 2004; Ren et al., 2008; Samanta et al., 2009; Shin et al., 2008; Zhang & Fang, 2009). However, the textile processing utilising plasma technique, especially the atmospheric pressure plasma, is different from that of the conventional wettability modification (Samanta et al., 2009; Shin & Yoo, 2008; Zhang & Fang, 2009).

Low-temperature atmospheric pressure plasma etching

Theoretically, the application of plasma under ambient conditions is the most ideal. The plasma technology, however, is still limited by a small scale production with respect to the system pressure, uniformity, high capital cost and high labour skills. Plasma system which is able to run on fabric rolls in open width condition is yet to emerge. Manipulation and fine tuning of the process are not extensively available as yet.

In order to achieve the industrial realisation of continuous plasma treatment, it is necessary to understand the basic dependence of the resultant surface properties with respect to process parameters. This helps the manipulation of nano-structure formation and designs the appropriate surface properties for a substrate. Hitherto, atmospheric pressure plasma treatment is lack of quantitative investigation about the formation of topographical structures related to plasma operation parameters. The focus of the present study is the quantitative analysis of the dimension of the plasma-induced structures and the formation of the nano-scale surface texturisation on the substrates.

Plasma modification is a time-dependent physicochemical interaction between plasma and substrate. Plasma is capable of modifying a substrate irrespective of the nature of the substrate. To design an appropriate plasma treatment for a substrate, plasma operation parameters are the main factors to be considered (Kan & Yuen, 2007; Wang & Qiu, 2007). With regard to the restriction of APPJ instrumentation, the system pressure adopted in the present study cannot be varied as it is fixed at the atmospheric pressure. Other operation parameters including 1) treatment time; 2) ignition power; 3) plasma gas composition and 4) jet distance are being investigated as well.

The findings obtained from this study can afford a better understanding of the interaction between atmospheric pressure plasma and different textile substrates. Furthermore, the optimum conditions used for the wettability modification can also be determined and provided as the empirical formulation of the atmospheric pressure plasma processing for textile materials.

1.2   Objectives

This project is focused on the development of a nano-scale surface modification of textile materials utilising atmospheric pressure plasma. The principle objectives of the thesis are summarised as follows:

1. To modify the surface of textile materials in nano-scale using plasma technology in relation to the process parameters.

2. To study the changes in textile properties of the plasma-modified textile materials with respect to different textile wet processing agents.

3. To explore the reaction model of plasma-surface interactions on textile materials and to predict the outcomes of plasma treatment using novel process parameters.

1.3   Methodology

The following methodologies have been adopted to achieve the objectives:

1. To review the material properties and characteristics as well as the background knowledge and recent development of low-temperature atmospheric pressure plasma treatments

2. To perform atmospheric pressure plasma treatment on a polyethylene terephthalate film which acts as the reaction model to help determine the optimum treatment parameters for textile materials in order to achieve a nano-scale topography.

3. To perform atmospheric pressure plasma treatment on different textile materials in order to achieve a nano-scale topography using appropriate operation parameters.

----

4. To characterise the plasma-modified substrates using the advanced characterisation techniques such as scanning electron microscopy (SEM), Fourier Transform infrared spectroscopy (FTIR) and X-ray photoelectron spectroscopy (XPS) etc., and to deduce the optimum conditions for a nano-scale plasma modification.

5. To evaluate the wetting behaviour of the plasma-modified substrates in response to a nano-scale atmospheric pressure plasma modification.

1.4   Scope of thesis

The thesis comprises chapters which are outline as follows:

Chapter 1 introduces the background information, objectives, methodology and scope of the thesis.

Chapter 2 summarises the comprehensive literature review of textile substrates, development of atmospheric pressure plasma in textile industry, and the characteristics of atmospheric pressure plasma.

Chapter 3 presents a preliminary simulation and evaluation of a homogeneous polymer film which acted as a reaction model and milestone for the development of plasma modification of different textile substrates. He-O_2 plasma used for the development of the plasma etching-hydrophilisation system of the polyester substrate was studied. The modified film was characterised by the advanced instrumentations. Nano-scale plasma modification was achieved and optimised. In this chapter, the development of atmospheric pressure plasma etching system for polyester fabrics was explored. He-O_2 plasma system developed by the film model was put into practice using

----

----

polyester fabric. The modified fabric was characterised by the advanced instrumentations. Nano-scale plasma etching-hydrophilisation was achieved and optimised.

Chapter 4 evaluates the atmospheric pressure plasma etching system for wool fabric. He-O_2 plasma was employed for the development of the plasma etching-hydrophilisation system of the substrate. Two types of wool fabrics were used to study the effect of substrate dependence on the plasma-substrate interaction. The modified fabric was characterised by the advanced instrumentations. Nano-scale plasma etching-hydrophilisation was achieved and optimised without descaling.

Chapter 5 evaluates the atmospheric pressure plasma etching system for cotton fabric. Two plasma systems namely He-CF_4 and He-O_2 were studied for the plasma etching–hydrophobisation of the substrate. The systems were optimised based on the statistical optimisation tool to evaluate the optimum condition for attaining a nano-scale hydrophobisation. The surface properties of the substrate were revealed using the advanced instrumentations. The effect of plasma gases was evaluated using two different etchant gases in the present study.

Chapter 6 states the major results and findings obtained from the present research work and draws the final conclusion. The remaining problems and deficiencies in the present study associated with the development of the plasma systems for different textile materials are outlined. Some future research works are also recommended.

Chapter 7 includes all references in this thesis.

Chapter 2   Literature review

2.1   Nature of different textile materials: polyester, wool and cotton

Every textile material has its own distinctive and appreciable textile properties. Technologists are acquiring novel techniques to tailor-made textile materials with specific surface properties catering for a diverse of applications. A diversity of surface modifications is under exploration in order to afford desirable textile performances without deteriorating the original bulk properties. Low temperature plasma is one of the alternatives used as a substitution of the conventional wet chemical processing.

Pristine nature of different textile materials has to be well-studied before applying appropriate treatments on each type of materials. In the present study, polyester, wool and cotton are subjected to experimentation. Nature of each type of textile materials is summarised as follows.

2.1.1   Polyester

Polyester is derived from petroleum via condensation reaction of diols and dicarboxylic acids conventionally. Polyester is chemically composed of at least 85% by weight of an ester of a substituted aromatic carboxylic acid. Polyester polymers are not restricted to terephthalic units and para-substituted hydroxybenzoate units in a long-chain of linear polymer. Two varieties of polyester filaments, namely polyethylene terephthalate (PET) and poly-1,4-

---

cyclohexylene   dimethylene   terephthalate   (PCDT),   are   commercially

manufactured in textile sector as illustrated in **Figure 2-1**.

polyethylene terephthalate   poly-1,4-cyclohexylene dimethylene terephthalate
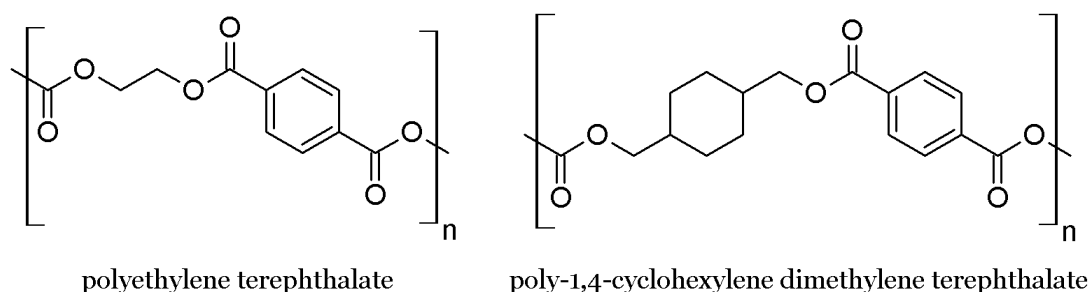
Figure 2-1   Chemical structures of PET and PCDT

Polyester fibre is typically produced by melt-spinning affording circular

shape with smooth surface without distinguishable features. There are other

variants of polyester fibres manufactured to provide specific textile properties.

In general, polyester filament is hydrophobic in nature. During super drawing,

polymer chains are oriented along the fibre axis. The filament is composed of

axially-oriented linear polymer molecules. High regularity furnishes the

hydrophobicity of polyester. Polyester fibre possesses high mechanical strength,

dimension stability and elastic recovery. With respect to the close proximity of

polymer chains oriented in lengthwise direction, polyester has high mechanical

properties where electron clouds between benzene rings extensively interacting

with each other.

The bulk properties such as high mechanical strength and excellent

chemical inertness of polyester are attractive in textile industries. However, the

main defect of most of the synthetic fibres is that they do not have surface

reactivity. Hydrophobicity without surface reactivity leads to accumulation of

---

electrostatic charge and poor fabric comfort for polyester. Smooth polyester filament without voids has poor wickability and low moisture regain. Without reactive functional groups, polyester is not easy to be wetted nor dyed. Polyester is usually dyed by disperse dye with moderate colourfastness. Lacking surface reactivity has to be surmounted in order to achieve appreciable textile performances for different applications.

2.1.2   Wool

Wool is an animal fibre composed of heterogeneous proteins. Wool proteins are natural polyamides, i.e. polypeptides, linking different amino acids together via peptide bonds as shown in Figure 2-2. Wool is chemically complex containing 18 naturally-occurring amino acids. Wool proteins are amphoteric with the presence of both the ionisable carboxyl groups and amino groups. These ionic groups are dye sites for ionic dyes. The physical structure of wool fibre is unique. The fibre is characterised with surface cuticles which act as a barrier to protect the interior cortex of wool. It is made up of two main parts, namely cuticle and mesocortex as illustrated in Figure 2-3.

polyamide
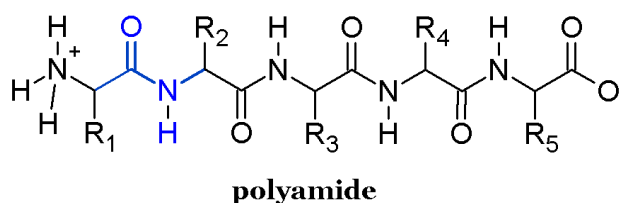
Figure 2-2   General chemical structure of wool protein

The cuticle cell of wool fibres overlapping in one direction is comprised of at least four sub-layers. The cell consists of epicuticle, the A-layer and the B-layer of exocuticle, and endocuticle. The surface of epicuticle is composed of covalently bound fatty acids, chiral 18-methyleicosanoic acids (18-MEA), probably via thioester linkages, namely the F-layer (Negri et al., 1993). The epicuticle is about 2.5nm thick and highly resistant to attack of alkalis, oxidising agents and proteolytic enzymes. Predominantly hydrophobic cuticle is made up of proteins with a high density of disulphide bonds, i.e. cystines. These crosslinks are water insoluble and exhibit water-repellence. The cystine content is progressively decreasing from the outer exocuticle to the inner endocuticle. In other words, the degree of crosslinking is reducing in the radical direction of the fibre. Endocuticle with low sulphur content is readily permeable and acts as the radical pathway for diffusion of water and other reagents.

Wool fibre having natural crimp is made up of bilateral segmentation of mesocortex cells naming ortho- and para-cortex cells. With respect to the variation in sulphur content of the two types of cortex cells, toughness is different resulting in stable crimps of the fibre. The cortex cell is subdivided into macrofibrils and microfibrils which are organisations of α-keratin polymers. Good elasticity and resilience of wool are due to the presence of internal helical microfibrils. Microfibrils are alpha helix of keratins acting as springs inside the wool fibre.
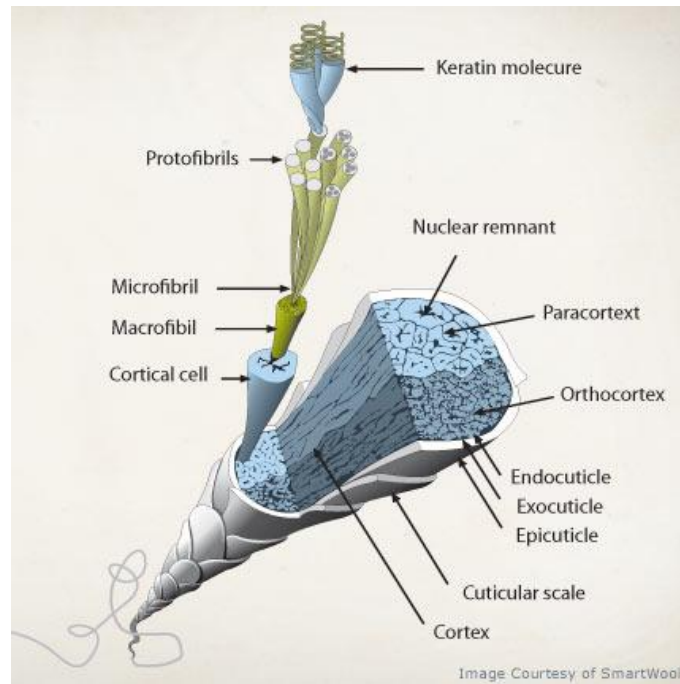
Figure 2-3   Sub-microscopic structure of wool fibre (Wood, 2009)

Descaling of wool fibre is an essential treatment to determine the processability of wool in textile applications. Wool cuticles constraining directional movement of the fibres hinders the processing of wool fibres. Felting and shrinkage of wool fabrics are problematic. Cuticles inhibit yarn spinning and dyeing of wool. To facilitate wool processing, pretreatment of wool fibres is needed. Conventional wet descaling processes impose environmental stress and degradation of wool fibres. Low temperature plasma (LTP) being a dry processing technique which has been established to improve surface wettability and dyeing properties of wool (Hesse et al., 1995; Kan et al., 1999; Molina et al., 2002, 2003; Ryu et al., 1991), and would be a potential alternative to alleviate the stress. Chlorination employed for descaling is difficult to limit the effect on the surface level of fibre. Fibres are usually severely damaged by aggressive wet chlorination and lose bulk mechanical properties. Other descaling methods are

----

----

acquired to prevent degradation of interior of wool fibres. Controlled descaling is also beneficial in wool dyeing and other wet processing of wool fibres. Chlorination of wool cleaves disulphide bonds and hence reduces the degree of surface crosslinks.

2.1.3   Cotton

Cotton is structurally distinctive. Unlike other natural and synthetic fibres, cotton is inherently hollow fibres. Cotton fibre is unicellular with lumen at the centre. This help to trap air for warmth retention of garments. Cotton fibre is a flat, twisted ribbon which facilitates yarn spinning as shown in **Figure 2-4**. Multiple walls of spiral fibrils give convolutions to the fibre. Since convolutions scatter incident light, thus cotton fabric usually exhibit poor lustre. **Figure 2-5** illustrates the sub-microscopic structure of a cotton fibre.
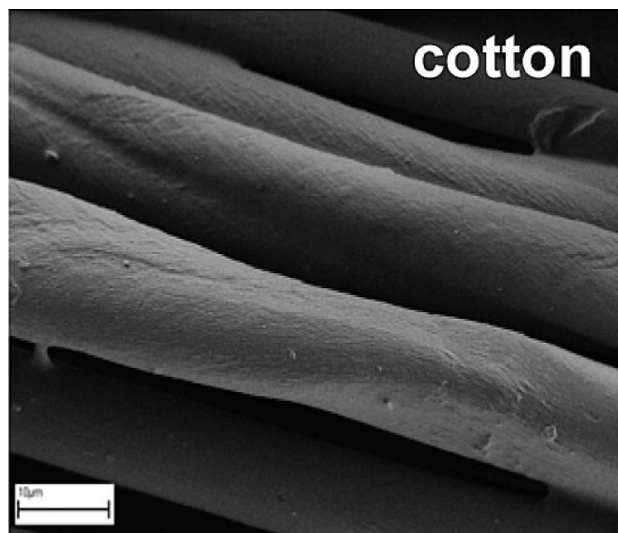
Figure 2-4   Surface morphology of cotton fibres (Vince et al., 2006)
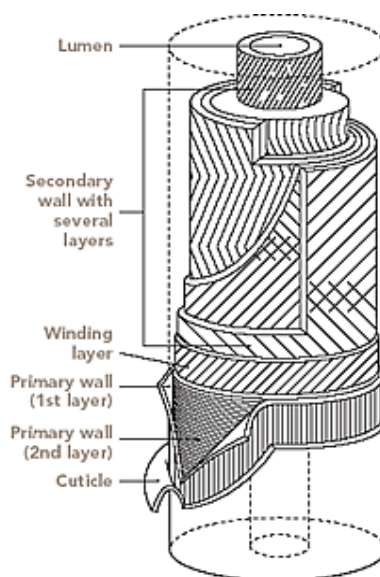
Figure 2-5   Sub-microscopic structure of a cotton fibre (Worsham, 2010)

Cotton is a botanic fibre made up of cellulose which is a homopolysaccharide of D-glucoses linked by *β*-1,4 glycosidic bond as illustrated in **Figure 2-6**. On one hand, a large amount of polar hydroxyl groups present in glucose units offers hydrophilicity to the fibre. On the other hand, hydroxyl groups forming the extensive intermolecular and intramolecular hydrogen bonding give strength to the fibre. Well-defined intermolecular hydrogen bonding between the linear and unbranched cellulose polymer chains allows regular molecular packing in close proximity.
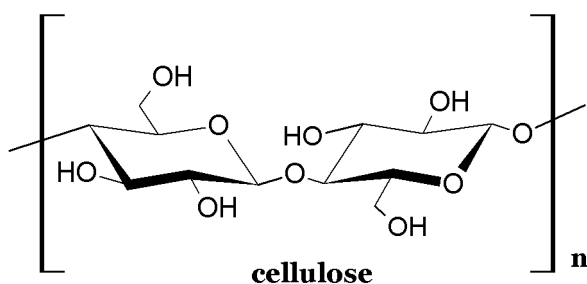
Figure 2-6   Chemical structure of cellulose

Moreover, hydroxyl groups give surface reactivity to the fibre with respect to various wetting agents and chemical finishing. For example, hydroxyl groups are dye sites for reactive dyes. Nevertheless, cotton possesses excellent wettability and wickability. However, high moisture content of this natural fibre possesses low resistance to microorganisms. Different finishing are aimed at improving anti-microbial activity of cotton so as to maintain fibre durability. For examples, cotton using in medical sectors requires anti-microbial activity and haemorepellence to prevent accumulation of aqueous contaminants. Surface hydrophobicity is needed to cater for the requirements.

The depletion of non-renewable resources is leading to a resurgence of interest in the plant-derived materials in various textile sectors. Cellulosic fibre possesses attractive inherent bulk properties which is widely be used in diverse sectors with surface modifications (Allan et al., 2002; Baltazar-Y-Jimenez et al., 2007; Canal et al., 2009; Hoa et al., 2007; Karahan & Özdoğan, 2008; Mejía et al., 2009; Sinha & Panigrahi, 2009; Tsafack & Levalois-Grützmacher, 2007; Temerman & Leys, 2005). The acquisition of hydrophobic surface offering liquid repellency is exploitable for diverse applications catering.

2.2 Background and current development of plasma treatments on textile materials

2.2.1 Fundamentals of plasma

Plasma is regarded as "the fourth state of matter". Plasma is a fully or partially ionised gas generated by the thermal, magnetic or electrical discharge. It is composed of many reactive species including positive and negative ions, electrons, neutrals, excited molecules, metastables, free radicals and photons from ultraviolet to visible electromagnetic radiation depending on the degree of ionisation as shown in **Figure 2-7**. These constituents are responsible for the surface modification of a substrate, especially metastables. Metastables with a long decay lifetime are capable of transferring energy to other species. They are crucial in generating and sustaining the production of various types of excited and atomic species in plasma. Luminosity is one of the observable macroscopic features of plasma. In addition, plasma is electrically conductive containing free charge carriers while exhibiting quasi-neutrality. Plasma possesses a unique property by inducing surface modifications confined to about 1-10µm depth without altering the bulk properties of a substrate.
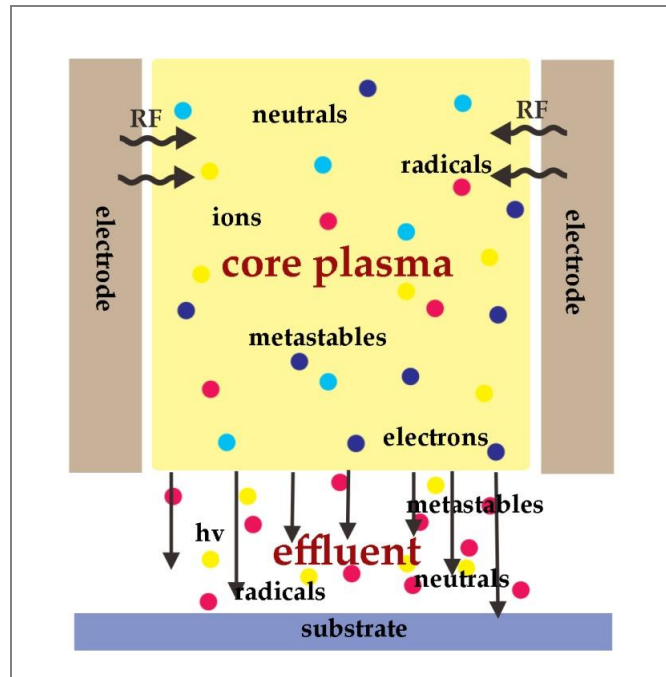
Figure 2-7   Schematic diagram of plasma constituents in an atmospheric
pressure plasma jet (Niemi et al., 2007)

The degree of modification of a substrate is determined by the penetration power of plasma. Plasma is composed of different types of active species having different power. Plasma is regarded as a surface treatment as most of the plasma constituents responsible for the outermost surface-substrate interaction are usually in nanometre depth. Photons such as vacuum ultraviolet (VUV) photons are able to penetrate deeper into the sub-surface region and even into the bulk region (Holländer et al., 1999). **Figure 2-8** illustrates the penetration power of plasma constituents.
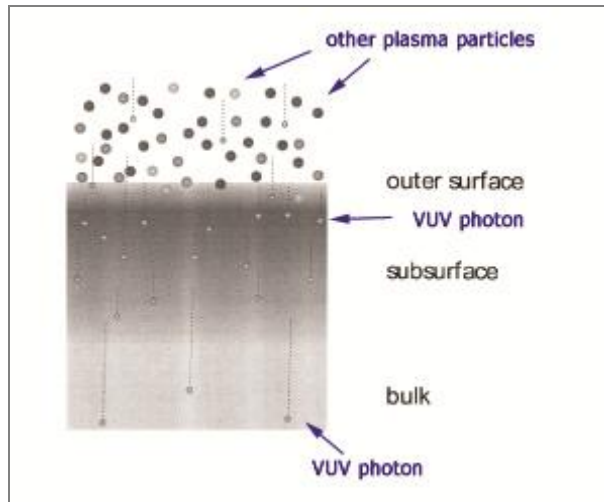
Figure 2-8   Penetration power of different plasma constituents
(Holländer et al., 1999)

Plasma is classified into two main categories, namely equilibrium (thermal) and non-equilibrium (low-temperature) plasmas. The overall temperature of plasma is determined by the thermodynamic equilibrium between plasma constituents. **Table 2-1** indicates the main difference between the two categories of plasmas.

Table 2-1   Classification of plasmas

	Equilibrium plasma	**Non-equilibrium plasma**
Temperature	$T_e \approx T_i \approx T_n$	$T_e \gg T_i \approx T_n$
Electron density	High	low
Type of collision	Gas particles are being heated by frequent collision with electrons elastically	Minimal elastic collision to heat up plasma gas particles

(T_e = electron temperature, T_i = ion temperature; T_n = neutral temperature)

2.2.2 Low-temperature plasma in textile industry

Plasma is well-developed for a variety of industrial surface modifications. Application of gas plasma for micro-electronics dates back to the 70s. For example, thermal plasma has been applied to surface cleaning, etching and coating deposition on semi-conductors. In these few decades, suitable low-temperature plasma is being developed for surface modification of heat sensitive substrates. Low-temperature plasma (LTP) is attained without achieving a thermodynamic equilibrium between different plasma constituents. Electrons acquire a much higher energy of 0.1 to several eV as compared to the other ions and neutral molecules ($T_e \gg T_i \approx T_n$). Bulk gaseous plasma remains at low temperature without causing thermal degradation of heat sensitive materials. With this distinct property, LTP is recently put forward in textile sectors.

LTP is attractive in textile industry with the bulk gas temperature near ambient temperature. Thermal degradation of heat sensitive textile materials is avoided. Non-thermal plasma treatment has been applied to a diversity of textile materials in the past few decades with reference to the detailed review by Morent in 2007 (Morent et al., 2007). Plasma is a prospective choice as a pre-treatment or finishing technique which is a dry process. In textile industry, a large consumption of water and chemicals in the pre-treatment and finishing processes requires a high material input and sequential effluent treatments. To surmount the shortcomings of wet chemical processing, plasma offers a potential alternative. Solventless plasma treatment without the production of massive amount of effluent is ecological and environmentally friendly. Furthermore, plasma treatment is a versatile treatment which is compatible

----

with different gases or precursors in a system. A diversity of surface functionalities can be incorporated into the textile materials to cater for different applications. LTP is competent to supersede the conventional chemical finishing of textile materials.

2.3   Background, advantages and applications of atmospheric pressure plasma treatment

2.3.1   Atmospheric pressure versus reduced pressure

LTP operated in vacuum at low pressure has been industrialised and applied to textile materials in the past few decades. The reduced pressure plasma generates a high concentration of active species while maintaining low gas temperature. Starting from the late 20th century, researchers and technologists exploit to use more economical plasma operating at atmospheric pressure. Plasma operating under atmospheric pressure will bring manifold potential advantages to textile industry including 1) enable continuous processing of fabric rolls without limitation of the vacuum system architecture; 2) reduce capital and maintenance cost without the vacuum system implantation; and 3) offer a milder surface treatment to substrates with short lifetime active species. **Table 2-2** summarises the characteristics of plasma operating under different system pressures.

Table 2-2   Summary of the characteristics of plasma operated in different ranges of system pressure

	reduced pressure	atmospheric pressure
Operation	Batch	Batch/continuous
Capital /maintenance cost	High	Relatively low
Lifetime of active species	Long	Short
Mean free path length	Long	Short
Breakdown voltage V$_b$	Similar	

Although atmospheric pressure plasma is attractive for continuous textile modifications, yet a high breakdown voltage is required under atmospheric pressure (Schütze et al., 1998). The breakdown voltage–gas pressure relationship is illustrated in **Figure 2-9**. Breakdown voltage, V$_b$ depends on the inter-electrode gap, d, and system pressure, p as illustrated in **Equation 2-1**. In order to achieve a reasonable breakdown voltage in the atmosphere, the inter-electrode gap has to be reduced. Various atmospheric pressure plasma sources are developed based on this prerequisite (Shenton & Steven, 2001).
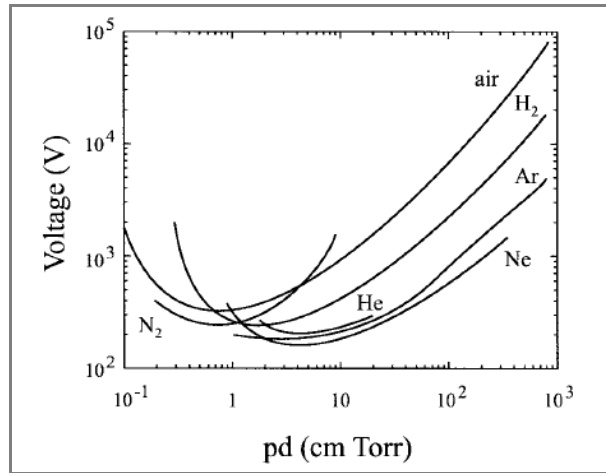
Figure 2-9   Breakdown voltage – gas pressure relationship
(Schütze et al., 1998)

$$V_b = \frac{B(p \cdot d)}{\ln\,[A(p \cdot d)] - \ln[\ln(1+1/\gamma_{se})]} \qquad \text{Equation 2-1}$$

Nature of plasma is pressure-dependent. Collision between electrons and other heavy particles intensifies with the increasing system pressure. As a result, atmospheric pressure plasma approaches thermodynamic equilibrium as shown in **Figure 2-10**. In order to prevent the establishment of thermal plasma, one way is to use low density current or short-pulsed feeding power to ignite the plasma (Tendero et al., 2006). To sustain non-equilibrium plasma under atmospheric pressure, radio wave (13.56MHz or 27.12MHz) or microwave (2.54GHz) electromagnetic radiations are commonly employed as the ignition source.

Other than the nature of ignition source, the size of plasma influences the non-equilibrium state of plasma (Mariottia, 2008). Te and Tg departing from each other with the reducing size of plasma enhances the non-equilibrium state

----

----

as illustrated in **Figure 2-11**. Furthermore, the nature of feeding gas or gas mixture will affect the non-equilibrium state of atmospheric pressure plasma (Mariottia, 2008). For example, adding methane gas into a system can reduce T_g. When feeding oxygen gas, T_g will increase as shown in **Figure 2-12**. Active oxygen species present in the plasma can heat up the gas.
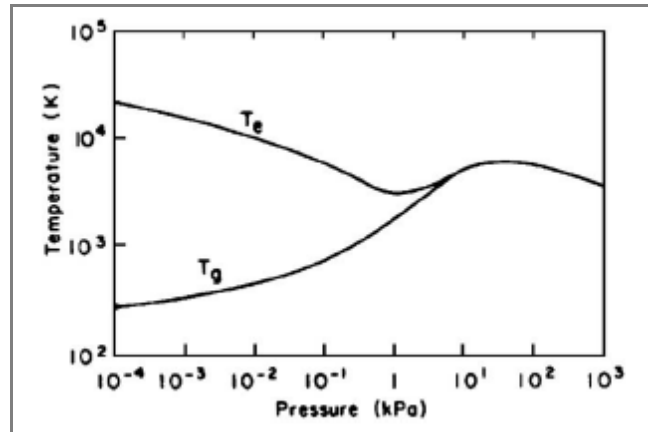
Figure 2-10 T_e and T_g relationship with system pressure
(Schütze et al., 1998; Tendero et al., 2006)
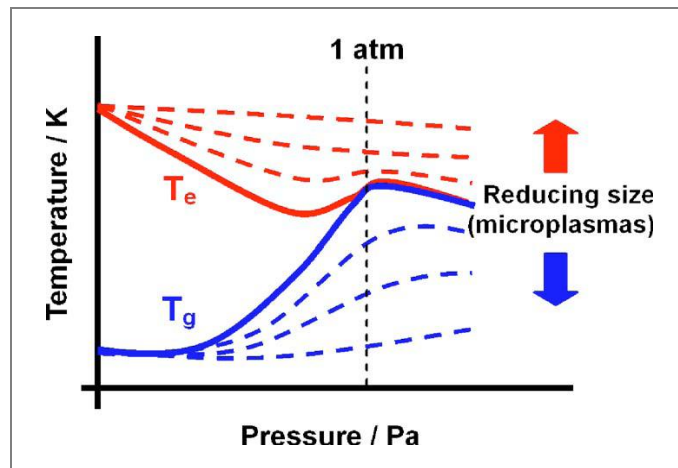
(red line: T_e; blue line: T_g)

Figure 2-11   Effect of size of plasma at the non-equilibrium state varies with
pressure (Mariottia, 2008).

---
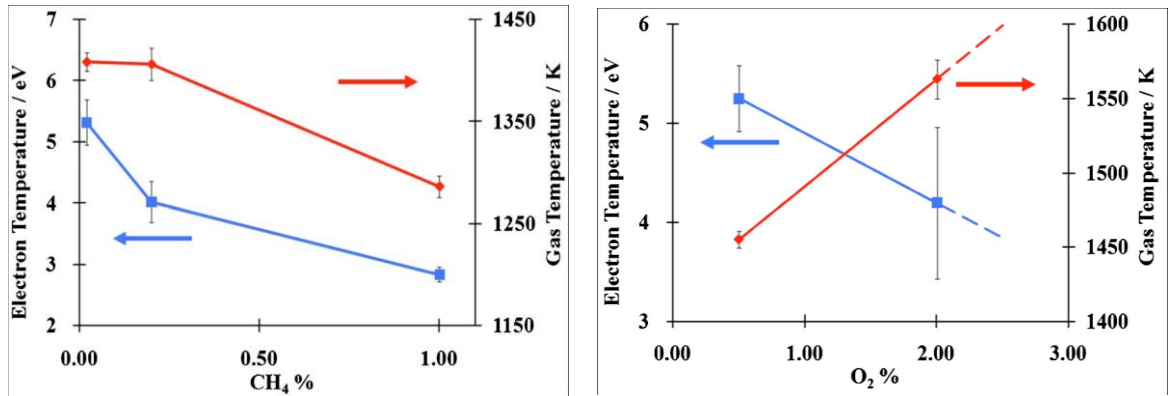
a) T_e and T_g decrease with increasing methane concentration

b) T_e decreases while T_g increases with increasing oxygen concentration

Figure 2-12   Effect of gas nature on T_e and T_g (red line: T_g; blue line: T_e) (Mariottia, 2008)

2.3.2   Different atmospheric pressure plasma sources

In recent years, atmospheric pressure plasma arouses an increasing interest in textile industry. Plasma modification is a promising technique in textile pre-treatment and finishing, especially operating under ambient conditions, i.e. at atmospheric pressure and near room temperature. There are ongoing researches using atmospheric pressure plasma to enhance the surface reactivity of textile materials. Plasma-modified textile materials show improvement in wettability (Karahan & Özdoğan,, 2008; Leroux et al., 2006; Samanta et al., 2009; Song, 2006; Temmerman & Leys, 2005; Tsai et al., 2005; Wang, 2007), dyeability (Černákorá et al., 2005; Cai & Qiu, 2006; Carneiro et al., 2001; Karahan et al., 2008; Sung-Spitzl, 2003), shrinkage resistance (Tokino et al., 1993), adhesion to different chemical finishing including UV screening metal/metal oxides (Szabová et al., 2009; Šimor et al., 2003), and anti-microbial agents etc. (Kostić et al., 2008). Functional coatings, e.g. UV screening and anti-microbial, can be

---

----

deposited directly on the substrates using plasma grafting and polymerisation with organic precursors (Allan et al., 2002, Virk et al., 2004; Fiala et al., 2006, Herbert, 2003, 2006, Kim et al., 2006; Lee et al., 2001; Lei et al., 2000; Masaaki et al., 2008).

As compared to the reduced pressure plasma, atmospheric pressure plasma reduces the complexity and cost for material processing. In addition, atmospheric pressure plasma enables the continuous processing of fabric rolls. Various novel atmospheric pressure plasma sources have been developed. There are three main classes of atmospheric pressure plasmas, namely corona discharge, dielectric barrier discharge (**DBD**) and glow discharge. Corona discharge operates in ambient atmosphere while DBD and glow discharge can be operated under both reduced and atmospheric pressure. When compared with corona discharge, DBD and glow discharge are relatively homogeneous. Glow discharge is more volumetric, homogeneous, and free of arcs and streamers as compared to corona and dielectric barrier discharge. With the above advantages, both DBD and glow discharge are gaining prosperity in textile industry for uniform surface modifications.

There is a variety of DBD and glow discharge plasmas sources including atmospheric pressure glow discharge (**APGD**) (Meade et al., 2008; Samanta et al., 2009), atmospheric pressure non-equilibrium plasma (**APNEP**) (Shenton & Stevens, 2001, Shenton et al., 2002), atmospheric pressure plasma jet (**APPJ**) (Song & Wang, 2006; Wang & Qiu, 2007a, b; Wang et al., 2007), one atmosphere uniform glow discharge (**OAUGD**) (Tsai et al., 2005; Zhu et al., 2008), surface dielectric barrier discharge (**SDBD**) (Černákorá et al., 2005; Fiala et al., 2006), atmospheric pressure plasma liquid deposition (**APPLD**) (Herbert, 2003; 2006)

----

etc. Each type has its own characteristic architecture and featured plasma discharge.

APGD is capable of improving the wettability of water and oil on cotton, nylon and polyester fabrics. This glow discharge is free from micro-discharges. As compared to other non-uniform atmospheric pressure plasmas, **APGD** is able to induce nano-scale indentations without damaging textile materials. Using He, Ar, O_2 and air in the system, the modified fabric surfaces can improve the spreading and wetting of both hydrophilic and hydrophobic liquids via the nano-scale channels formed by plasma (Samanta, et al, 2009). **APNEP** is operated using microwave electromagnetic radiation as the ignition source. Uniform glow discharge generated is successful to modify various polymeric films (Meade et al., 2008; Samanta et al., 2009). APNEP is also used to modify polyester garment by plasma graft polymerisation of acrylic acid (Masaaki et al., 2008). Synthetic electrospun nano-fibre fabric and melt-blown micro-fibre fabric were hydrophilised by **OAUGD** using air plasma. Upon exposure to the plasma source for a few seconds, only a minimal degradation is imposed on the textile materials with a significant increase in wettability (Tsai et al., 2005). **APPLD** is a novel technique especially developed to deposit functional coatings on fabrics. In this system, a substrate is exposed to the afterglow plasma with the atomised droplets of precursors being directly nebulised and deposited on the substrate surface. As there is no electrons present in the afterglow region, thus the precursors do not dissociate or being fragmented. Therefore, a coating formed retains all the functionalities of the original liquid precursor. Additionally, no solvent is required in this system. APPLD has been used to depositing hydrophobic coating on cotton fabrics as

----

---

well as hydrophilic coatings on polyester and polyolefin synthetic fabrics (Herbert, 2003, 2006; Tyner, 2007).

In the present study, an APPJ developed by Selwyn and his co-workers in 1998 (Selwyn et al., 1999-2000) utilised for an atmospheric pressure plasma treatment on substrates. **APPJ** can be operated at low ignition power with the gas temperature being around 100°C. Low gas temperature is able to minimise the thermal degradation of heat sensitive textile materials. Low temperature atmospheric pressure plasma is excited by a capacitive discharge using the radio-frequency (RF) of 13.56MHz or 27.12MHz. A close proximity of a pair of parallel plate electrodes allows lower power operation avoiding thermal plasma generation. Narrow gap (1.6mm) between the electrodes in APPJ enables a reasonable breakdown voltage (V_b) under atmospheric pressure. A schematic diagram as shown in **Figure 2-13** illustrates the APPJ architecture. Wang and her colleagues have utilised APPJ extensively to modify the natural (cotton and wool) and synthetic (polyester, polyamide and polyethylene) fibres and fabrics (Song & Wang, 2006; Wang & Qiu, 2007a, b; Wang et al., 2008; Zhu et al., 2008). Additionally, the system architecture allows plasma to be applied onto the substrates in complex shapes and unlimited dimensions.
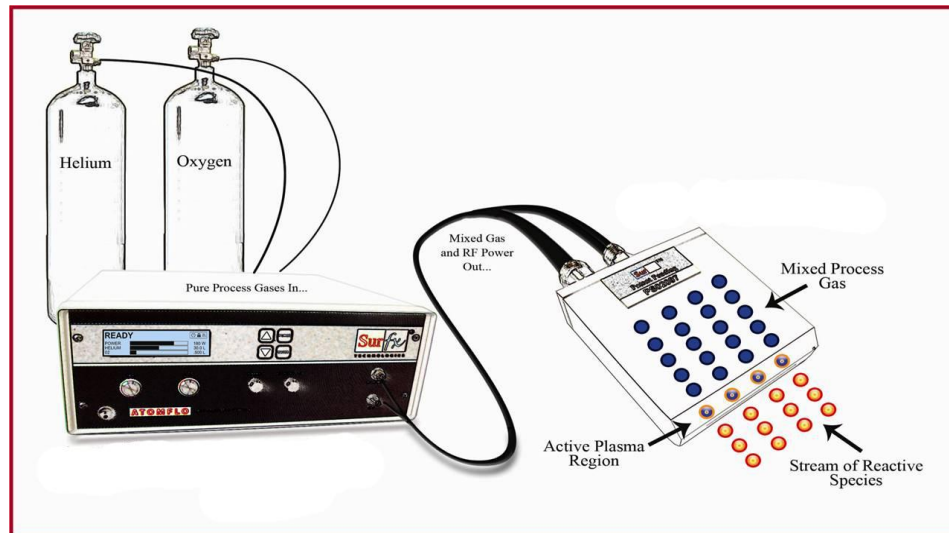
Figure 2-13   Architecture of APPJ (Surfx Tech., US)

APPJ produces plasma comparable to that of the low pressure glow discharge with a high concentration of active species (Schütze et al., 1998). As compared to the other atmospheric pressure plasma sources, APPJ discharge is more uniform, homogeneous and volumetric. Glow discharge is less powerful than filament discharge at a lower discharge voltage. When compared with corona and DBD, the plasma generated by APPJ is free of filaments, streamers and arcs with respect to the close proximity of the planar electrodes (Park et al., 2000, Selwyn et al., 1999-2000, Schütze et al., 1998; Tendero et al., 2006). This avoids severe deterioration of textile materials leading to adverse effect on textile properties such as reduction in mechanical strength. A simplified comparison between corona discharge, DBD and APPJ is listed in **Table 2-3**.

Table 2-3   Comparison of atmospheric pressure plasma sources

	Corona	**DBD**	**APPJ**
Uniformity of plasma	Non-uniform	Non-uniform	uniform
Bulk gas temperature	50-400 °C	50-400°C	25-200°C
Electron concentration [e]	10^{15}-10^{19}m^{-3}	10^{18}-10^{21} m^{-3}	10^{17}-10^{18}m^{-3}
Breakdown voltage V$_b$	High	medium	Low-medium

(Selwyn et al., 1999-2000, Tendero et al., 2006)

Furthermore, a substrate is exposed to the afterglow of APPJ in the downstream plasma treatment. **Figure 2-14** indicates different plasma composition present in the direct glow region and afterglow region. A substrate positioned in different regions usually experiences different plasma-substrate interaction. The afterglow of atmospheric pressure plasma is dominated by the neutral reactive species including the ground-state atoms and metastables which are the chief components (Jeong et al., 2000; Schütze et al., 1998) owing to free of electrons in the downstream afterglow, the milder physical ablation can be induced by using APPJ which has a great potential to achieve nano-fabrication of textile materials.

28
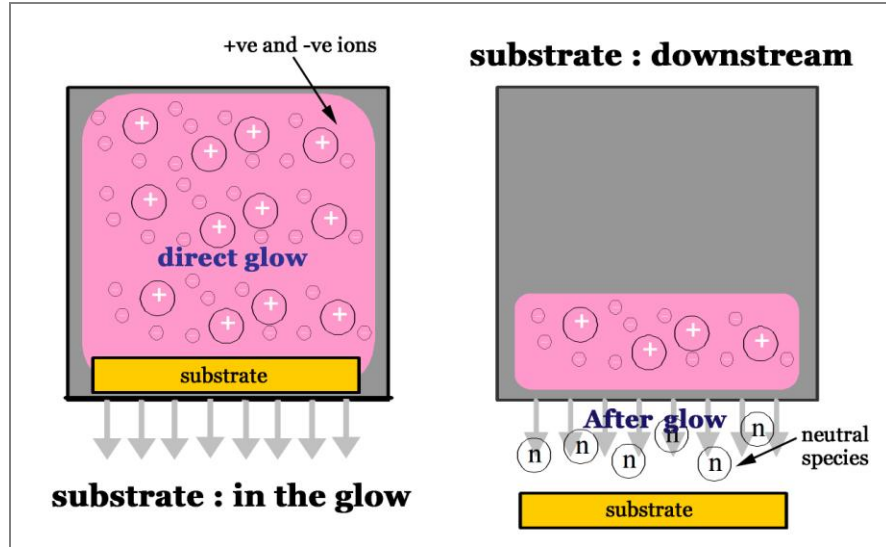
Figure 2-14   Composition of plasma afterglow

2.3.3   Understanding plasma chemistry and plasma-substrate interaction in designing appropriate atmospheric pressure plasma treatments

2.3.3.1   Types of plasma-substrate interactions

Plasma modification is a time-dependent physicochemical interaction between plasma and substrate. The interaction is fundamentally based on the types of plasma used. Plasma is a gaseous mixture of various active species including electrons, ions, excited states, metastables, molecules, atoms and photons. By feeding different gases and precursors into the system, a wide range of modifications can be imposed on a substrate. Plasma produced by the non-polymerising gases, e.g. argon (Ar), helium (He), nitrogen (N_2), oxygen (O_2), tetraflouromethane (CF_4) and ammonia (NH_3) induces surface etching and functionalisation. Plasma grafting or polymerisation is induced by using

----

----

polymerising precursors including various organic compounds, e.g. acrylic acid and siloxane.

Plasma etching of substrates relies on two main principles, namely physical ablation and chemical etching. Physical ablation is induced by ion and electron bombardment of inert gases such as argon and helium. Chemical etching is caused by the reactive gases including oxygen and nitrogen. Reactive gases react with the substrate to form low molecular weight materials which can be easily removed from the substrate surface. Plasma grating polymerisation is induced by photons and free radicals generated from plasma. Surface exposed to plasma is activated and sequentially the monomers of a precursor can be grafted and/or further polymerised on the substrate *in situ* or post plasma treatment.

In order to alter the surface wettability of different textile materials, various reactive gases are required to incorporate into the plasma system. Plasma hydrophilises a surface by increasing surface energy of the substrate. Oxidation and ammonisation using O_2 or N_2 respectively are useful for generating polar functionalities and enhancing surface wettability. In opposite, plasma hydrophobises a surface by reducing the surface energy of the substrate. Fluorination and deposition of hydrophobic precursors using CF_4 or silicones and fluorocarbons respectively are useful for generating non-polar functionalities reducing surface wettability.

In the present project, O_2 and CF_4 were used as the reactive gas for coupling He in the plasma modifications. These two etchant gases were utilised for two distinct applications. O_2 has been employed for hydrophilisation

----

(Karahan & Özdoğan, 2008; Leroux et al., 2006; Samanta et al., 2009; Song & Wang, 2006; Temmerman & Leys, 2005; Tsai et al., 2005; Wang, 2007) while CF_4 has been employed for hydrophobisation (Gao et al., 2009; McCord et al., 2003; Sigurdsson & Shishoo, 1997, Vohrer et al., 1997) of the substrates. By applying the appropriate type of reactive gas, the surface wettability of a substrate can be reverted.

2.3.3.2   Plasma chemistry diagnosis

The composition of plasma constituents in the reduced and atmospheric pressure plasma has been extensively studied by different researchers and scientist using various spectroscopic techniques such as optical emission spectroscopy (**OES**), ultraviolet absorption spectroscopy (**UAS**), Infrared spectroscopy, laser induced fluorescence (**LIF**), mass spectroscopy (**MS**) and Langmuir probe (Fanelli et al., 2008; Foltin et al., 2006; Gheorghiu et al., 1997; Holländer et al., 1999; Jeong et al., 2000; Mariottia, 2008; Niemi et al., 2007; Schütze et al., 1998;   Sasaki & Kadota, 1999; Tichý et al., 2009; Vinogradov et al., 2003, 2004; Vinogradov & Lunk, 2005).

In the case of using He-O_2 plasma operated under ambient pressure, the atomic O, metastable O* and O_2 are identified as the neutral active species in the plasma afterglow responsible for the plasma hydrophilisation of substrates (Niemi et al., 2007; Schütze et al., 1998,). Their analyses confirmed the postulation of Shibata M. in 1996. **Figure 2-15** illustrates the changes of the composition of plasma active species with respect to the system pressure. Plasma, being luminous, emits a wide range of UV and vacuum-UV electromagnetic irradiation which plays an important role in plasma chemistry

----

----

for the excitation of atomic O species in the afterglow region in addition to the

Penning reaction with He metastables (He*) inside the plasma as referred to the

following equations. With the persisted lifetime, active species can transport

and interact with the substrate surface.

$He^* + O_2 \rightarrow O_2^+ + He + e^-$

$He^* + O_2 \rightarrow O^* + O^+ + e^-$

$He^+ + O_2 \rightarrow He^+ + O + O^*$

$He^+ + O_2 \rightarrow He + O^+ + O^*$
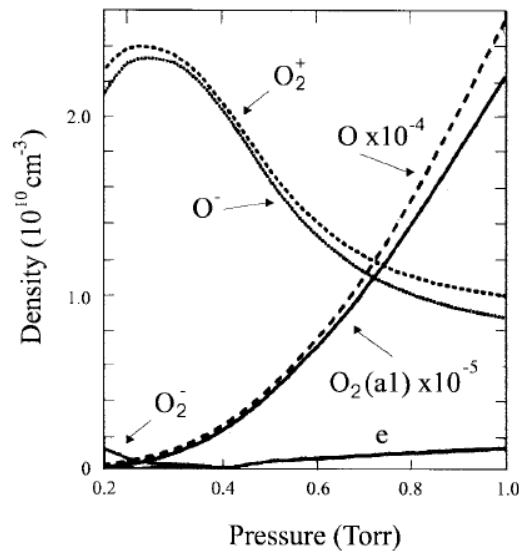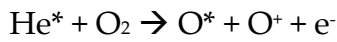
Figure 2-15   Density of oxygen plasma species in relation to system pressure
(Shibata et al., 1996)

In the case of using He-CF_4, the fluorine and the related fluorocarbon ions

including F^-, CF_3^-, CF_3^+, and CF_2^+, are generated by i) electron bombardment and

2) He* bombardment similar to the plasma chemistry of He and O_2 as referred

to the following equations.

Electron bombardment: Penning reaction:

$e^- + CF_4 \rightarrow CF_3 + F^-$ $He + e^- \rightarrow He^+ + 2e^-$

$e^- + CF_4 \rightarrow CF_3^- + F$ $He^* + CF_4 \rightarrow CF_3^+ + F + He + e^-$

$e^- + CF_4 \rightarrow CF_3 + F + e^-$
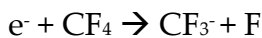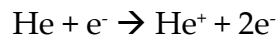
CF_4, F, CF_3, CF_2, CF, C_2F_6, C_2F_5, C_2F_4, C_2F_3, and F_2 are identified as the neutral active species evolved in time and distance downstream of the nozzle in the plasma afterglow responsible for the hydrophobisation of substrates (Hicks & Herrmann, 2003; Fresnais et al., 2009). **Figure 2-16** depicts the density of the individual species in the glow region and afterglow region of the atmospheric pressure plasma.
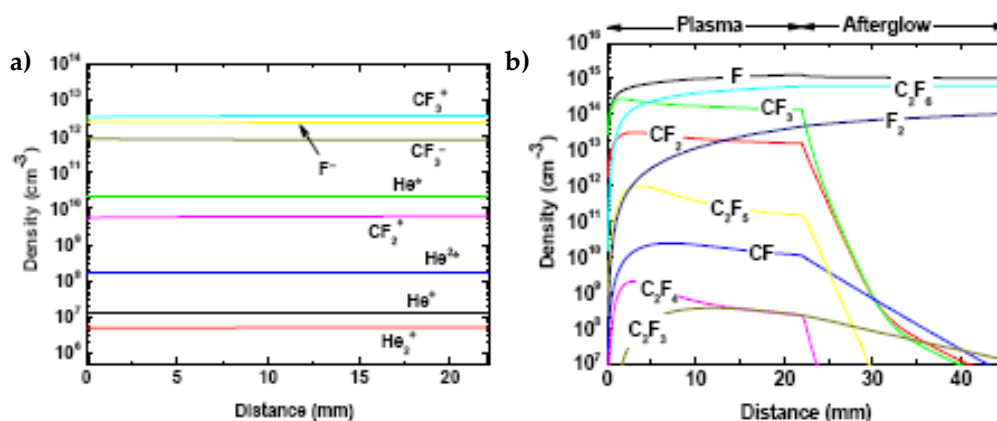
Figure 2-16   Densities of CF_4 plasma species depicted in (a) the plasma glow region and (b) the afterglow region (Hicks & Herrmann, 2003)

Electronic and vibrational emission of the excited plasma gas at a wide scope of wavelengths, especially in UV and near-UV range, are the primary sources of free radicals and photons. Photo-assisted and radical assisted dehydrogenation, dehydroxylation and heterolytic cleavage open up the

----

----

substrate molecules to further reactions. Such kind of reactions assists sequential functionalisation of the substrates such as oxidation and fluorination (Holländer et al., 1999; McCord et al., 2003; Sahin, 2007). Plasma is luminous and the luminosity of plasma is characterised by the feeding plasma gases in the system. By feeding various mixtures of gases and altering the relative ratio of gases in the plasma, the chemistry of plasma will be different and hence the chemical reaction induced on the substrate surface will be various.

Diagnosis of atmospheric pressure plasma is not an easy job. The conventional standard techniques are designed for analysing the reduced pressure plasma. Due to high collision frequency between plasma active species and the atmosphere, the plasma chemistry is different from that operated at the reduced pressure. A well-defined reaction model of atmospheric pressure plasma has not yet been established. Owing to the complexity of the plasma active species, numerous variations of chemical reactions can be induced with respect to the complex composition of different nature of textile materials. The exact chemical reactions occurred on different substrates are still under investigation.

2.3.3.3 Degree of plasma modification in relation to plasma operation parameters

Plasma is capable of modifying a substrate irrespective of the nature, i.e. physical and chemical reactivity, of the substrate. To design an appropriate plasma treatment for a substrate, various plasma operation parameters have to be considered (Kan & Yuen, 2007; Wang & Qiu, 2007). With respect to the restriction of APPJ instrumentation, the system pressure cannot be varied in the

----

----

course of the present study. System pressure is fixed as the ambient pressure. Other operation parameters including 1) duration of treatment; 2) ignition power; 3) nature of plasma gas, and 4) jet distance are going to be investigated.

(1) Duration of treatment

Treatment time defined as the duration of a substrate being exposed to plasma afterglow is the prime parameter which has to be monitored in the course of a plasma study. For example, plasma etching is a progressive reaction with respect to the concentration of plasma active species accumulated on a substrate surface. Time is required to accumulate a sufficient amount of active species on a substrate for the reaction. However, prolonging the exposure to a non-polymerising plasma will induce substrate degradation due to a continuous etching reaction.

(2) Ignition power

Radio frequency of 13.56MHz or 27.12MHz (RF power) is the ignition power employed in the APPJ instruments. Ignition power is a direct control of the plasma power in the discharge. Plasma power is determined by both the density, i.e. concentration of active species, and kinetic energy of the plasma active species. In general, plasma power is proportional to ignition power.

(3) Nature of plasma gas

Nature of plasma gas determines the resultant surface properties of the plasma-modified substrate. Plasma treatment is miscellaneous with respect to diverse kinds of feeding gases and precursors. In general, plasma etching and functionalisation produce oxygen, nitrogen and hydrogen. Plasma grafting or

----

----

polymerisation is induced by using polymerising precursors including various organic compounds, e.g. hydrocarbons, organosilicons and fluorocarbons.

When considering plasma etching, the inert and reactive gases are usually fed into the system. Inert gas, e.g. helium or argon, is commonly used as the diluent and stabilisers. Inert gas physically ablates a surface via bombardment and CASING process (Crosslinks via Activated Species of Inert Gases) simultaneously (Grill, 1994; Placinta et al., 1997). Reactive gas etches a substrate chemically and the nature of reactive gas contributes to the specific chemical reaction. For example, oxygen induces oxidation while tetrafluoromethane induces fluorination. As a result, the surface composition and characteristics vary from gas to gas. Furthermore, helium is employed as the inert gas carrier in the APPJ system. The ratio of reactive gas to carrier gas changes the plasma chemistry and hence influences the plasma-substrate interaction.

(4) Jet distance

APPJ is a downstream treatment. Substrate is always located below the nozzle as shown in **Figure 2-17**. Jet distance is the perpendicular distance between the plasma nozzle and substrate. On one hand, the active plasma species experience a severe collision with air molecules when travelling towards the substrate surface in the atmosphere. Velocity and energy content decrease with time and distance transported. On the other hand, the active species bounce off from substrate surface with respect to a close vicinity of the plasma nozzle. Appropriate proximity between the plasma nozzle and substrate affects the efficacy of the active species when etching a surface.
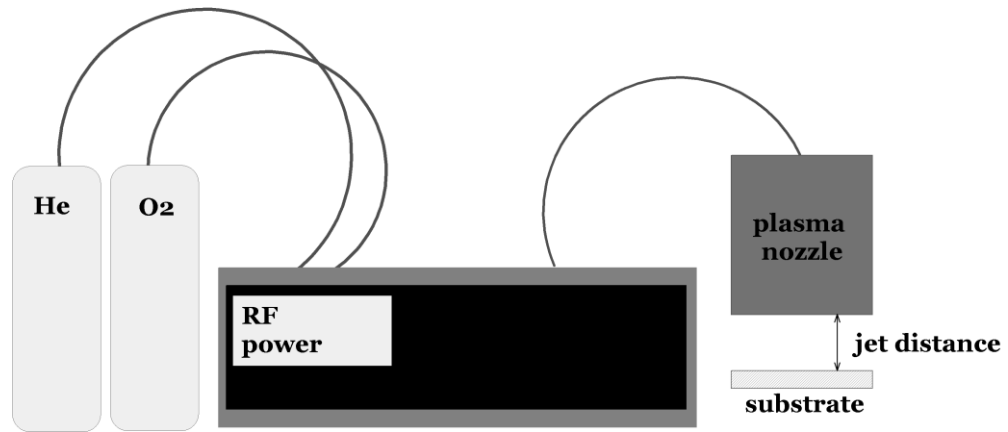
Figure 2-17   Schematic diagram of He-O$_2$ plasma treatment of substrates

2.4   Potential development, possibilities and limits of atmospheric pressure plasma nano-fabrication on textile material

2.4.1   Acquisition of atmospheric pressure plasma nano-fabrication on textile materials

Conventionally, nano-scale refers to a dimension of a structure or a feature in less than 100nm. Limiting the treatment of textile materials on the surface layer is essential to afford a reactive surface while retaining the inherent bulk properties. Severe surface treatment will lead to the degradation of fibres. For examples, plasma etching will reduce the mechanical properties of the fibres and fabrics when the treatment exceeds nano-scale. When considering the applications in apparel textile, the hand, comfort and lustre of fabrics are essential. Various plasmas impose different effects on apparel properties. Severe plasma etching will induce surface fibrils thereby affecting the apparel

----

---

properties of textile materials. Plasma polymer coating forming the individual fibres rather than the "overall" pores present on the fabric retains the bulk properties and breathability of a garment (Rombaldoni et al., 2008).

Nano-structures and nano-architectures exhibit some distinctive properties with respect to a high area-to-volume ratio. In other words, the surface reactivity of nano-texturised substrate will be promoted. Nano-fibres and nano-composites have been developed aiming to achieve the prospective functionalities and performances (Almetwally, 2007). Hitherto, only limited studies are developed in relation to the plasma-induced nano-structures and textile performances. In this aspect, quantifying the surface topography in accordance with the plasma operation parameters is useful for designing the optimum fabrication for different textile materials. Plasma is able to alter the uppermost atomic layers of a material surface while leaving the desirable bulk properties unaffected especially under the controlled condition. In this aspect, the development of plasma nano-fabrication becomes popular (Samanta et al., 2009; Shin & Yoo, 2008).

Micro-scale to nano-scale plasma modification in vacuum or under medium pressure for the synthetic textile materials has been attained in the past 10 years. Recently, researches are achieving the nano-scale plasma modifications under ambient pressure. AFM revealing the nano-scale surface roughness has been observed in vacuum or under medium pressure (Gupta et al., 2000; Raffaele-Addamo et al., 2006; Shin & Yoo, 2008; Wei et al., 2007; Wong et al., 1999) Micro-structures to nano-structures can also be formed using the atmospheric pressure plasmas with some examples being listed in **Table 2-4** (Leroux et al., 2006; Meade et al., 2008; Samanta et al., 2009; Shin & Yoo, 2008).

In order to attain a nano-scale modification via plasma treatment, optimisation of treatment parameters is critical. For example, the choice of plasma gas is one of the factors. O_2 plasma with higher etching power and etching rate will induce a higher vertical roughness as compared to N_2 plasma (Shin & Yoo, 2008; Vesel et al., 2008).

Table 2-4 Examples of some nano-scale plasma modifications on textile materials

Examples

- 12-35nm etched by N_2 or O_2 plasma on PET film (Vesel et al., 2008)

- <200nm nano-channels etched by He plasma enhanced fluid spreading (both hydrophilic and hydrophobic liquid) due to capillary action without significant deterioration of mechanical properties of the fabrics. (Samanta et al., 2009)

- 20-30nm protrusions interspersed across the wool cuticle surface (Meade et al, 2008)

- <25nm nano-porous amine coating deposited on polyester fabric using acetylene/ammonia admixture plasma (Hegemann et al., 2007)

2.4.2   Hurdles of atmospheric pressure plasma nano-fabrication

   in textile industry

Atmospheric pressure plasma is gaining interest in different industrial sectors. Without the prerequisite of the vacuum architecture for a treatment, atmospheric pressure plasma is prospective without physical boundaries in a operating system. Atmospheric pressure plasma is still in the early stage of development in textile industry. There are various factors hindering the prospective growth:

1.   limited knowledge of the physicochemical nature of atmospheric pressure plasma in application to diverse types of textile materials,

2.   poor reproducibility of a plasma treatment without (a) a well-defined plasma-substrate interaction and (b) the sequential interaction between the plasma-modified substrate and the processing agents,

3.   an appropriate application of atmospheric pressure plasma onto a substrate is difficult to monitor,

4.   a controlled degree of surface modification, especially in nano-scale, is crucial in order to ensure that a modification does not induce any alteration of bulk properties of the substrate.

Researchers are attempting to exploit the reactive constituent(s) responsible for a particular surface reaction. At this stage, only limited reaction models have been developed for the atmospheric pressure plasma-substrate interaction, especially quantifying the resultant surface topography in relation to the plasma operation parameters.

2.5   Conclusion

Textile technologists are continuously exploiting the possibilities of dry treatments and processing of textile materials. Low temperature plasma is one of the potential alternatives, especially the atmospheric pressure plasma techniques. The ambient operation condition allows the possibility of scaling up to industrial scale catering for various applications in textile sectors. As the trend, dry treatment using plasma is becoming more and more popular for material design and processing in textile industries. Distinct properties of this technique have been stated in the literature mentioned above. In significant, atmospheric pressure plasma afterglow is milder as compared to direct plasma glow In order to investigate the possibility of development of nano-scale plasma modification of textile materials, atmospheric pressure plasma is used in the present study.

With the aim of manipulating the technique applying to diverse types of textile materials, a fundamental knowledge of the substrate is required. The properties of three different kinds of textile materials including polyester, wool and cotton have been reviewed prior to the application of the technique. This is the foundation of the understanding of the plasma-substrate interaction. Concurrently, the profound knowledge of the plasma is inevitable. Excitation sources and chemistry of plasma were studied prior to all experiments.

In the present study, O_2 was selected as the reactive gases for hydrophilisation of polyester and wool while CF_4 was selected as the reactive gases for hydrophobisation of cotton.

Chapter 3   Plasma systems for polyester substrates

3.1   Introduction

Synthetic polymeric materials with superior mechanical properties and chemical inertness are popular in various industrial sectors. However, synthetic polymers lack surface properties. Originally, substrate with smooth surface can be texturised to offer the improved surface performances such as wettability, adhesion and anti-staticity etc. Atmospheric pressure plasma (APP) treatment becomes a potential alternative for an efficient dry surface processing of textile materials (Kan & Yuen, 2008; Samanta et al., 2009; Šimor et al., 2003; Wang et al., 2008a, b; Zhang & Fang, 2009).

Plasma-surface interaction is a physicochemical reaction. In order to manipulate the process, a polymeric thin film was firstly subjected to the APP treatment. A biaxially-drawn polyethylene terephthalate (PET) film with a homogeneous surface was used to reduce the complexity of studying the plasma-substrate interaction. The film model would yield a better understanding of the formation of a distinctive surface modification corresponding to various operation parameters of an APP treatment. The PET film was subjected to the plasma etching-hydrophilisation using helium and oxygen (He-O$_2$ plasma) generated with a radio frequency using an atmospheric pressure plasma jet (APPJ). This empirical study would assist in the design and control a treatment for actual textile materials. Based on the preliminary study of the film model, the APP treatment was then applied to the textile materials to evaluate the practical application and realisation of industrialisation in textile industry. A polyester fabric was then subjected to the plasma treatment.

In order to obtain the optimum condition to attain nano-scale etching -hydrophilisation of polyester substrates, a number of parameters including 1) treatment time, 2) ignition power, 3) O_2 concentration and 4) jet distance were investigated. The surface properties of the plasma-modified polyester substrates were characterised using the scanning electron microscopy (SEM), static contact angle goniometry, wetted area measurement, X-ray photoelectron spectroscopy (XPS) and Fourier Transform Infrared Spectroscopy - attenuated total internal reflectance (FTIR-ATR).

3.2   Experimental

3.2.1   Materials

PET film

The biaxially-drawn polyethylene terephthalate (PET) film of 0.1mm thickness supplied by the Goodfellow Ltd., Cambridge was used as the substrate. The film was rinsed with acetone (AR grade) and absolute ethanol (AR grade) to remove grease and dirt adhered to the surface during manufacturing. The cleaned film was dried and conditioned under the standard condition of 65±2% relative humidity and 21±1°C for at least 24 hours prior to all experiments.

Polyester fabric

100% plain weave polyester fabric of 188g/m^2 with thickness of 5.04mm supplied by the Yuen Lee Piece Goods was used as the substrate. The fabric was

----

----

washed with 2% non-ionic detergent at pH7 and 40°C for 20min, and subsequently rinsed with deionised water for about 5 min to remove oils and impurities. The scoured, cleaned fabric was tumble-dried and then conditioned under the standard condition of 65±2% relative humidity and 21±1°C for at least 24 hours prior to the experiments

Helium (He, 99.9% purity) and oxygen (O_2, 99.9% purity) were applied as the carrier and reactive gases respectively in the plasma treatment. Distilled water and glycerol (99%, extra pure, PhEur, USA) were used as probing liquids for contact angle goniometry.

3.2.2   Instrumentation

Atmospheric pressure plasma jet (APPJ) manufactured by the Surfx Technologies LLC, CA was used as a downstream atmospheric pressure plasma treatment with substrates being exposed to the plasma afterglow. In this part of study, APPJs Atomflo™ 200 and Atomflo™ 400 were utilised for the plasma treatment of PET film and polyester fabric respectively.

3.2.3   Atmospheric pressure plasma treatment

In the APP treatments of the polyester substrates, He and oxygen O_2 were supplied as carrier and reactive gases respectively. A schematic diagram of the plasma treatment is shown in **Figure 3-1**. Four operation parameters including 1) treatment time, 2) ignition power, 3) O_2 concentration and 4) jet distance were evaluated with respect to the development of a nano-scale etching-hydrophilisation of the polyester substrates.
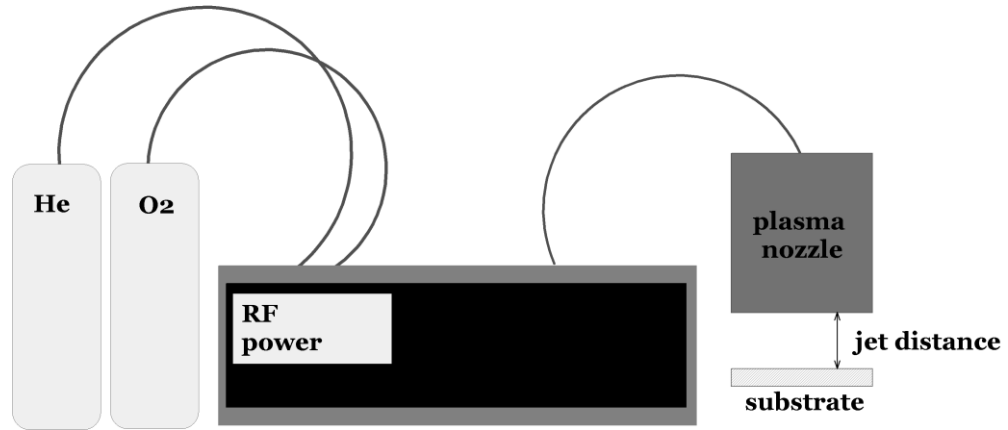
Figure 3-1   A schematic diagram of He-O_2 plasma treatment of polyester substrates

3.2.3.1   PET film

APP treatment of **PET film** model was conducted by an **APPJ (Atomflo™ 200)** with a rectangular nozzle (AH-250L, Surfx Technologies LLC, CA) which covered an active area of 25×1 mm². The nozzle was mounted vertically above the substrate which was moving at a constant speed of 2mm/s exposing to the plasma afterglow generated from the radio frequency of 13.56MHz. The flow rate of He was fixed at 15L/min. The four variable operation parameters are listed in **Table 3-1**. After atmospheric pressure plasma treatment, the PET samples were conditioned at the relative humidity of 65±2% and 21±1°C for at least 24 hours prior to further evaluation.

Table 3-1   Operation parameters studied in the plasma treatment

Operation parameters	Variables
Treatment time (s/mm)	1, 2, 3, 4, 5, 6, 8, 9
Ignition power (W)	60, 70, 80
O_2 concentration (%)	1, 2
Jet distance (mm)	5, 7

3.2.3.2   Polyester fabric

APP treatment of **polyester** was conducted by an **APPJ (Atomflo™ 400)** with a rectangular nozzle **(AH-500L**, Surfx Technologies LLC, CA) which covered an active area of 50×1 mm^2. The nozzle was vertically mounted above the substrate which was moving at a constant speed of 2mm/s exposing to the plasma afterglow generated from the radio frequency of 27.12MHz. The flow rate of He was fixed at 30L/min. The four variable operation parameters are listed in **Table 3-2**. After atmospheric pressure plasma treatment, the polyester samples were conditioned at the relative humidity of 65±2% and 21±1°C for at least 24 hours prior to further evaluation.

Table 3-2   Operation parameters studied in the plasma treatment of polyester fabric

Operation parameters	Variables		
Ignition power (W)	120	150	180
O_2 concentration (%)	0.3, 0.7, 1	1.3, 1.7, 2	2.2, 2.5, 2.8
Treatment time (s/mm)	0.5, 1.5, 2.5		
Jet distance (mm)	3, 5		

3.2.4   Characterisation

3.2.4.1   Scanning electron microscopy (SEM)

Surface topographical feature of the plasma-modified polyester substrates were analysed using a scanning electron microscope (SEM, JSM-6490, JEOL Ltd., Japan). The samples were gold-coated with a sputter coater (SCD005, BAL-TEC, Liechtenstein) prior to SEM analysis. Images of the modified substrates were captured at the magnification of 5,000x, 10,000x and 15,000x with the accelerating voltage of 20kV for the investigation and comparison of the nano-structures formed in the course of the treatment.

3.2.4.2   Contact angle goniometry

Wettability modification of the plasma-modified polyester substrates were characterised by the contact angle goniometry using the sessile drop technique with the aid of a micro-litre dispenser (GS-1200, Gilmont, Barnant Company, US) and a contact angle meter (Tantec Inc., US patent No.5,268,733) according to the standard testing method of ASTM D5946. Two probing liquids including distilled water (72.8mN/m) and glycerol (63.4mN/m) were used and the drop size was 3μL. The recorded contact angle was reported as the average of 10 measurements of an individual sample. The paired comparison t-test was employed to confirm the significant difference of the reported data to be within a confidence level of 95%. Surface energies of the plasma-modified samples were determined using the Kaelble's two-liquid method as referred to the respective **Equations 3-1 and 3-2** (Kaelble, 1970).

$$\gamma_l(1 + \cos\theta) = 2 \cdot [(\gamma_s^p \gamma_l^p)^{1/2} + (\gamma_s^d \gamma_l^d)^{1/2}] \qquad \text{Equation 3-1}$$

$$\gamma_s = \gamma_s^p + \gamma_s^d \qquad \text{Equation 3-2}$$

θ is the static contact angle between the film and the probing liquid

γ_l is the surface tension of the probing liquid

γ_l^p and γ_l^d are the polar and dispersive components of the probing liquid respectively

γ_s is the overall surface energy of the film

γ_s^p and γ_s^d are the polar and dispersive components of the film respectively

3.2.4.3   MATLAB image processing

SEM micrographs of the **plasma-modified PET films** were subjected to image processing using the MATLAB software to predict the formation of nano-structure induced by the atmospheric pressure plasma treatment.

3.2.4.4   X-ray photoelectron spectroscopy (XPS)

The surface chemistry of **PET film** was investigated by the X-ray photoelectron spectroscopy (XPS). XPS was carried out by a SKL-12 spectrometer (Sengyong, China) modified with VG CLAM 4 multi-channel hemispherical analyser equipped with Al/Mg twin anode. The spectrometer was operated with non-monochromatic Mg Kα (1253.6 eV) radiation for the characterisation of the plasma-modified substrate under the vacuum condition of 8 x 10^{-8}Pa. Spectra were analysed using XPSPEAK 4.1.

3.2.4.5   Fourier transform infrared spectroscopy (FTIR-ATR)

Perkin Elmer spectrophotometer (Spectrum 100, Perkin Elmer Ltd.) equipped with a horizontal attenuated total internal reflectance (HATR) accessory was used to analyse the surface chemical composition of the plasma-modified polyester substrates. ZnSe was employed as the ATR crystal. Each FTIR spectrum obtained was an average of 128 scans with a resolution of $4cm^{-1}$.

3.3   Results and discussion

The plasma treatment, using He and O_2 gases, was a physicochemical modification capable of etching-hydrophilisation of the surface of polyester substrates. The modification relied on two main principles, namely physical ablation and chemical etching. Physical ablation was induced by the inert helium bombardment while chemical etching was driven by the reactive oxygen oxidation.

3.3.1   Simulation of PET film model

3.3.1.1   Surface topographical modification

Surface etching is predominantly caused by physical ablation. In addition, surface etching formed a great deal of volatile low molecular weight oxidised fragments (LMWOF) which are easily removed from the substrate surface via sublimation in the open system. Dual reactions simultaneously acting on the substrate elicited a distinctive surface topography. Nano-structures on the plasma-modified PET substrate were revealed using a scanning electron

----

----

microscope (SEM) at the magnification of 15,000x. The original PET film was smooth without distinguishable features on the surface. After exposure to the He-O_2 plasma, the modified PET films were texturised with micro-scale and nano-scale surface structures. Nano-structures included nano-cones and nano-honeycomb structures were developed at different stages of the treatment as illustrated in **Figures 3-2 and 3-3** respectively. Detailed analysis of the relation between the development of surface structure and operation parameters was illustrated in **Section 3.3.1.3**.
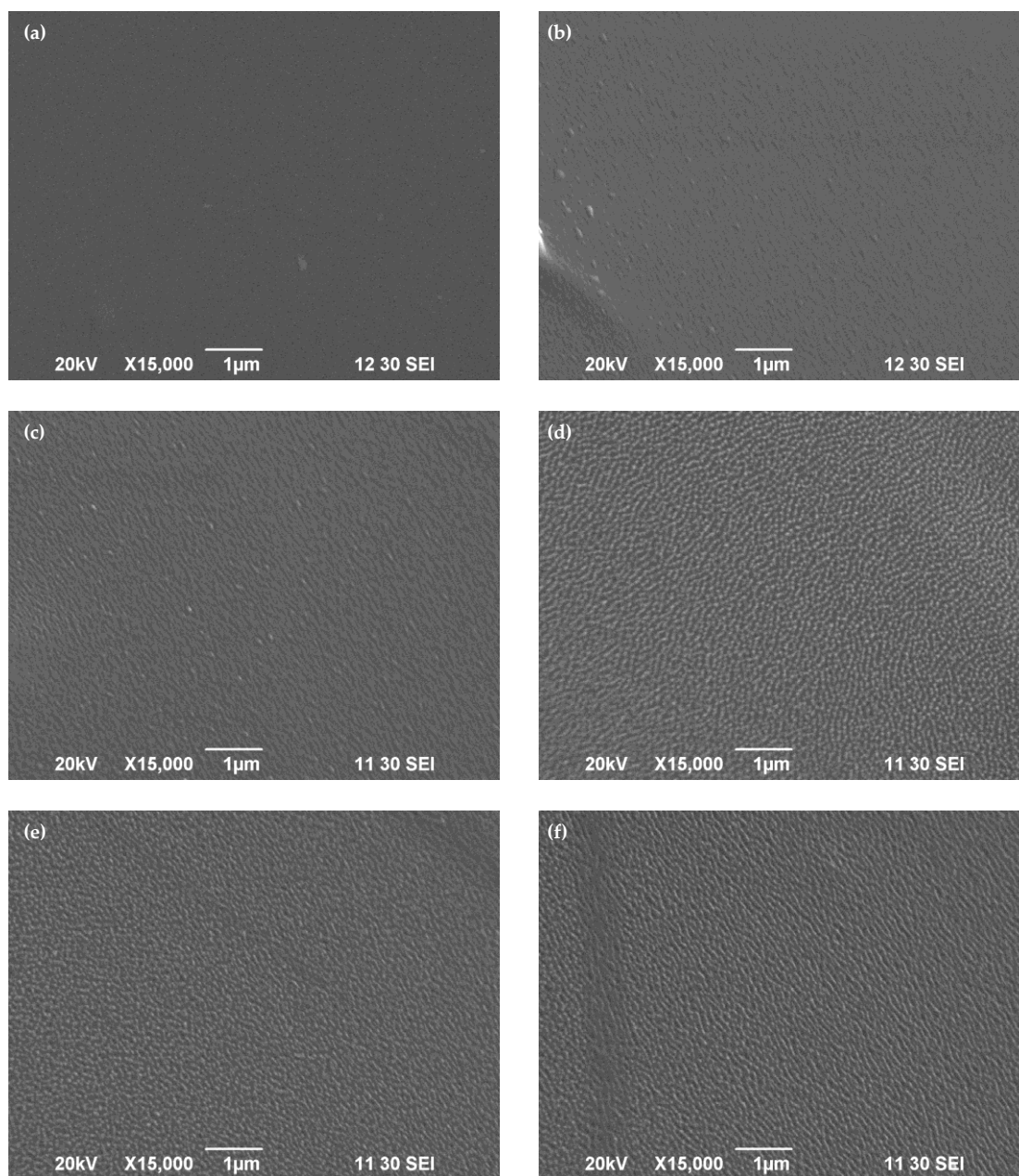
(a)control, (b) 1s/mm exposure, (c) 2s/mm exposure, (d) 3s/mm exposure, (e) 4s/mm exposure, (f) 5s/mm exposure (Constant parameters: 80W, 5mm and 2% O_2)

Figure 3-2   SEM micrographs illustrate a time-dependent nano-bump formation on the surface of PET film exposed to He-O_2 atmospheric pressure plasma (magnification 15,000x, top view)
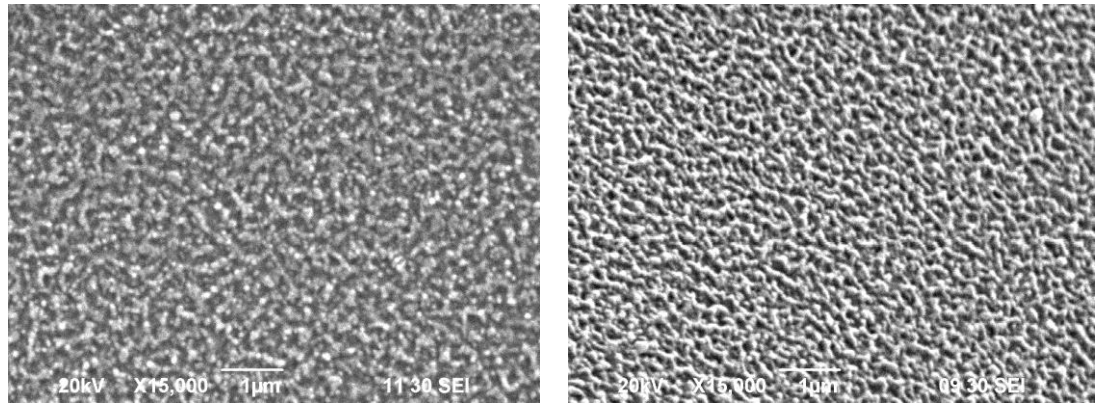
Top view   Side view (45° tilted)

Operation parameters: 60W, 5mm, 8s/mm and 2%O_2

Figure 3-3   SEM micrographs show the nano-porous honeycomb after the prolonged plasma treatment (magnification of 15,000x).

Preferential etching involved in the formation of distinctive surface topography

Plasma-induced surface topographical ablation is a preferential etching. Preferential etching of a substrate surface attributes to the development of a distinctive surface texturisation. Since PET is in polymeric phase, thus different phases react with the plasma etchants at different rates. Amorphous region is more susceptible to plasma etching and will be etched away with respect to the bombardment of active species in the plasma (Borcia et al., 2008; Matthews et al., 2004, Vesel et al., 2008; Wong et al., 2000) and other electromagnetic irradiations (Bahners et al., 1993; Jang & Jeong, 2006; Wong et al., 2000). Nano-cones appeared on the PET film in globular form specifying the drawn nature of the substrate, i.e. biaxially-drawn. Similar to other electromagnetic irradiations and electrical discharges, the plasma-induced surface topographical modification is characterised by the intrinsic properties of a substrate. The modification is controlled by the inherent molecular orientation and the distribution of

----

----

different amorphous-crystalline regions, i.e. drawn ratio and drawn direction. In other words, stress field determines the topography going to be developed in a plasma treatment (Bahners et al., 1993; Gupta et al., 2000; Vesel et al., 2008; Yip et al., 2006).

Characteristic plasma chemistry of the afterglow produced by APPJ

Degree of physical ablation induced by the APP is different from the reduced pressure plasma. Plasma is a complex gaseous mixture of ions, electrons, metabstables, neutrals, photons and radicals. Ion and electron bombardment are responsible for the physical ablation of a substrate. Nano-scale topographical modifications have been achieved under the reduced pressure (Beake et al., 1998a, b; Gupta et al., 2000; Kan & Yuen, 2008; Shin et al., 2008; Vesel et al., 2008; Wong et al., 2000). The composition of plasma is pressure-dependent. With the increasing pressure of the system, the densities of ions and electrons are dramatically diminished. As a result, physical ablation under atmospheric pressure will be less significant as compared to the operations under reduced pressure. In other words, nano-scale etching will be more favourable for the plasma systems operated under atmospheric pressure.

In the experiment, the PET film was exposed to the afterglow plasma produced by the downstream APPJ treatment. In the afterglow of APP using He and O_2 gases, neutral reactive species including ground-state He, ground–state $O(^3P)$, metastables, $O_2(a^1\Delta_g)$, $O_2 (b^1\Sigma_g^+)$ and ozone O_3 are the chief components (Jeong et al., 2000; Schütze et al., 1998). The substrate was hydrophilised via surface oxidation by the active oxygen species. With regard to the neutral

----

----

reactive species detected in the downstream afterglow, a milder physical ablation was confirmed using APPJ.

3.3.1.2   Alteration of surface chemistry

In addition to etching, He-O_2 plasma was competent of hydrophilising the PET substrate. On one hand, physical ablation increased the order of randomness by cleaving polymeric chains into smaller fragments. On the other hand, the oxidation of PET substrate increased surface polarity by introducing more polar carboxylic and hydroxyl derivatives. The plasma-modified substrate possessed improved wettability (Gupta et al., 2000; Ren et al., 2008; Shin & Yoo, et al, 2008).

Contact angle goniometry was employed to evaluate the degree of hydrophilisation of the modified PET film. Contact angles were measured with two polar probing liquids, namely water and glycerol. A reduction of contact angles (ΔCA) was observed. The change was defined as $\Delta CA = (CA_P - CA_o)/CA_o$ where CA_P was the contact angle of the plasma-modified samples and CA_o represented the contact angle of the control. Complementarily, an alteration of the surface energy (γ_s) of the modified film was revealed based on the calculation of Kaelble's two-liquid method (Kaelble, 1970). The calculation expressed the surface energy components, i.e. polar (γ_s^p) and dispersive (γ_s^d) types, clearly as referred to **Figure 3-4**. In significance, a drastic increase of the polar component of the modified film was discovered. The original film possessed low polar surface energy of about 4mN/m. The polar component boosted to more than 15 times, i.e. 60mN/m, after exposure to the plasma for

----

1s/mm. This explained that ΔCA in the goniometry was caused by the polar interaction at the liquid-solid interface.

Another piece of information revealed from the goniometry was that plasma hydrophilisation was the most predominant phenomenon at the initial stage without any significant change of the surface morphology of the film as shown in **Figure 3-4**. The initial increment of the polar type of surface energy at 1s/mm was found to be the most significant. Further increasing the treatment time did not show significant effect on the enhancement of the surface wettability. Moreover, the plasma-modified PET film did not show complete wetting in the probing liquids with respect to the operation parameters being studied.
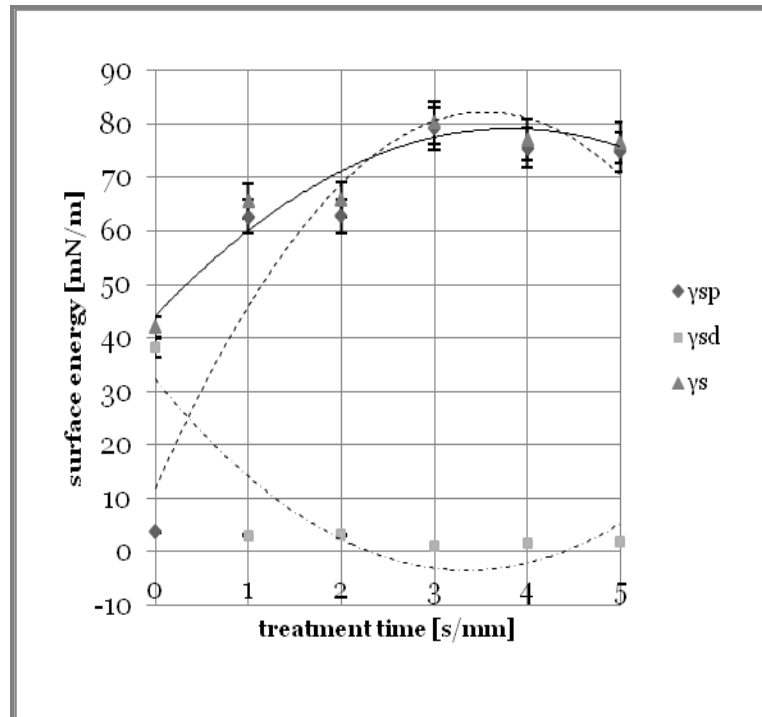
(Constant parameters: 80W, 5 mm and 2% O_2)

γ_s is the overall surface energy of the film. γ_s^p and γ_s^d are polar and dispersive components of the film respectively.

Figure 3-4   Time-dependent variation of surface energy and the respective components of the plasma-modified PET film

----

In order to confirm the physical experimental results obtained from the contact angle goniometry, XPS was conducted to evaluate the surface chemical composition of the plasma-modified PET films. The original PET film was composed of three elements, namely carbon (C), oxygen (O) and silicone (Si), with reference to **Figure 3-5**. Since the particulate Si surface additives were incorporated in the production of polymeric PET films (Beake et al., 1998a, b), thus a trace amount of Si present in the original PET film was formed.
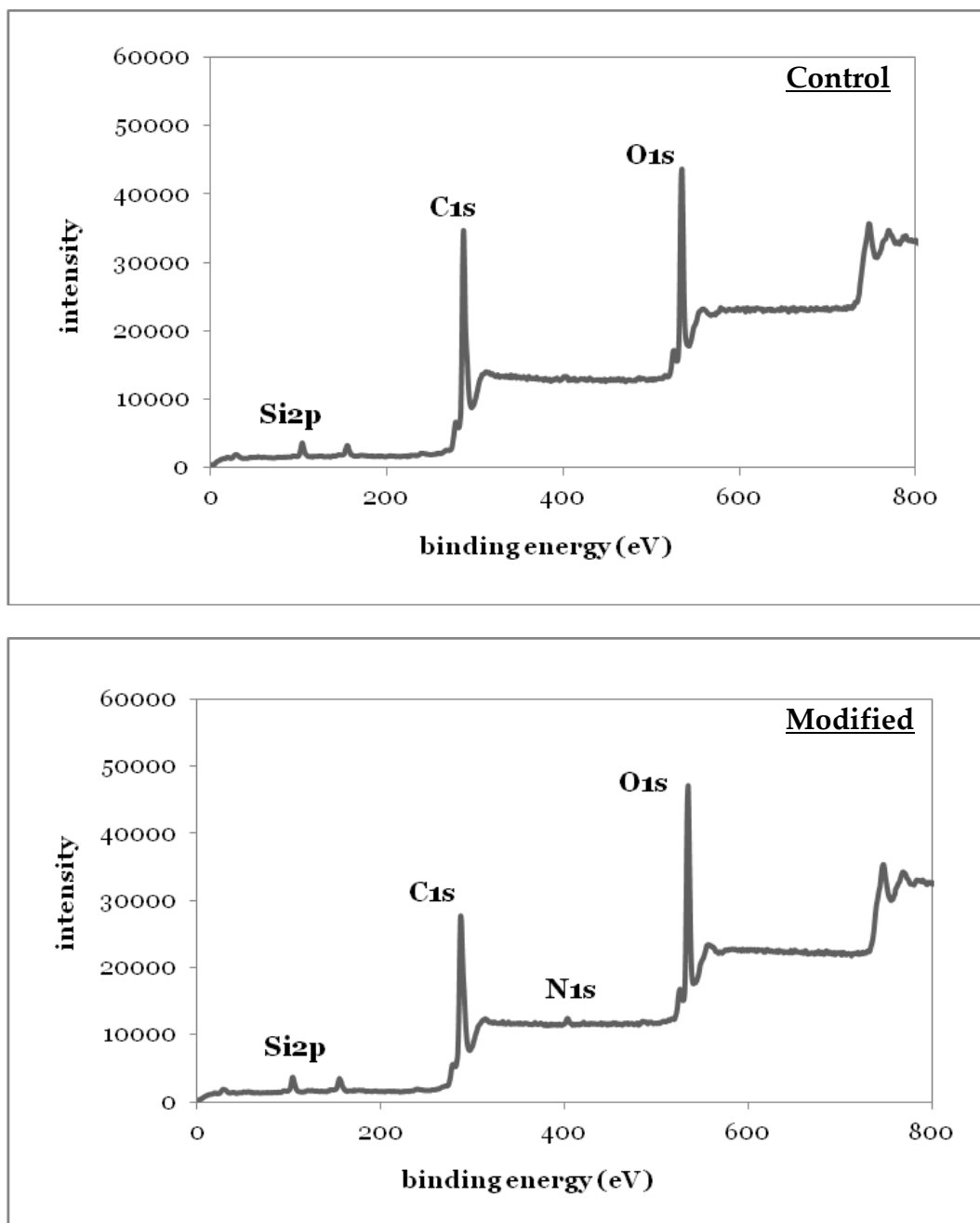
(Constant parameters: 80W, 2%O_2, 5mm and 5s/mm)

Figure 3-5   Surface elementary composition of He-O_2 plasma-modified PET films

----

The nature of He-O$_2$ plasma is oxidative. The result of XPS indicated an increase in O content and a reduction in C content of the plasma-modified PET film as presented in **Table 3-3**. The ratio of O and C atomic content (O/C ratio) was an indicator of the surface polarity of a substrate. This ratio indicated the relative quantity of polar O-containing functionalities present on the substrate surface. The higher the O/C ratio, the more the hydrophilicity of a substrate surface will be. The O/C ratio of the original PET so obtained was **0.5**. The He-O$_2$ atmospheric pressure plasma incorporated an additional O into the substrate via surface oxidation. The O/C ratio of the plasma-modified substrate was increased up to **>0.6**. In general, O-containing functional groups being hydrophilic and having a strong affinity towards polar wetting agents are essential to determine surface wettability. Simultaneously, a small amount of N detected on the modified films was proposed to be grafted under ambient condition. Polar N-containing functional groups also contributed to the increment of surface wettability. Additional polar functionalities incorporated on the substrate surface indicated that APP treatment would further assist in the wet processing of textile materials. The XPS results confirmed the physical phenomenon observed in the contact angle goniometry.

The exact surface composition of the modified films was evaluated by the deconvolution of individual elemental peak via XPSpeak4 software. Deconvulation of PET films revealed that C$_{1s}$ atomic peak was assigned to be C-H, C-O and C=O bonds as shown in **Figure 3-6**. No new bonds were detected in the present study. However the atomic content of individual bonds varied with the plasma operation parameters.

Table 3-3   Surface elementary composition of the He-O_2 plasma-modified PET film

	C	O	N	O/C
Control film	0.64	0.32	N/A	**0.50**
Modified film	0.58	0.36	**0.02**	**0.62**

(Treatment parameters: 80W, 2%O_2, 5mm and 5s/mm)
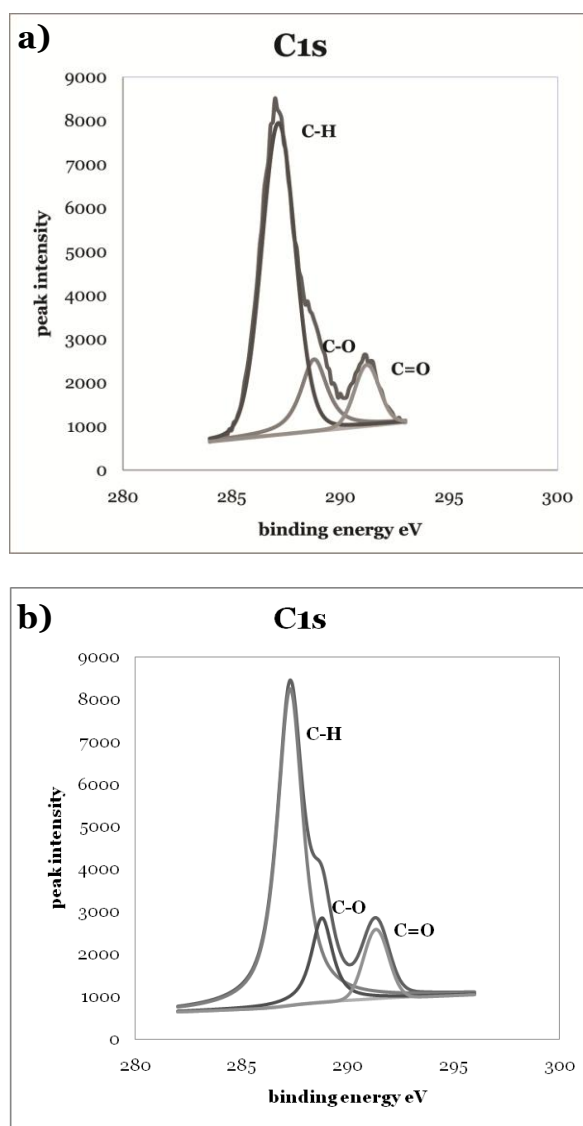
(Constant parameters: 80W, 2%O_2, 5mm and 5s/mm)

Figure 3-6   XPS deconvoluted C_{1s} peak of a) control film and
b) plasma-modified PET film using XPSPeak4 software.
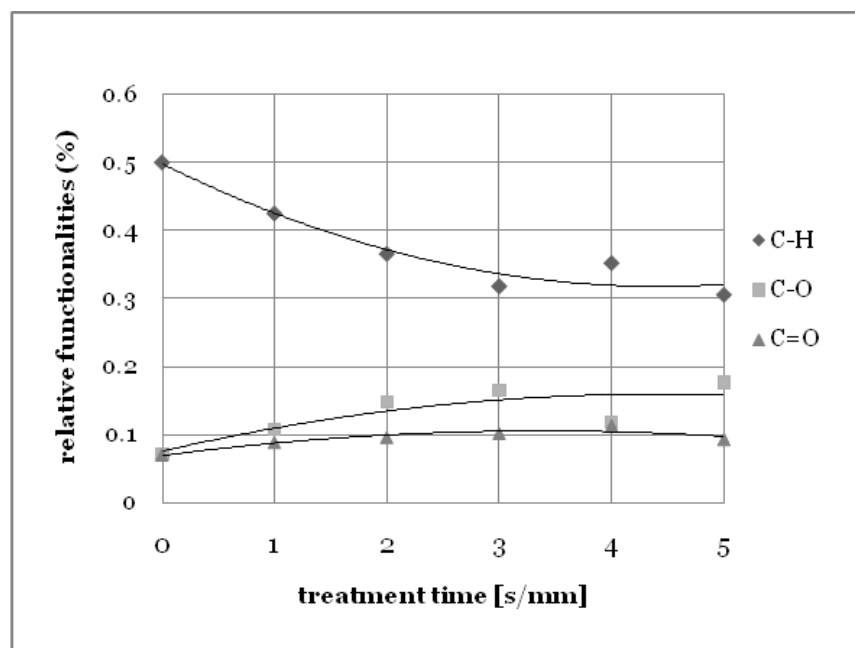
(Constant parameters: 80W, 5 mm and 2% O_2)

Figure 3-7   Time-dependent surface functionalities of plasma-modified PET
film determined by the deconvolution of C_{1s} peak

With reference to **Figure 3-7**, the concentration of individual surface functionalities was found to be time-dependent. With respect to the deconvolution of C_{1s} peak, C-H was found to be reducing with treatment time while C-O and C=O were increasing with time. This opposite trend in relation to treatment time indicated that the plasma hydrophilisation was a progressive and continuous reaction via surface oxidation. **Figure 3-7** illustrates the deconvolution analysis of XPS data complied with the variation of polar and dispersive components of surface energy of the plasma-modified films.

Deconvolution analysis of C_{1s} peak indicated the reaction mechanism of surface hydrophilisation of the substrate. He-O_2 plasma induced surface oxidation predominantly in 1 to 3s/mm treatment. A C-H reduction with a C-O increment indicated that oxidation occurred at the ethylene units of the PET

----

polymer chains. The increased C-O bonds improved the surface polarity of the plasma-modified PET films. After the optimum point, i.e. **3s/mm**, C-H content increased while C-O reduced. When exceeding the optimum point, the change of individual functionality was saturated with time. This indicated that the equilibrium between etching and oxidation had reached.

3.3.1.3   Nano-scale etching-hydrophilisation in relation to individual plasma parameters

In the course of plasma treatment, the surface topography and chemistry varied with the four operation parameters including 1) treatment time, 2) ignition power, 3) O_2 concentration and 4) jet distance. Plasma modification was a progressive reaction with respect to the concentration of plasma active species on the PET surface. Time was required to accumulate sufficient amount of active species on the substrate for the reaction. This variation was an indicator representing the equilibrium shifting between the physical ablation and chemical etching in the plasma treatment. Variation with respect to two interactive parameters, namely ignition power and O_2 concentration, determined the stability and effective energy content of the plasma gaseous admixture. The jet distance representing the proximity of the nozzle to the substrate surface demonstrated how the effective transfer and accumulation of the active species could affect the overall surface etching-hydrophilisation reaction.

3.3.1.3.1 Variation of surface properties with treatment time

Plasma modification is a progressive reaction with respect to the concentration of plasma active species present on the substrate surface. Time is required to accumulate a sufficient amount of the active species on the substrate for the reaction. Surface topographical modification was found to be time-dependent. Under the operation of 80W plasma with 2% O_2 at 5mm-jet distance, a progressive topographical alteration was illustrated in the SEM images as shown in **Figure 3-2**. The degree of etching was expressed in terms of the surface structure density, i.e. number of surface structures per unit area μm^2 in a SEM micrograph.

For the 1s/mm of exposure, plasma only induced the elongated micro-bumps of **125 to 185nm** (expressed as the longer diameter of the bump) on the PET film. When exposed to the plasma for 2s/mm, the size of the micro-bumps reduced to 99 to 150nm. The density of micro-bumps per unit micro-area was found to be ranging from 10 to 15/μm^2. It was obvious that insufficient treatment time of 1 to 2s/mm was not able to generate nano-structures as shown in **Figure 3-2**. However, surface energy increased rapidly by almost 15 times within an instant exposure to plasma. The enhancement in wettability of the modified PET film was mainly due to the increase in the polar functionalities of the substrate surface with reference to the characterisation of contact angle goniometry as illustrated in **Figure 3-4.** At the initial stage, i.e. within 1 to 2s/mm, chemical etching was predominant versus physical ablation. Surface wettability increased without any nano-structure being formed.

After 3s/mm of exposure, appreciable amounts of round nano-cones were developed on the surface. The dimension of the surface structures induced by plasma reduced with time. The diameter of the majority of nano-cones formed on the modified PET films was in nano-scale ranging from **60 to 99nm**. The density of surface structures was amplified by up to 9 times. The density of nano-structures with a maximum of **85 to 90/μm²** was achieved at 3s/mm in response to the highest surface energy of **84mN/m** attained using 80W at 5mm-distance of treatment.

Further exposure to plasma for 4 and 5s/mm, the white dots representing the nano-cones were more standout from the surface in terms of colour contrast with respect to the dark background. This indicated that the height of the nano-cones increased with the plasma treatment time. Simultaneously, the nano-cones started to merge to form the elongated micro-ridges. The dimension of the surface structure began to increase after the optimum treatment time of 3s/mm. The plasma reaction was actually a cascade process via the radical-initiated chain reaction. The density of nano-structure formed was reduced with time after achieving a maximum value at 3s/mm, indicating that plasma would ablate the newly formed nano-structures and polar LMWOF. 3s/mm of exposure was found to be the optimum treatment time in the present study.

The accumulated active plasma species continuously ablated the modified surface and the newly formed polar LMWOF were being etched away with treatment time. As a result, the density of nano-cones did not increase with treatment time in the course of continuous treatment. The formation of

----

nano-structures was found to be in a quadratic relationship with treatment time and appropriate plasma parameters as illustrated in **Figure 3-8.**
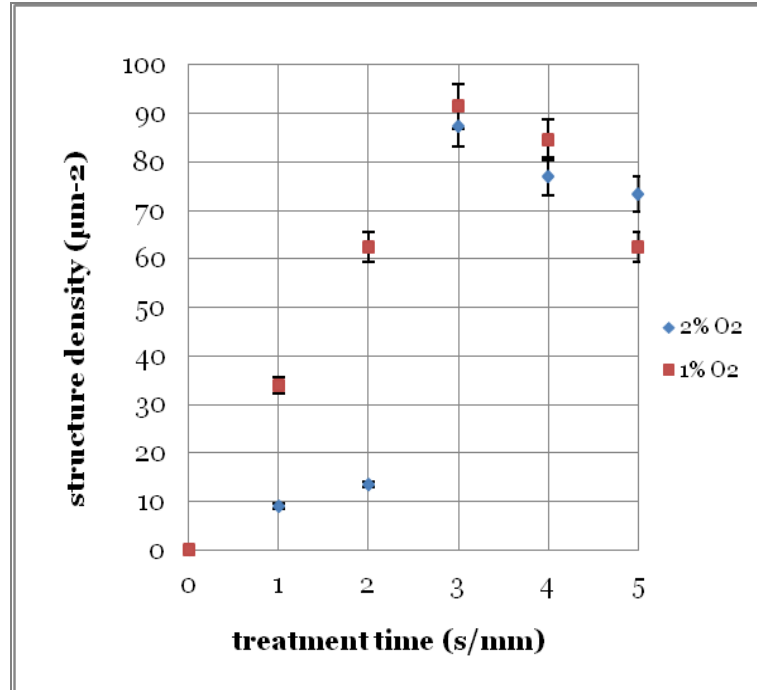
(Constant parameters: 80W and 5 mm)

Figure 3-8   Time-dependent surface structure density of the plasma-modified PET film with respect to different O_2 concentration of plasma

Differentiated from the physical ablation of the substrate, surface hydrophilisation was found to be directly proportional to treatment time using the optimal operation power and reactive gas concentration. Based on the calculation of $\Delta(O/C)$ from the XPS data, the increment of O/C with respect to treatment time was found to be in a linear relationship using 80W plasma with 2% O_2 at 5mm-jet distance. Increasing treatment time would promote surface hydrophilisation of PET substrate as shown in **Figure 3-9**.
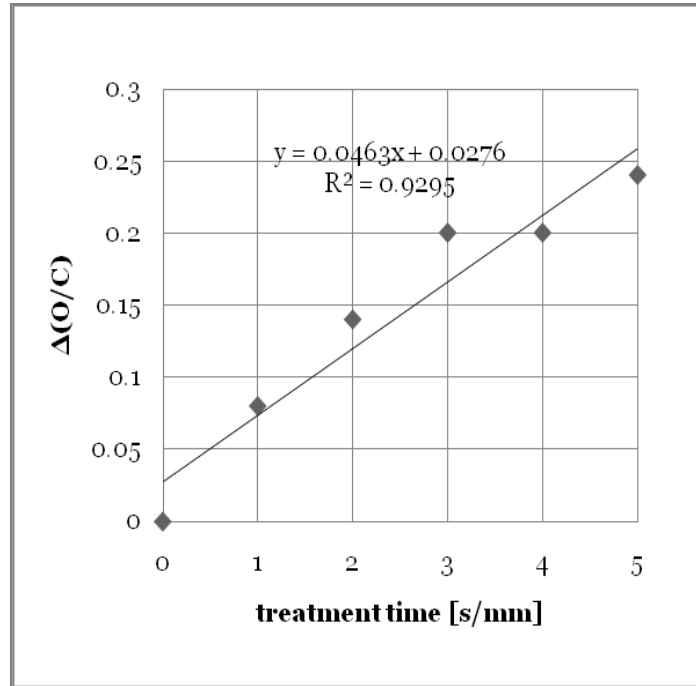
(Constant parameters: 80W; 5 mm and 2%O_2)

Figure 3-9   Time-dependent plasma hydrophilisation of PET substrate with
linear relationship

In order to evaluate the effect of prolonged exposure to plasma imposed on the substrate, 60W-plasma operating with 2% O_2 at 5mm-jet distance was employed instead of using 80W-plasma. A weaker 60W-plasma was used to minimise thermal degradation of the substrate. At a high ignition power, thermal degradation of the substrate was induced leading to the alteration of the bulk which was undesirable.

Prolonged exposure, i.e. 8s/mm, to active plasma gas would generate a distinctive nano-scale honeycomb structure as shown in **Figure 3-3**. Physical ablation which was a cascade process became predominant with an appreciable amount of the accumulated active species continuously etching the surface via the radical-initiated chain reaction. Active plasma species ablated the newly

----

formed plasma-induced nano-structures and penetrated into the sub-surface, resulting in the formation of porous nano-honeycomb topography. When the contact angle goniometry of the modified film was performed, spreading of probing liquids on the plasma-modified film was observed. It was probably due to the fact that the spreading was induced by the diffusion of liquids into the porous sub-surface of the modified film via the voids present in the honeycomb structure.

The degree of ablation was depicted by both the variation of the density of nano-structures and dispersive surface energy of the modified substrate. Dispersive surface energy symbolised the plasma-induced chain scission on the film surface. This energy constantly remained at a low value during the plasma treatment of 1 to 8s/mm in **Figure 3-10** indicated that the plasma-induced etching would not impose severe degradation of the bulk polymer film.
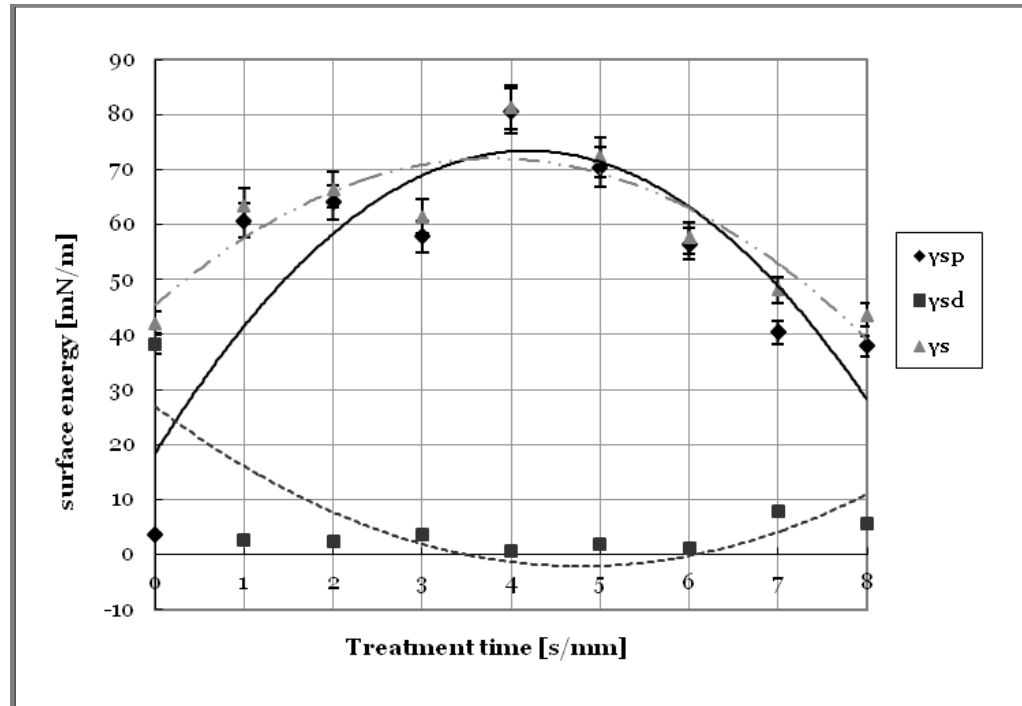
(Constant parameters: 60W, 5 mm, and 2% O_2)

γ_s is the overall surface energy of the film.

γ_s^p and γ_s^d are polar and dispersive components of the film respectively.

Figure 3-10   Time-dependent variation of surface energy
and the respective components of the plasma-modified PET film

3.3.1.3.2   Variation of surface properties with ignition power and O_2 concentration

Ignition power is a direct control of the plasma power in a plasma discharge. A higher ignition power would be capable of attaining nano-cones at a higher rate as the plasma active species possesses higher energy when bombarding the substrate. Physical ablation was comparatively more rapid at 70W to 80W than at 60W. During the study duration of 1 to 5s/mm, 60W was not able to induce the observable nano-structures of the PET film subjected to 2% O_2 plasma at a jet distance of 5mm. In contrast, both 70W and 80W counterparts generated some distinctive nano-cones within 3s/mm of exposure.

Ignition power did play an important role at the initial stage of the nano-cone formation. There was no significant change in the dimension and density of nano-cones in the course of the treatment once the nano-structures were formed. Likewise, the surface energy of the plasma-modified PET film demonstrated a similar relationship between the nano-cone density and ignition power. This indicated that ignition power was the prime driving force for both the physical ablation and chemical etching.

The effect of ignition power on the surface chemistry was investigated by XPS. The degree of hydrophilisation was presented as the variation of O/C ratio of the modified films. The change was expressed in terms of Δ(O/C) which was the increment of the ratio of O/C of the modified fabrics (($O/C)_P$) against the control fabrics (($O/C)_o$) as illustrated in **Equation 3-3**.

$$\Delta(O/C) = \frac{(O/C)_P - (O/C)_o}{(O/C)_o} \qquad \text{Equation 3-3}$$

Increasing the ignition power could promote the surface hydrophilisation of PET substrate as shown in **Table 3-4**. It was obvious that the O/C ratio increased with ignition power. A higher ignition power was capable of producing more active species, resulting in a higher concentration of He and O active species present in the plasma afterglow. As a result, both the etching and oxidation reactions were more effective using a larger ignition power. Based on the calculation of Δ(O/C), the increment of O/C with respect to ignition power was in a linear relationship using the optimal 80W-plasma with $2\%O_2$ at 5mm-jet distance.

Table 3-4   The alteration of O/C atomic ratio with respect to ignition power

Ignition power (W)	C	O	O/C	Δ(O/C)
Control	0.64	0.32	0.50	**0**
60	0.61	0.33	0.53	**+0.06**
70	0.59	0.34	0.57	**+0.14**
80	0.58	0.36	0.62	**+0.24**

Positive value represents the increase of Δ(O/C) with respect to the control sample. (Constant parameters: 80W, 2% O_2 and 5s/mm)

In general, higher O_2 concentration should be able to incorporate more polar functionalities into the substrate. However, the experimental results obtained were contradictory, which could be explained by the plasma chemistry. It was anticipated that O active species were not directly formed by the electrical discharge in the APPJ. On the contrary, O active species were generated mainly by Penning reaction with He metastables (Jeong et al., 2000; Schütze et al., 2000). It was believed that higher O_2 concentration would consume more He metastables. As a result, the reduced concentration of He metastables consequentially hindered the production of O active species. The experimental results did support the above proposed explanation. When taking 80W-plasma as an example, the density of nano-cones observed on the modified substrate treated by 1% O_2 plasma was found to be higher than that modified by 2% O_2 plasma as shown in **Figure 3-8**. Simultaneously, the improvement of surface energy of the substrate modified with 1% O_2 was found to be greater than that with 2% O_2 plasma as illustrated in **Figure 3-11**. As a result, 1% O_2 plasma was found to be comparatively effective for etching-hydrophilisation.
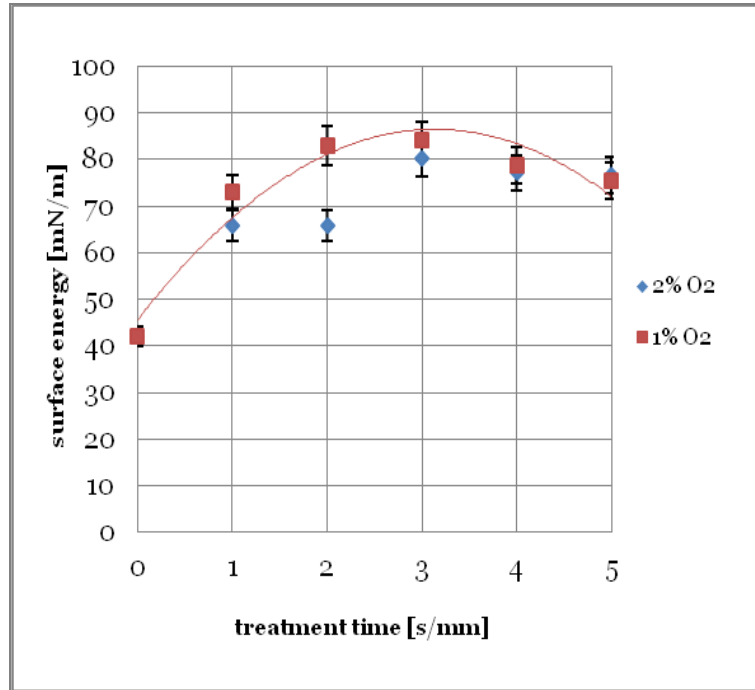
(Constant parameters: 80W and 5 mm)

Figure 3-11   Time-dependent plasma hydrophilisation of PET film with respect
to different O_2 concentration of plasma

The ignition power and the ratio of O_2 to He not just affected the etching-hydrophilisation power, but also determined the stability of the plasma. Plasma was suggested to be more stable when operated at a higher ignition power and a lower O_2 concentration. Under a given ignition power, a lower O_2 concentration used in the plasma offered a more stable plasma modification of the substrate. As referred to **Figures 3-12 and 3-13**, both the nano-spot density and surface energy gave a coherent quadratic relationship with the treatment time using 1% O_2 plasma at 80W. The coherence was proposed as an indicator of the plasma stability. The quadratic relationship deviated when lower ignition power and higher percentage of O_2 were used in the treatment. Although 70W induced an appreciable amount of nano-cones similar to that of 80W, the correlation was deviated from the quadratic relationship. Reducing ignition

----

power at a given O_2 concentration could not provide sufficient energy for the formation of stable plasma for surface etching. The stability of plasma generated was the prime attribute for the experimental design and prediction of the resultant modification.
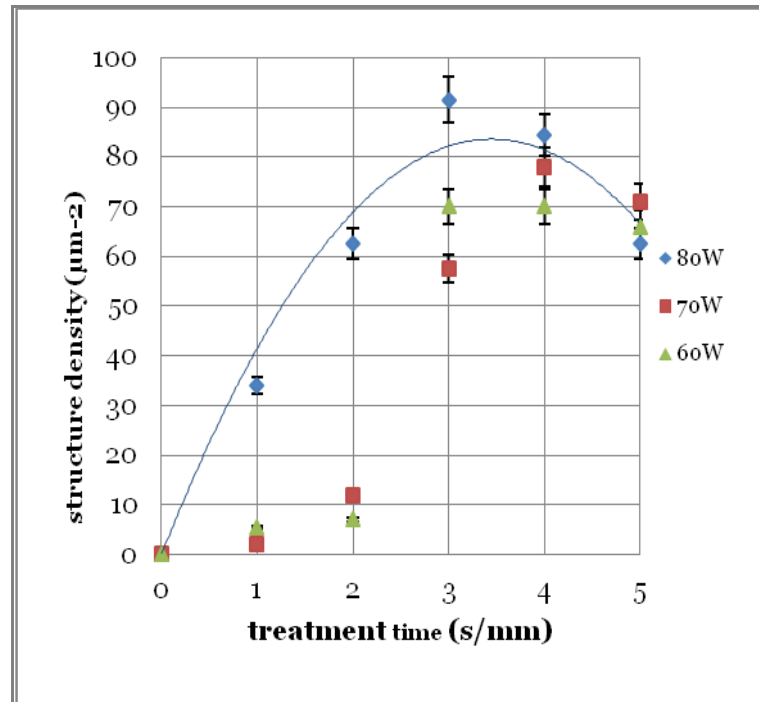
(Constant parameters: 5 mm and 1% O_2)

Figure 3-12   Coherent time-dependent variation of surface structure density of the plasma-modified PET film
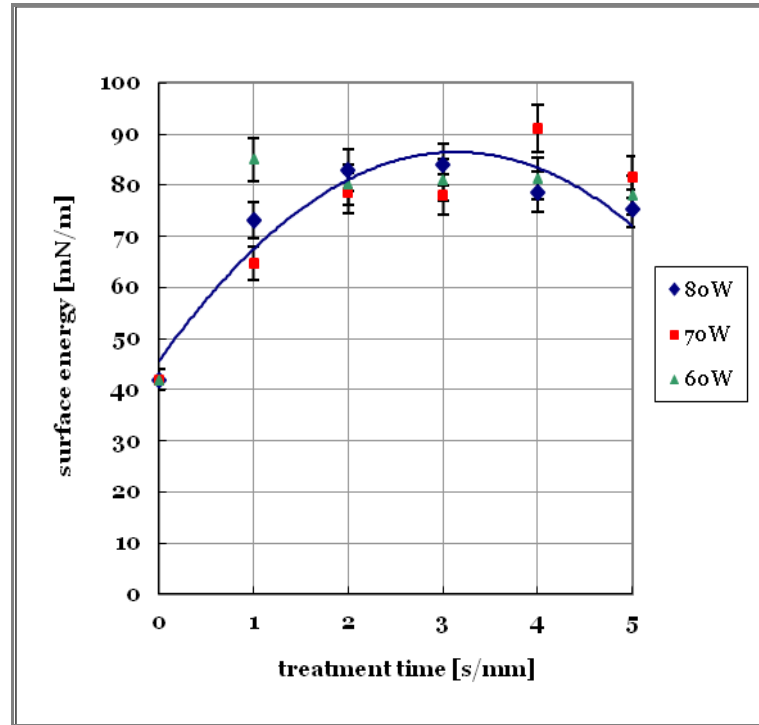
(Constant parameters: 5 mm and 1% O_2)

Figure 3-13   Coherent time-dependent variation of surface energy of the plasma-modified PET film

3.3.1.3.3   Variation of surface properties with jet distance

APPJ was a downstream treatment. Jet distance was the perpendicular distance between the plasma nozzle and the substrate located below as shown in **Figure 3-1**. In the experiment, the jet distance of 5mm and 7mm were studied respectively. The non-porous PET film inherently possessing a low glass transition temperature Tg of ~80°C with poor heat dispersion could not withstand a low jet distance of <5mm. A close proximity to the plasma nozzle would induce glass transition on the substrate and hence alter the bulk properties as the nozzle was heated up to almost 100°C during the treatment.

An appropriate proximity between the plasma source and the substrate affected the efficacy of the active species when etching a surface. In the APP treatment, the active plasma species experienced a severe collision with air molecules when travelling towards the substrate surface. Velocity and energy content decreased with respect to the time and distance transported. The initial formation rate of nano-structure at 5mm was almost 7 times of that modified at 7mm as referred to **Figure 3-14**. As a result, 5mm-plasma treatment was more effective and efficient in attaining the nano-structures.
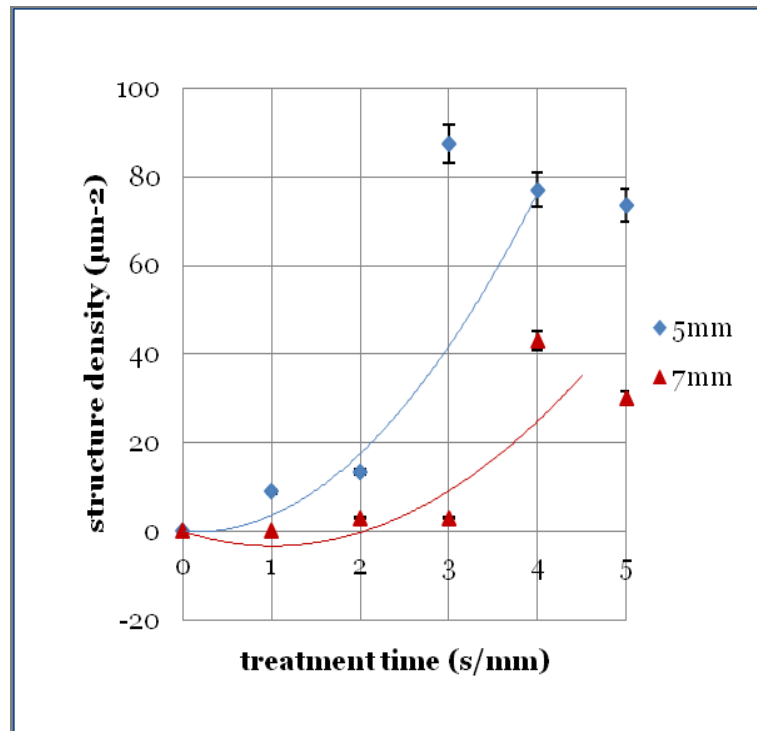
(Constant parameters: 80W and 2% O_2)

Figure 3-14   Time-dependent nano-cone density of the plasma-modified PET film with jet distance

----

The amount of additional O incorporated into the substrate surface was also found to be distance-dependent. A closer proximity allowed effective energy transfer from the plasma active species to the polymeric substrate surface. As a result, 5mm jet distance could achieve the largest increment in O/C ratio of +0.24 as compared to the other two counterparts shown in **Table 3-5.**

Table 3-5   The alteration of O/C atomic ratio with respect to jet distance

Jet distance (mm)	C	O	O/C	Δ(O/C)
Control	0.64	0.32	0.50	**0**
5	0.58	0.36	0.62	**+0.24**
6	0.60	0.34	0.56	**+0.12**
7	0.60	0.34	0.58	**+0.16**

Positive value of represents the increase of Δ(O/C) with respect to the control sample. (Constant parameters: 80W, 2% O_2 and 5s/mm)

3.3.1.4   Imaging prediction of plasma-substrate interaction

MATLAB image processing

SEM micrographs were subjected to image processing using the MATLAB software to predict the formation of surface structures induced by the atmospheric pressure plasma treatment with respect to various plasma parameters. This software predicted the formation of surface structures of a substrate based on the colour contrast of the micrographs captured. The structure density was quantified in terms of the number of surface structures

(black spots) per unit area of the plasma-modified PET film (white background) as illustrated in **Figure 3-15**. The structure density was expressed in terms of image level and NK.

SEM micrographs   **MATLAB processed images**
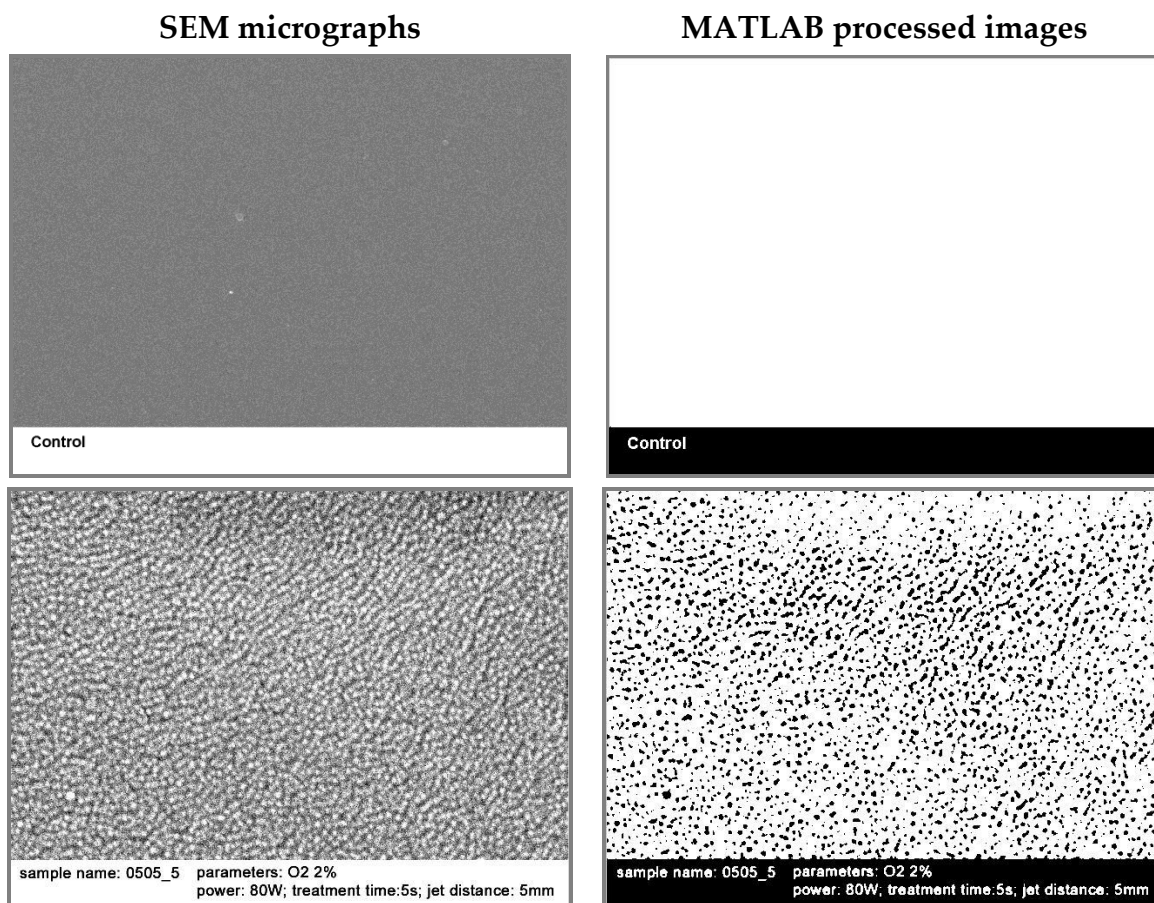
Figure 3-15   Images of the plasma-modified PET films processed via
SEM-MATLAB image processing

Image level indicated the overall colour gradient of the micrograph. Taking grey colour as the reference point, i.e. the value of 0, the whiter the image, the more the positive value of image level would be obtained. On the contrary, the darker the image, the more the negative value of image level would be attained. In **Figure 3-16**, the image level of the plasma-modified PET samples was decreasing with treatment time. NK represented the number of black spots at a defined image level of an image, i.e. NK was proportional to the number of surface structure of the plasma-modified film. In **Figure 3-17**, MATLAB imaging predicted that the quantity of surface structures was increasing with time and ignition power in general. The MATLAB image processing compiled with the SEM micrographs obtained.
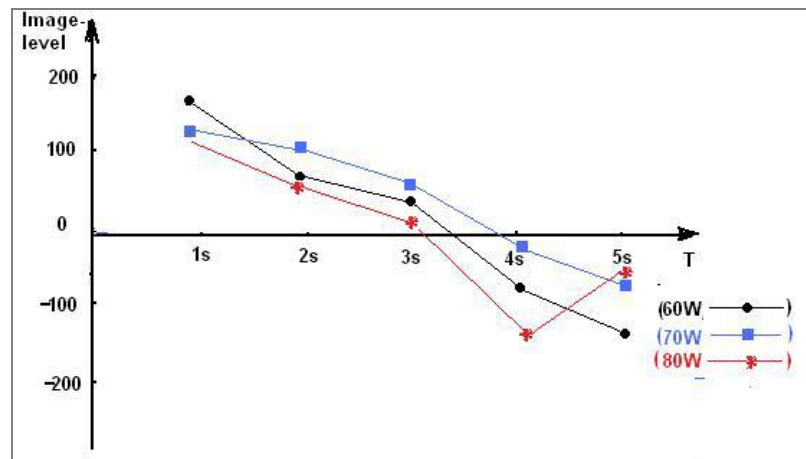
Figure 3-16   MATLAB imaging prediction of the plasma-modified PET film
with respect to different ignition power based on image level

----
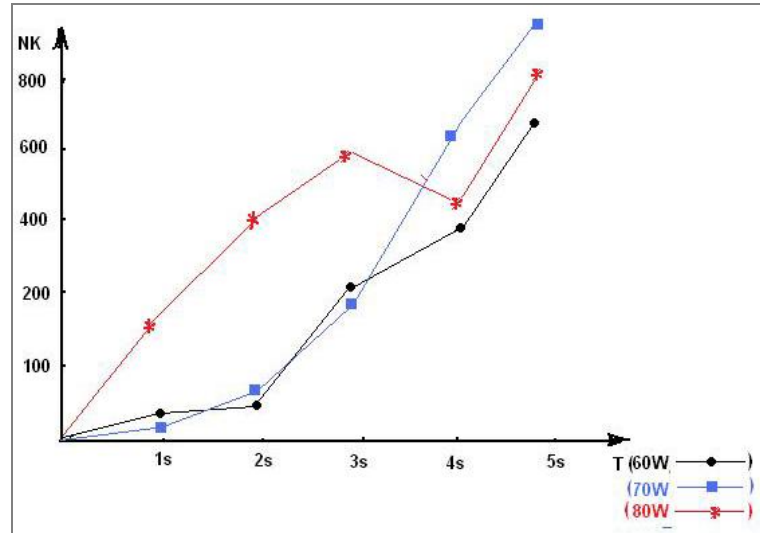
Figure 3-17   MATLAB imaging prediction of plasma-modified PET film with
respect to different ignition power based on NK value

With the assistance of image processing, an empirical trend of the plasma-substrate interaction was achieved. This concurred with the etching mechanism of plasma proposed, i.e. plasma etching was a progressive reaction. The degree of plasma etching was predicted to be proportional to time and ignition power of the plasma system.

SEM-MATLAB image processing would be a quick tool to quantify the degree of surface etching of APP treatment. As a matter of fact, coupling these two techniques offered several advantages. Firstly, SEM micrographs of the modified-substrates could be obtained with simple sample preparation and quick detection. Sample size required for SEM analysis was so small that it would condense the time for sample treatment in laboratory scale. This would reduce the expenditure of time suitable for the preliminary treatment prediction and simulation. Furthermore, SEM inherently in grey scale facilitated sequentially the image processing of MATLAB based on the grey colour

----

gradient. Coupling SEM with MATLAB would allow a relatively more reliable quantification of the surface structures as compared to manual counting of the number of structures induced.

However, prediction using MATLAB may have certain defects and limitations as it only predicts surface structures based on the colour contrast of the SEM micrographs. Capturing a SEM micrograph with appropriate colour contrast would be determined. Simultaneously, the choice of the appropriate reference point during processing is influential as it will affect the resulting image level and NK value. The image processing requires skillful and experienced technologists. In addition, the colour background ought to be uniform for comparison between different samples. Non-uniform coloured background would affect the result of image level i.e. the choice of probing location of sample using SEM would be essential to affect the sequential MATLAB processing. Besides, MATLAB is not able to quantify the dimension of the structures. Further image processing is needed to determine the scale of an etching modification.

3.3.2   Application of polyester fabrics

With reference to the film model, He-O_2 atmospheric pressure plasma was applied to a polyester fabric to evaluate the plasma-substrate interaction during etching-hydrophilisation. The surface properties of the modified fabric were quantified thoroughly.

3.3.2.1   Surface topographical modification

When the polyester fabric was subjected to the plasma afterglow for a few seconds, an alteration of surface topography was observed using SEM. The SEM micrographs showed an observable surface roughening of individual polyester fibres. The original polyester fibre had smooth surface without distinguishable surface topography as shown in **Figure 3-18**. Plasma etching induced surface features to this synthetic filament. Micro-granules and nano-grooves were observed under SEM using different parameters at the magnification of 10,000x as referred to **Figures 3-19** and **3-20**.
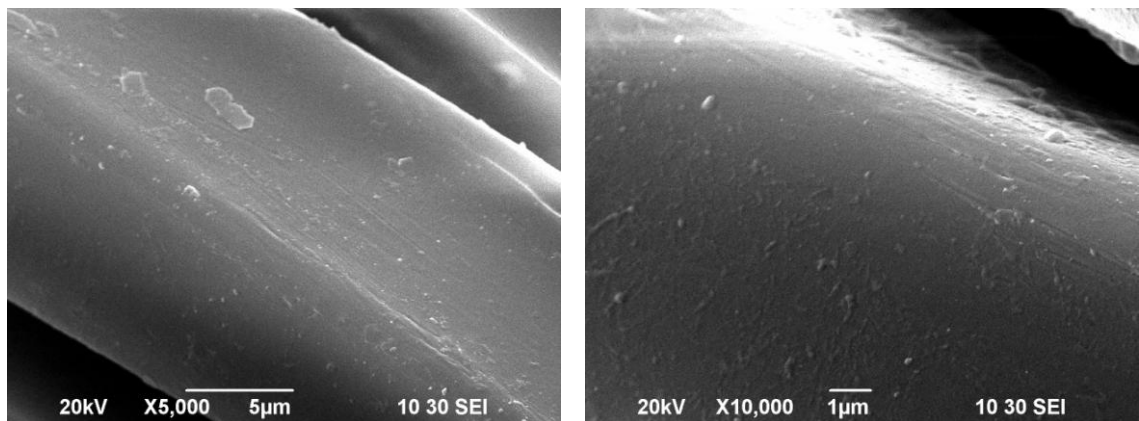
Left: magnification of 5,000X; Right: magnification of 10,000x

Figure 3-18   SEM micrographs of the original polyester fibre

----
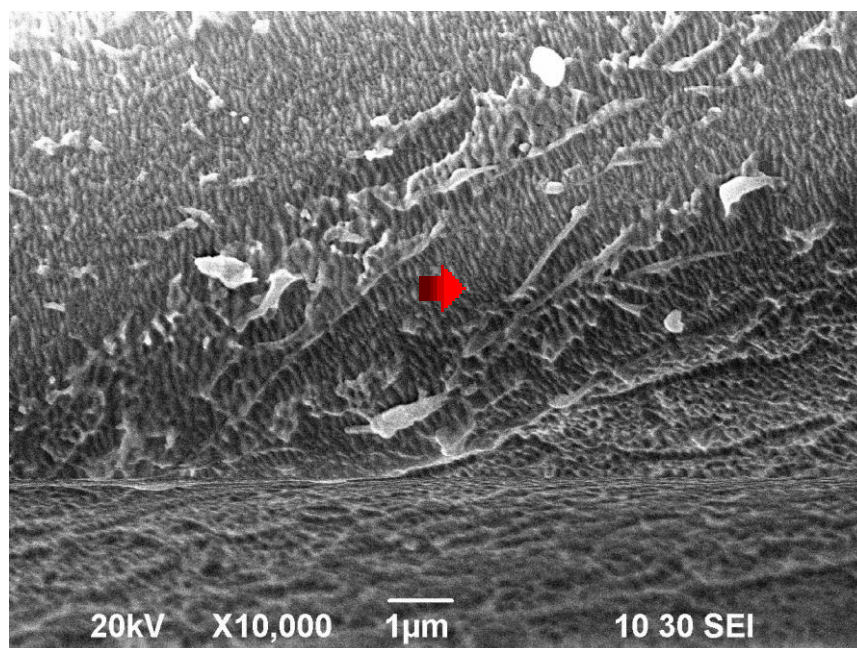
(Constant parameters: 180W, 2.5% O_2, 3mm and 2s/mm)

Figure 3-19   Nano-grooves developed on the polyester fibre perpendicular to the fibre axis under SEM at the magnification of 10,000x

----
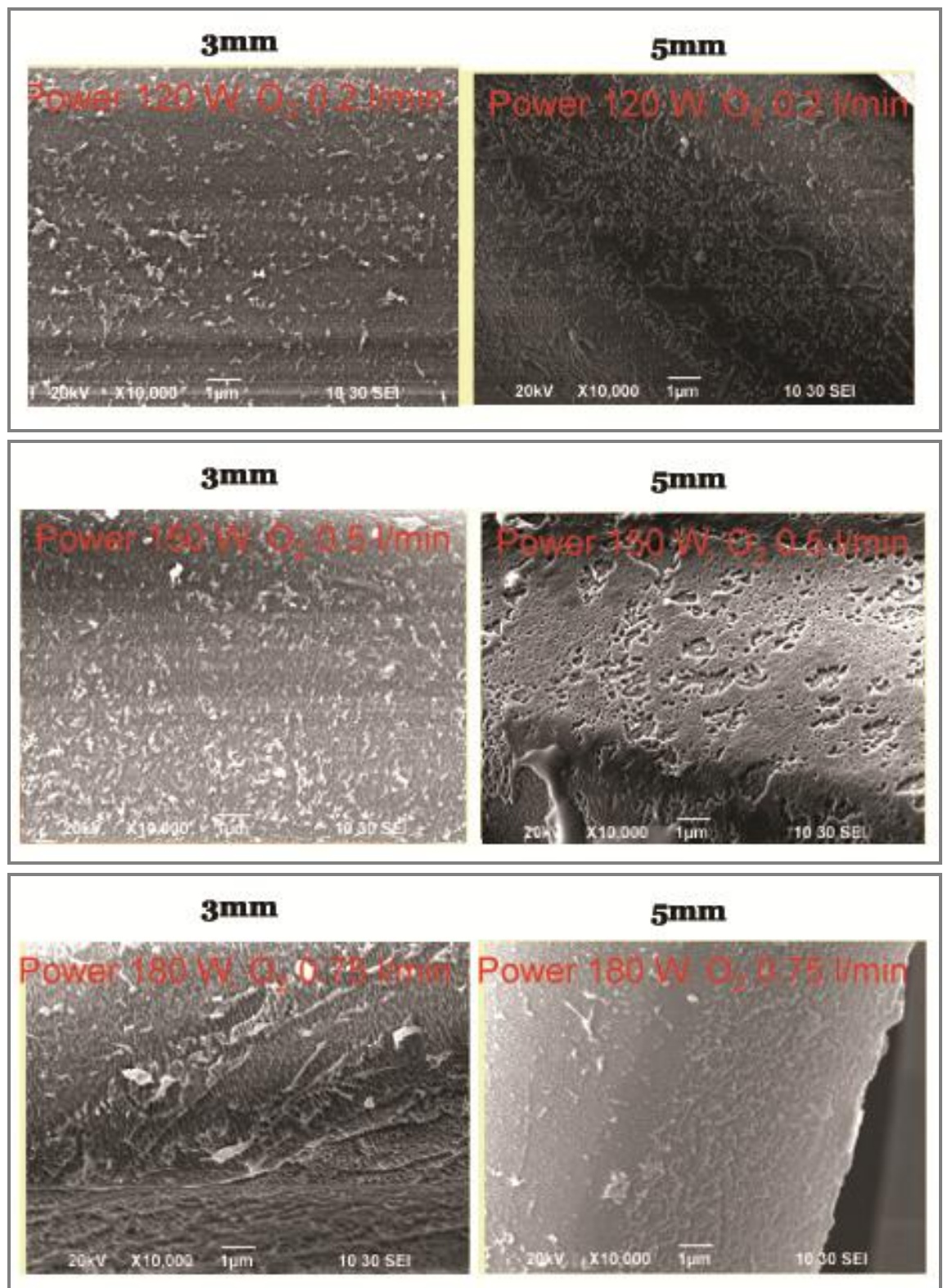
Figure 3-20   Variation of etching pattern of polyester fibres with respect to
ignition power of plasma and jet distance

With respect to the analysis of the PET film model, the ignition power and jet distance were the two prime parameters contributing to the surface etching of a substrate in the formation of characteristic topography. Variation in surface topographical modification related to these two parameters is illustrated in **Figure 3-20**. In general, ignition power determines etching power of plasma and hence the degree of etching. Within the jet distance of 3mm, ignition power of 120W did not possess sufficient amount of energy to generate nano-grooves. When increasing power to 150W and 180W, nano-grooves on the substrate fibres were induced. Ignition power of **180W** possessing higher energy did induce distinct nano-grooves with higher roughness as compared to those induced by 120W and 150W at a given treatment time. Moreover, the jet distance determined the etching pattern of the substrate surface. At the jet distance of 5mm with all the ignition powers being used in the study range, the modified polyester fibres were covered with granular micro-structures without distinguishable grooves. Granular structures were proposed to be induced by the glass transition of surface materials and re-deposition of etched substances. When the jet distance was reduced to **3mm**, nano-grooves perpendicular to the fibre axis were developed. A close proximity was necessary for the development of nano-grooves. This indicated that the proximity between the plasma source and the substrate surface essentially affected the etching efficacy.

Linear polyester polymeric chains allowed a close packing of molecules by introducing a large intermolecular dispersive force. Polyester fibre manufactured by super-drawing with well-oriented amorphous regions was resistant to the atmospheric pressure plasma etching. A high ignition power and a short jet distance were required for the formation of nano-grooves on the

----

Chapter 3   Plasma systems for polyester substrates

----

fibres. The development of nano-grooves was essential in improving the wicking behaviour of synthetic textile materials.

Topographical modification of polyester fibre differentiated from that of the PET film. Stress field of individual substrate attributed to the discrepancy. Polyester fibres were extruded and drawn in unidirection in contrast to the two-directional drawing when manufacturing the biaxially drawn PET film. As a result, nano-grooves developed on the polyester fibres were transverse to the fibre axis. Interestingly, the micro-pitches were developed at the ignition power of 150W with the jet distance of 5mm. The development of micro-pitches instead of nano-grooves needs further investigations in the future.

3.3.2.2   Surface chemistry alteration

He-O_2 plasma was oxidative resulting in surface chemistry alteration of a substrate. Contact angle goniometry was taken as a physical phenomenon of surface wetting behaviour of a substrate and water was used as the probing liquid. The experimental results showed that there was a reduction of water contact angle (WCA) in the course of the plasma treatment. The degree of hydrophilisation was quantified by the change of WCA, i.e. $\Delta WCA = (WCA_P - WCA_o)/WCA_o$, where WCA_P and WCA_o represent the WCA of the plasma-modified samples and the control fabric respectively.

The results shown in **Table 3-6** demonstrated that He-O_2 etching-hydrophilisation was efficient and effective in improving the surface wettability of polyester fabrics. The original polyester fabric was confirmed to be hydrophobic with a large WCA_o of 128°. Within 2.5s/mm of treatment time, WCA_P induced by a low ignition power of 120W was found to be reduced by

----

83

30-48%. A complete wetting was observed after 2.5s/mm treatment when the ignition power was tuned to a high value of **180W**. Increasing ignition power facilitated surface hydrophilisation of hydrophobic polyester substrate. For all ranges of parameters, polyester fabrics showed tremendous improvement in surface wettability with negative values of ΔWCA.

Table 3-6   Improved surface wetting based on the water contact angle goniometry

parameters	time [s/mm]	WCA [º]	ΔWCA [º]
control	**0**	**128**	**---**
120W, 0.3%O_2	0.5	125	-0.023
	1.5	84	-0.344
	2.5	67	-0.477
120W, 0.7%O_2	0.5	124	-0.031
	1.5	96	-0.250
	2.5	89	-0.305
120W, 1%O_2	0.5	108	-0.156
	1.5	66	-0.484
	2.5	75	-0.414

(to be continued)

----

parameters	time [s/mm]	WCA [º]	ΔWCA [º]
control	**0**	**128**	**---**
150W, 1.3%O_2	0.5	109	-0.148
	1.5	97	-0.242
	2.5	64	-0.500
150W, 1.7%O_2	0.5	118	-0.078
	1.5	100	-0.219
	2.5	117	-0.086
150W, 2%O_2	0.5	128	0.000
	1.5	105	-0.180
	2.5	92	-0.280
parameters	time [s/mm]	WCA [º]	ΔWCA [º]
control	0	128	---
180W, 2.2%O_2	0.5	78	-0.390
	1.5	87	-0.320
	2.5	0	-1.000
180W, 2.5%O_2	0.5	85	-0.336
	1.5	72	-0.438
	2.5	0	-1.000
180W, 2.8%O_2	0.5	110	-0.141
	1.5	107	-0.164
	2.5	0	-1.000

Negative values of ΔWCA represent the reduction of surface wettability (Constant parameter: 5mm)

* Values are statistically different at $P < 0.05$.

With reference to the film model, O_2 concentration did affect the plasma hydrophilisation of the polyester fabric. In general, increasing the ignition power would improve the wetting behaviour of polyester fabric to a larger extent. However ignition power was not an independent variable. As a matter of fact, both the ignition power and O_2 concentration were the interactive parameters determining the efficacy of a plasma etching-hydrophilisation.

Increasing O_2 concentration would reduce the hydrophilisation power of the plasma. With regard to **Table 3-6**, increasing O_2 concentration minimised the reduction of ΔWCA at each power level indicating the degree of hydrophilisation reduced accordingly. For example, 150W plasma with 1.7% and 2% O_2 was not a competent treatment for effective substrate hydrophilisation as compared to their counterparts with 1.3% O_2. ΔWCA reduced by less than 30% with a high concentration of O_2. With a higher O_2 content in plasma, the Penning reaction was predominant. As a result, the electrical energy produced by the ignition source was mostly consumed within the plasma before interacting with the substrate surface. Increasing the O_2% in the plasma gas required a higher ignition power. According to **Table 3-6**, 180W plasma having sufficient energy was capable of hydrophilising the polyester substrate to the greatest extent. A complete wetting was observed at high O_2% (>2%) within 2.5s/mm of treatment. At a higher ignition power, the effect of ignition power overrode the effect of O_2 concentration

The FTIR analysis explained the observed improvement in the wetting behaviour of the plasma-modified polyester fabrics. Based on the analysis, He-O_2 plasma was revealed to be capable of incorporating an appreciable amount of hydrophilic groups on the hydrophobic fibre surface. Original

----

----

polyester fabric was hydrophobic without hydrophilic hydroxyl groups (O-H). In **Figures 3-21 and 3-22**, the appearance of characteristic peaks at 3422cm^{-1} indicated the newly formed O-H groups such as carboxylic acids and hydroxyls. In addition, hydrogen bonds present on the substrate surface between the plasma-modified polyester fabric and atmospheric moisture afforded such a broad peak. The plasma-modified polyester fabric showed a reduction of C=O ester bonds located at **1720cm^{-1}**. Hydrolysis of ester bond was proposed as one of the reaction for the mild reduction in C=O functionalities. Oxidation of ethylene units generated polar functionalities such as C-O and O-H etc. which were the hydrophilic groups that could interact with atmospheric moisture. Sequentially, the moisture adsorbed on the fabric surface promoted further acid hydrolysis of ester bonds. In the etching-hydrophilisation reaction, the change in O-H groups and C=O groups was complementary as illustrated in **Table 3-7**. The degree of hydrophilisation was evaluated based on the peak area at 3422cm^{-1} and 1720cm^{-1}.
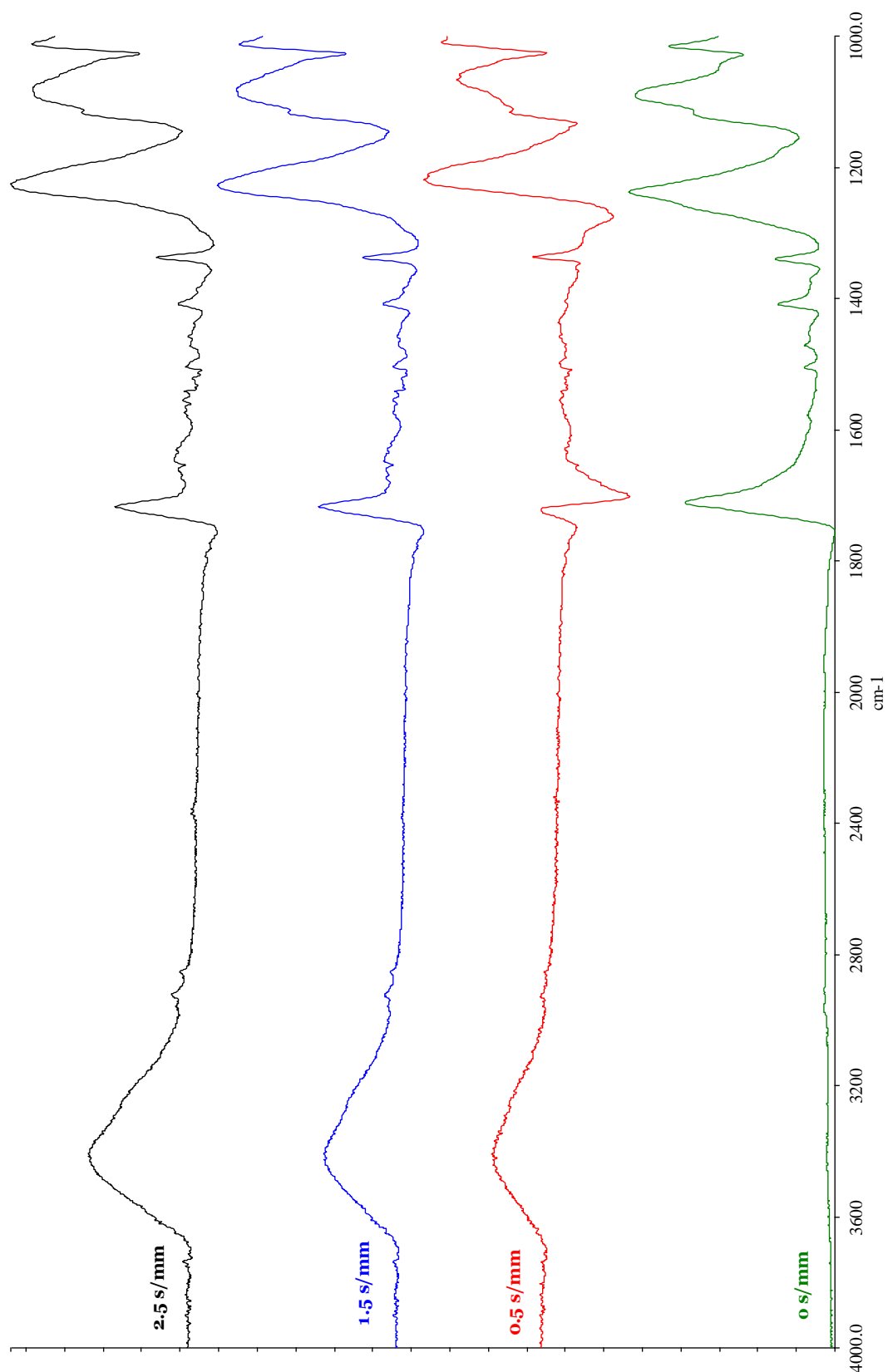
(Constant parameters: 120W, 5mm and 0.2% O_2)

Figure 3-21   FTIR spectrum of the plasma-modified polyester fabric exposed to
atmospheric pressure plasma
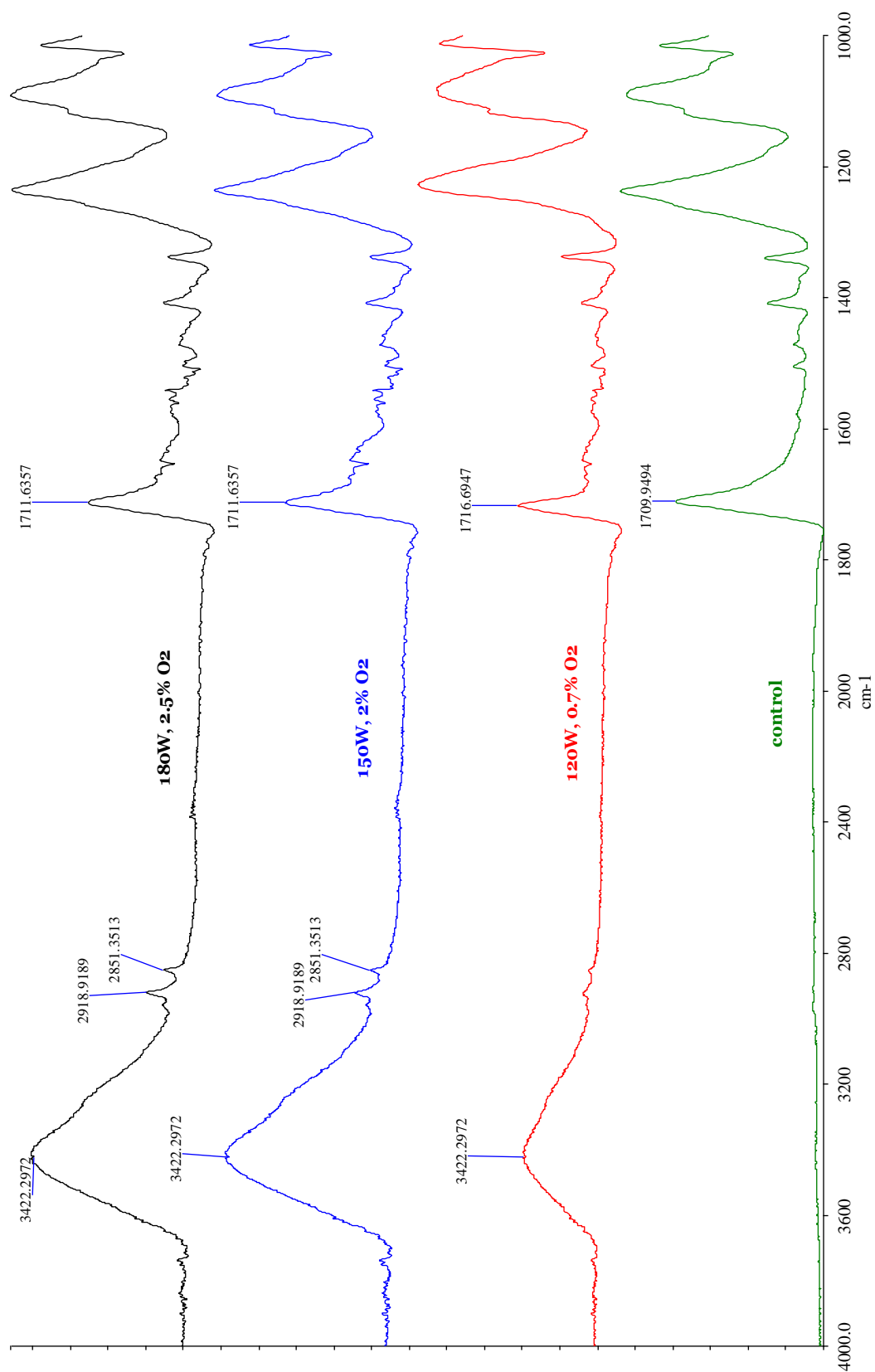
(Constant parameters: 5mm and 1.5s/mm)

Figure 3-22   FTIR spectrum of the plasma-modified polyester fabric exposed to
atmospheric pressure plasma

Table 3-7   Correlation between ignition power, treatment time
and hydrophilisation was evaluated by FTIR analysis.

parameters	time [s/mm]	O-H [A· cm^{-1}]	C=O [A· cm^{-1}]
control	**0**	**nil**	**527.52**
120W, 0.7%O_2	0.5	380.03	80.61
	1.5	779.61	72.15
	2.5	953.25	60.79
parameters	**time [s/mm]**	**O-H [A· cm^{-1}]**	**C=O [A· cm^{-1}]**
control	**0**	**nil**	**527.52**
150W, 1.7%O_2	0.5	1118.16	92.86
	1.5	1264.41	81.25
	2.5	1376.53	71.01
parameters	**time [s/mm]**	**O-H [A· cm^{-1}]**	**C=O [A· cm^{-1}]**
control	**0**	**nil**	**527.52**
180W, 2.5%O_2	0.5	1447.8	115.44
	1.5	1433.92	95.33
	2.5	1421.09	94

The peak area at 3422cm^{-1}, O-H represents carboxylic acids and hydroxyl groups and the related Hydrogen bonding. The peak area at 1720cm^{-1}, C=O represents hydrolysis of ester bond

Plasma functionalisation was a progressive reaction. The concentration of surface hydrophilic groups was amplified continuously during the course of treatment, i.e. degree of hydrophilisation increased with treatment time, as presented in **Table 3-6**. The phenomenon matched the PET film model as discussed in S**ection 3.3.1**.

Ignition power was another parameter needed to be considered carefully prior to the dry processing of the textile materials. Increasing ignition power sequentially promoted hydrophilisation because a higher power enabled to it could generate a higher concentration of active species in plasma as shown in **Figure 3-22** when considering the same treatment duration, e.g. 1.5s/mm, the higher the power, the larger and broader the peak at $3400cm^{-1}$ would be induced. For example, polyester fabric treated by APPJ operated at 120W with 0.7% O_2 at 5mm-jet distance was hydrophilised as shown in **Figure 3-21.** The other ignition powers of 150W and 180W showed a similar trend of hydrophilisation with respect to treatment time as tabulated in **Table 3-7**. The change in surface composition was complied with the physical phenomenon observed in the contact angle goniometry.

Other than hydrophilisation, increasing ignition power simultaneously promoted the etching of the polyester substrate. Free radical reaction could induce chain scission forming short chains of volatile low molecular weight oxidised fragments (LMWOF) as characterised by the peaks at $2918m^{-1}$ and $2851cm^{-1}$. The concentration of LMWOF was found to be increasing with ignition power as shown in **Figure 3-22.** Theoretically, increasing ignition power would promote hydrophilsiation proportionally. Power, however, should not be tuned to high values indefinitely as high power would induce severe chain scission of polymer chains leading to alteration of the bulk properties of the substrate.

3.4   Conclusion

Nano-scale He-O$_2$ atmospheric pressure plasma etching-hydrophilisation conducted on the PET thin film was achievable under controlled condition. Nano-surface structure density and surface energy were found to be varied with the treatment time in a quadratic relationship using stable plasma. Oxygen concentration acted as the coherence factor in the treatment. Ignition power and jet distance related to structure density and surface hydrophilicity in a linear manner. 3s/mm was determined to be the optimum treatment time to achieve the development of nano-spot within the range of 60-99nm in diameter on the PET substrate. In addition, the highest surface energy of 84mN/m was required by using the APPJ operating at 80W and 5mm jet distance by the feeding of 1% O$_2$/He gaseous admixture.

SEM-MATLAB image processing was found to be a potential tool for the prediction of surface etching of plasma of the film model. This technique allowed a quick prediction but required skillful technologists for processing manipulation.

The plasma treatment was applied to polyester fabric with reference to the film model. High ignition power plasma of 180W at a jet distance of 3mm with 2.2% O$_2$ was required for the optimal nano-scale etching-hydrophilisation of the polyester fabric. Surface wettability of the fabric modified under the optimum condition was improved significantly, allowing a complete wetting of the modified fabric after 2.5s/mm treatment. The effect of ignition power overrode the effect of O2 concentration at high levels.

After summarising the effect of individual parameter imposed on the etching- hydrophilisaiton of the substrates, it was found that both the ignition power and jet distance were the prime driving force for the distinctive topographical development and functaionlisation of a substrate surface. Reactive gas concentration and treatment time determined the equilibrium between etching and hydrophilisation reactions. The model demonstrated an empirical framework of atmospheric pressure plasma treatment for both the homogeneous and heterogeneous surface of polyester substrates.

Chapter 4   Plasma system for wool fabrics

4.1   Introduction

Conventional wet descaling processes impose environmental stress and cause degradation to wool fibres. Low temperature plasma (LTP) is a dry processing technique which has been established to improve surface wettability and dyeing properties of wool (Hesse et al., 1995; Kan et al., 1999; Molina et al., 2002, 2003; Ryu et al., 1991). It would be a potential alternative to alleviate the environmental stress. Hitherto, systematic evaluation of the plasma-textile processing is still insufficient. In the present study, a quantitative evaluation of the degree of wool surface modification utilising plasma technique was employed as a framework for the controlled dry processing of wool fabrics. Controlled descaling is also beneficial to wool dyeing and other post-wet processing of wool fibres.

Atmospheric pressure plasma (APP) treatment was employed for etching-hydrophilisation of the wool fabric substrates. In this section, two types of wool fabrics were used as the substrates to review the substrate dependence of the plasma treatment. These two fabrics were composed of different wool fibres with various fabric structures, namely the plain woven structure and twill woven structure. In order to study the optimum condition of attaining nano-structures on the wool fabrics, a number of parameters including 1) treatment time, 2) ignition power, 3) O_2 concentration and 4) jet distance were investigated. The surface properties of the plasma-modified wool fabric substrates were characterised using the scanning electron microscopy (SEM),

----

static contact angle goniometry, wetted area measurement, Fourier Transform infrared spectroscopy (FTIR-ATR) and X-ray photoelectron spectroscopy (XPS).

4.2   Experimental

4.2.1   Materials

100% twill 2/1 woven wool fabric of 180g/m^2 with thickness of 3.45mm, and density of 95 x 65 per inch supplied by Sun Fung Company, was used as the substrate called **wool A**. Another wool fabric with different fabric structure was studied to investigate the effect of fabric structure on the plasma-substrate interaction. 100% double-faced woven wool fabrics of 281g/m^2 with thickness of 5.30mm and density of 108 x 70 per inch supplied by the Hoa San & Co., Ltd., was used as the substrate called **wool B**. Fabric structures of these two types of wool fabric are shown in **Figure 4-1**. Wool fabrics were soaked in acetone for 30min and sequentially dried in oven at 50°C for 1hr. Dried fabrics were conditioned under the standard condition of 65±2% relative humidity and 21±1 ^{o}C for at least 24 hours prior to the experiments.

Wool A	Wool B
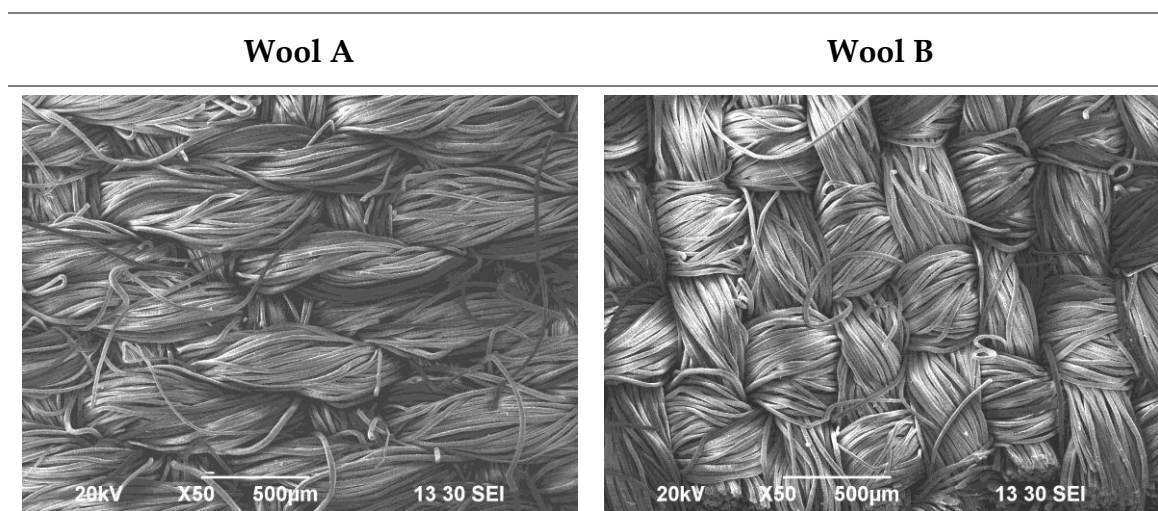
(Left: **wool A**; right: **wool B**)

Figure 4-1   Fabric structures of wool substrates at the magnification of 50x

Helium (He, 99.9% purity) and oxygen (O_2, 99.9% purity) were used as carrier and reactant gas respectively in the atmospheric pressure plasma treatment. Distilled water and glycerol (99%, extra pure, PhEur, USA) were used as probing liquids for contact angle goniometry.

4.2.2   Instrumentation

Atmospheric pressure plasma jet (APPJ) manufactured by the Surfx Technologies LLC, CA was used as a downstream atmospheric pressure plasma treatment with substrates being exposed to the plasma afterglow. In this part of study, APPJ Atomflo™ 400 was employed for the plasma treatment.

4.2.3   Atmospheric pressure plasma etching

In the APP treatment was conducted by an **APPJ, Atomflo™ 400** using a rectangular nozzle **(AH-500L**, Surfx Technologies LLC, CA) which covered an active area of 50×1 mm^2 vertically mounted above the substrate. Wool substrates were affixed to the stage of a 3-axis desktop robot (Model RB300-XY, Surfx Technologies LLC, CA). The substrate moving at a constant speed of 2mm/s was exposed to the afterglow plasma generated by the radio frequency of **27.12**MHz. He and O$_2$ were supplied as carrier and reactive gases respectively. The schematic diagram of the plasma treatment is shown in **Figure 4-2**.
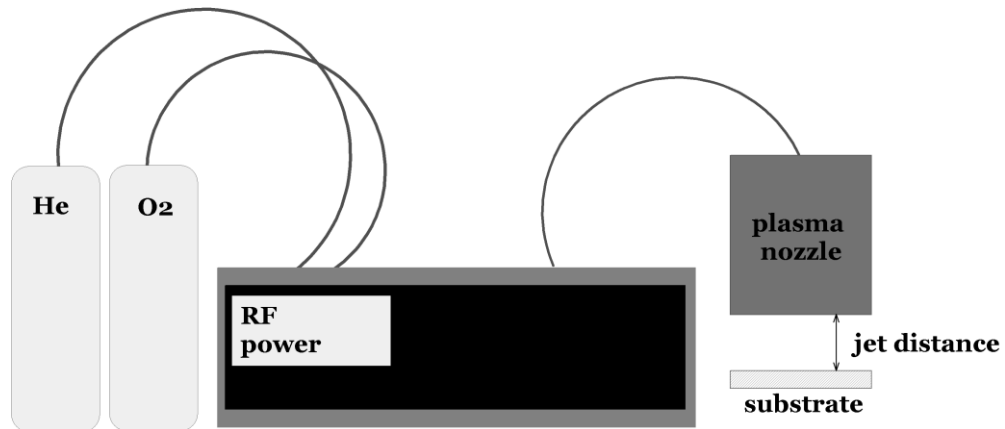
Figure 4-2   Schematic diagram of He-O$_2$ plasma treatment of wool substrates

Four operation parameters including 1) treatment time, 2) ignition power, 3) O$_2$ concentration and 4) jet distance were evaluated in order to study the formation of nano-structure on wool fabrics. The flow rate of He was fixed at 30L/min. Other variable operation parameters are listed in **Table 4-1**.

Table 4-1   Operation parameters studied in the plasma treatment of wool fabrics

Operation parameters	Variables
Treatment time (s/mm)	1-5
Ignition power (W)	120, 140, 160
Jet distance (mm)	3, 5, 7
O_2 concentration (%)	0.5, 1, 1.5

After APP treatment, the wool fabrics were conditioned at the relative humidity of 65 ±2% and 21 ±1°C for at least 24 hours prior to further evaluations.

4.2.4   Characterisation

4.2.4.1   Scanning electron microscopy (SEM)

Surface topographical feature of the plasma-modified wool fabrics was analysed using a scanning electron microscope (SEM, Model JSM-6490, JEOL Ltd., Japan). Samples were gold-coated with a sputter coater (Model SCD005, BAL-TEC, Liechtenstein) prior to SEM analysis. Images of plasma-modified fabrics were captured at the magnification of 10,000x with 20kV accelerating voltage for the investigation of nano-structures formed in the course of the treatment.

4.2.4.2   Contact angle goniometry

The change of surface wettability of the plasma-modified wool fabrics was characterised by the contact angle goniometry using the sessile drop technique with the aid of a micro-litre dispenser (GS-1200, Gilmont, Barnant Company, US). The contact angle defined as the tangential angle at the three-phase contact point was evaluated based on the image was captured by a digital microscope (AM413T- DinoLite Pro, ANMO Electronics Corp., Taiwan). Two probing liquids including distilled water (72.8mN/m) and glycerol (63.4mN/m) were used and the drop size was 3µL. The recorded contact angle was reported as the average of 10 measurements of an individual sample. The paired comparison t-test was employed to confirm the significant difference of the reported data to be within a confidence level of 95%.

4.2.4.3   Wetted area measurement

Unlike the polymer film, wool fabrics are non-isotropic and porous. To quantify the surface wettability of the plasma-modified wool fabrics, the wetted area with a dye solution was recorded (Wardman and Abdrabbo, 2010). All the experiments were carried out in a conditioned room at a temperature of 22°C and relative humidity of 65%. The dye solution was an aqueous solution of 0.1g/L Solophenyl Blue FGL-01 165% and the drop size was 10µL approximately. The wetted area was defined as the area within the liquid boundary after a complete drying in air. The wetted area recorded was reported as the average of 3 measurements of individual sample. The paired comparison t-test was employed to confirm the significant difference of the reported data to be within a confidence level of 95%. The wetting behaviour was quantified

----

----

through the change of the dimension of the wetted area with the dye solution with respect to the control fabrics. The change was calculated as the relative increment of the wetted area, $\Delta A = (A_P - A_o)/A_o$ where A_P is the wetted area of the plasma-modified wool fabrics, and A_o represents the wetted area of the control fabric respectively.

4.2.4.4   Fourier transform infrared spectroscopy (FTIR-ATR)

Perkin Elmer spectrophotometer (Spectrum 100, Perkin Elmer Ltd.) equipped with a horizontal attenuated total internal reflectance (HATR) accessory was used to analyse the surface chemical composition of the plasma-modified wool fabrics. ZnSe was employed as the ATR crystal. Each FTIR spectrum obtained was an average of 128 scans with a resolution of $4cm^{-1}$.

4.2.4.5   X-ray photoelectron spectroscopy (XPS)

The surface chemistry was investigated by the X-ray photoelectron spectroscopy (XPS). XPS analysis was carried out by a SKL-12 spectrometer (Sengyong, China) modified with VG CLAM 4 multi-channel hemispherical analyser equipped with Al/Mg twin anode. The spectrometer was operated with non-monochromatic Mg Kα (1253.6eV) radiation for the characterisation of the plasma-modified wool substrates under the vacuum condition of $8 \times 10^{-8}Pa$. Spectra were analysed using XPSPEAK 4.1.

Surface hydrophilicity was expressed in terms of the ratio of the total sum of the elemental content of O, N and S(VI) with respect to the C content ($\Sigma polar/C = [\Sigma O+N+S(VI)/C]$). The analysis of the individual polar functionalities was expressed as the ratio of O content versus C content (O/C)

----

and N content versus C content (N/C) respectively. In order to quantify the degree of hydrophilisation, the change of the relative concentration of surface polar functionalities compared to the control fabrics was taken into account. The changes was expressed in terms of $\Delta(\Sigma polar/C)$, $\Delta(O/C)$ and $\Delta(N/C)$. $\Delta(\Sigma polar)/C$ was the increment of the ratio of $(\Sigma polar)/C$ of the modified wool fabrics $((\Sigma polar)/C)_P)$ against the control fabrics $((\Sigma polar/C)_o)$. $\Delta(O/C)$ was the increment of the ratio of O/C of the modified wool fabrics $((O/C)_P)$ against the control fabrics $((O/C)_o)$, while $\Delta(N/C)$ was the increment of the ratio of N/C of the modified wool fabrics $((N/C)_P)$ against the control fabrics $((N/C)_o)$. Detailed calculation is illustrated in **Equations 4-1 to 4-3** respectively.

$$\Delta[\Sigma polar/C] = \frac{(\Sigma polar/C)_P - (\Sigma polar/C)_o}{(\Sigma polar/C)_o} \qquad \text{Equation 4-1}$$

$$\Delta(O/C) = \frac{(O/C)_P - (O/C)_o}{(O/C)_o} \qquad \text{Equation 4-2}$$

$$\Delta(N/C) = \frac{(N/C)_P - (N/C)_o}{(N/C)_o} \qquad \text{Equation 4-3}$$

As a complement, the variation in S(II) and S(VI) peaks of the modified wool substrates was studied in order to determine the degree of disulphide crosslink cleavage of surface cuticles. $\Delta[S(VI)/S(II)]$ was calculated as an indicator of the change of the relative concentration of surface disulphide crosslinks. $\Delta[S(VI)/S(II)]$ was determined as the change of the ratio of S(VI) to

----

S(II) of the modified wool fabrics ($[S(VI)/S(II)]_P$) against the ratio of the control

fabrics ($[S(VI)/S(II)]_o$). Detailed calculation is illustrated in **Equation 4-4**.

$$\Delta[S(VI)/S(II)]= \frac{[S(VI)/S(II)]_P - [S(VI)/S(II)]_o}{[S(VI)/S(II)]_o} \qquad \text{Equation 4-4}$$

4.3   Results and discussion

In the present study, two types of wool fabrics with different fabric

structure were used, namely wool A and wool B. These two fabrics represent

wool fibres in different natures. The two fabrics were obtained different breeds

of animals with respect to the difference in cuticle shapes as shown in **Figure**

4-3. The cuticles of wool A were comparatively rectangular with sharp edge

whereas wool B had round-edged cuticles. The variation from breed to breed

and the growth of a breed did affect the crystallinity of F-layer and A-layer, the

concentration of surface fatty acids, the composition of wool protein and hence

the cystine density, i.e. the degree of crosslinks (Appleyard, 1960; Wildman,

1954).

Wool A	Wool B
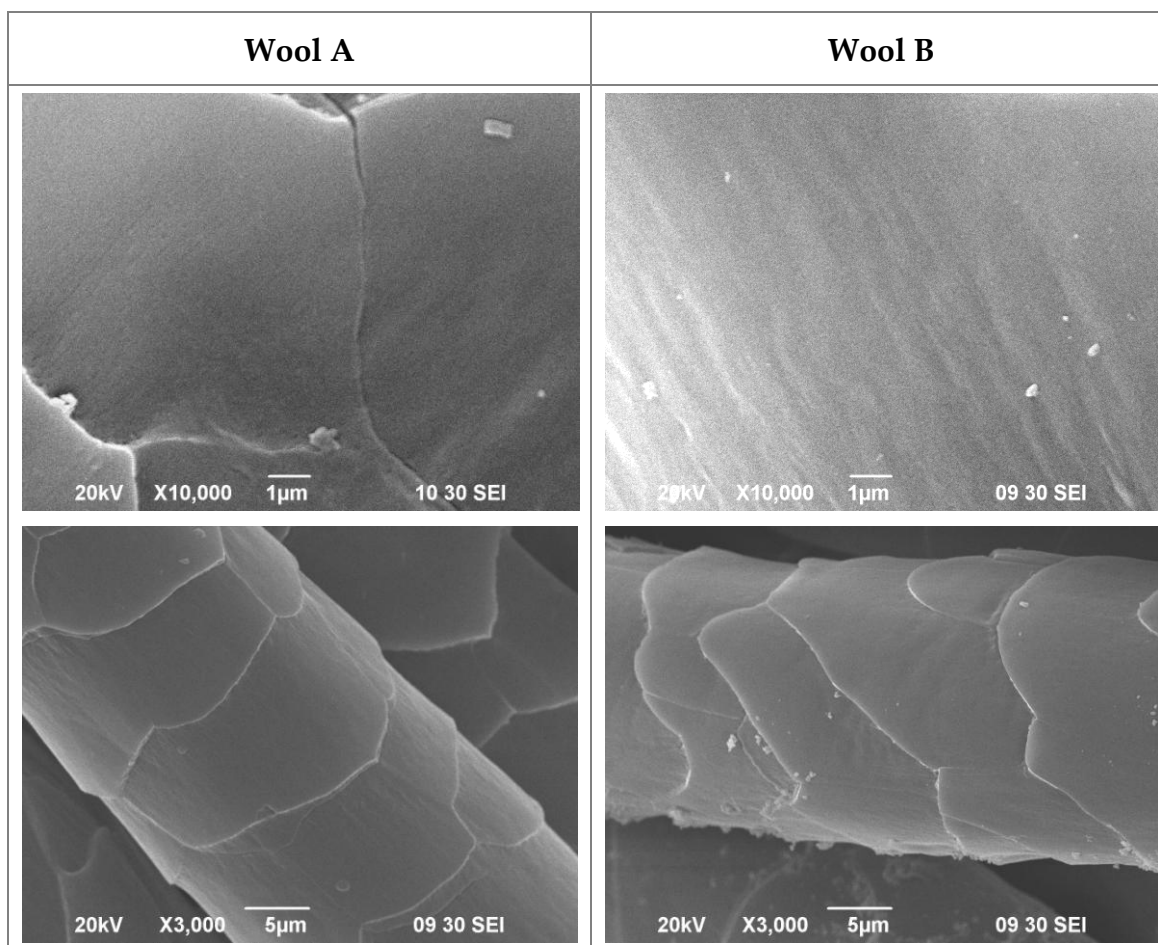
(Left: **wool A**; right: **wool B**)

Figure 4-3 Smooth cuticle surface of two different types of wool fibres at the magnification of 3,000x and 10,000x

The distribution of crystalline and amorphous regions was proposed to be the prime factor attributed to the development of nano-structures and the features of the surface structure formed. The distribution was intrinsically determined by the biological growth of the natural fibre of a particular breed of the animal. The shape of the plasma-induced features of wool A was different from that of wool B. Modified wool A with nano-bumps appeared in circular form while nano-bumps of wool B were in rod shape. With reference to the PET

----

film model, the stress field of a substrate determined the shape of structures formed on the substrate.

Similarly, the processing of natural fibres would induce the stress contributing to different characteristics of surface topography of these two types of wool.   Fibre processing, yarn spinning and fabric weaving induced stress to the fibre. Wool A and wool B with different fabric structure were manufactured by different companies. Stress and force imposed on these two types of wool fibres would be different. As a result, the optimum condition developed for obtaining the nano-scale etching was different for these two fabrics as shown in **Figure 4-4**.
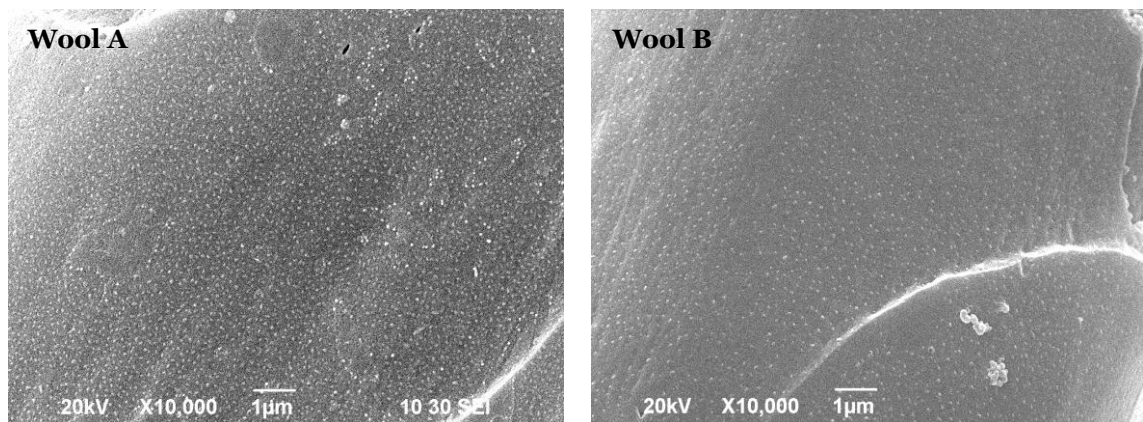
The optimum operation condition for wool A: 120W, **1%O$_2$,** 5mm and **4s/mm; wool B:** 120W, **0.5% O$_2$**, 5mm and **3s/mm.**
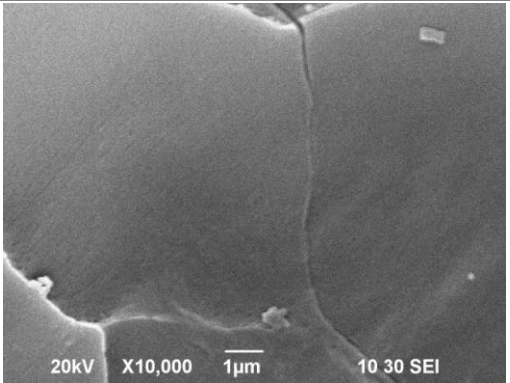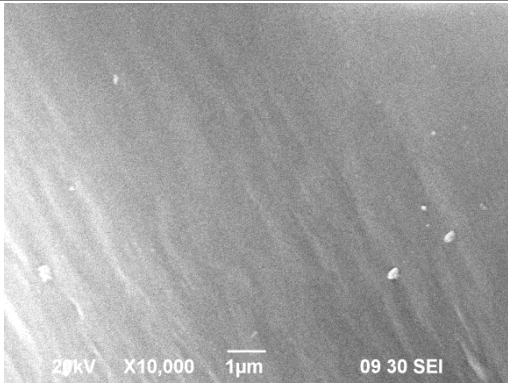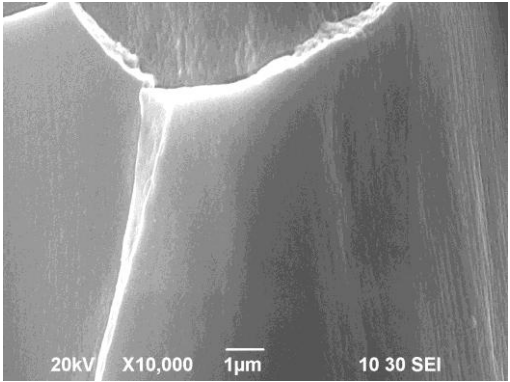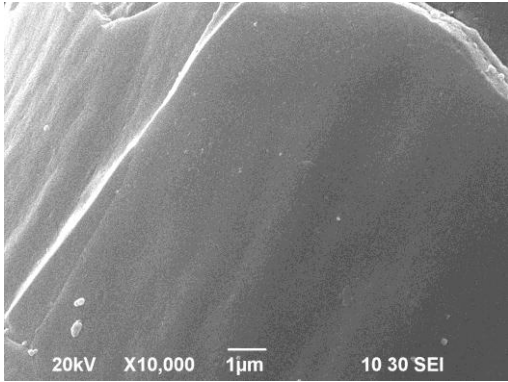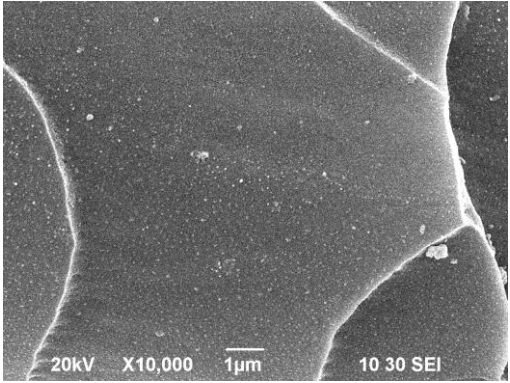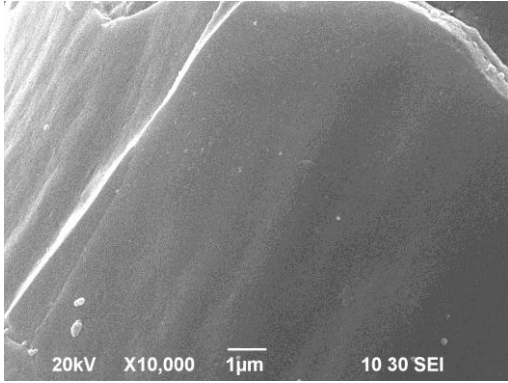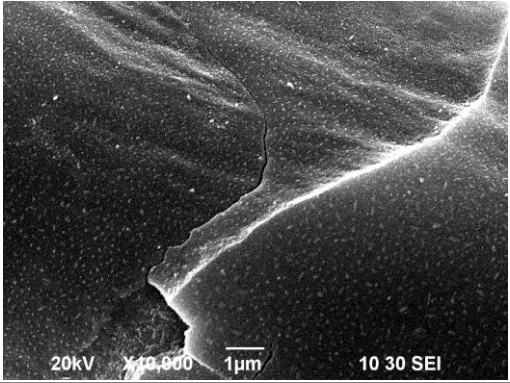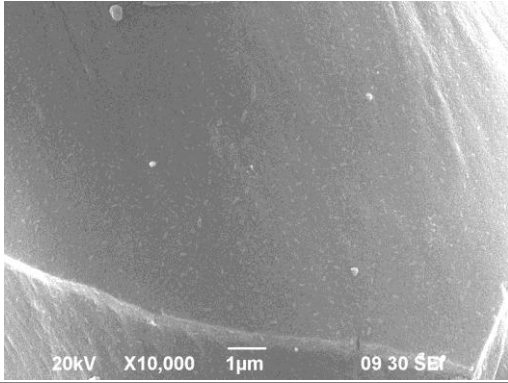
Figure 4-4   Nano-crystalline structures formed on two different types of wool fibres under SEM at the magnification of 10,000x.

With reference to the SEM micrographs shown in **Figures 4-4 and 4-5**, wool A was more susceptible to physical ablation with plasma as compared to wool B with respect to time. Under the same plasma operation condition, i.e. 120W plasma using 1% O_2 at 5mm-distance, the treatment time required for the formation of nano-structures of wool A was found to be relatively shorter as shown in **Figure 4-6.** It was obvious that 2s/mm treatment time was sufficient to induce nano-structures on wool A while 3 to 4s/mm treatment time was required for modifying wool B. When the etching power of plasma was enhanced, i.e. using a lower O_2 concentration of 0.5%, the dimension of the induced structure would increase to micro-scale with a more severe erosion of the cuticles being observed as shown in **Figure 4-7**. Susceptibility towards ablation was proposed to be caused by the variation in the crystallinity of the F-layer and the A-layer.
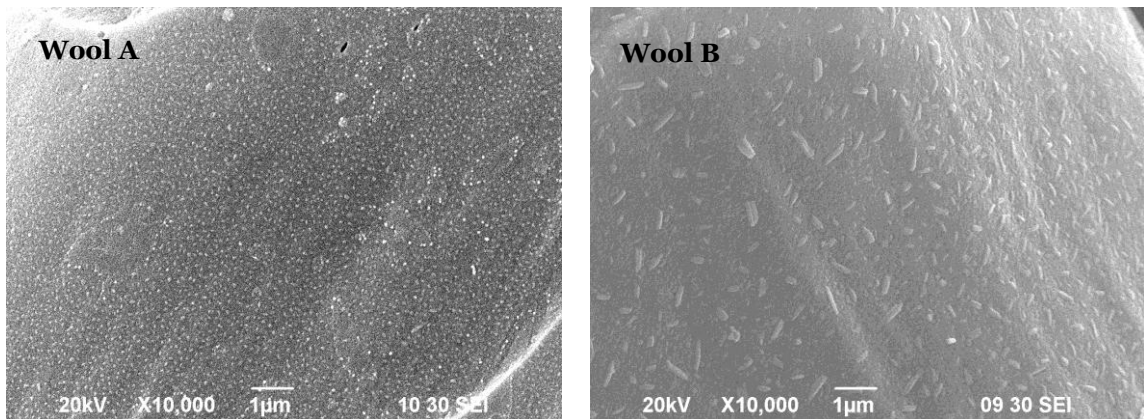
(Treatment parameters: 120W, 1% O_2, 5mm and 4s/mm)

Figure 4-5   Different characteristic surface topography induced by atmospheric pressure plasma treatment on wool A and B.
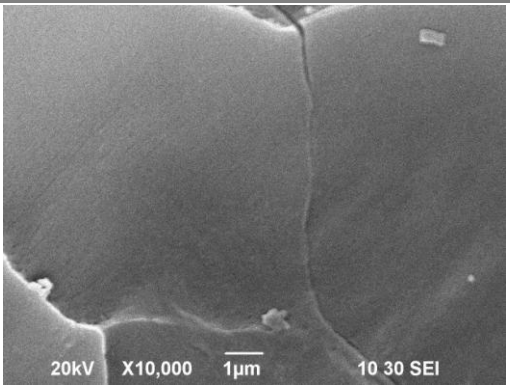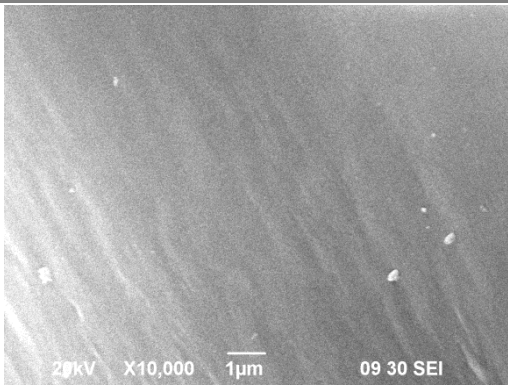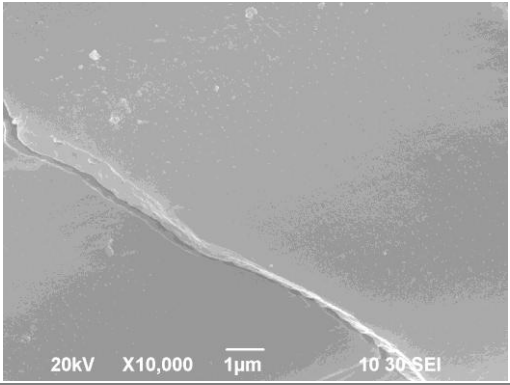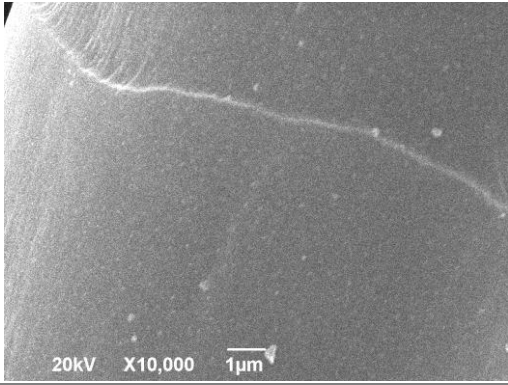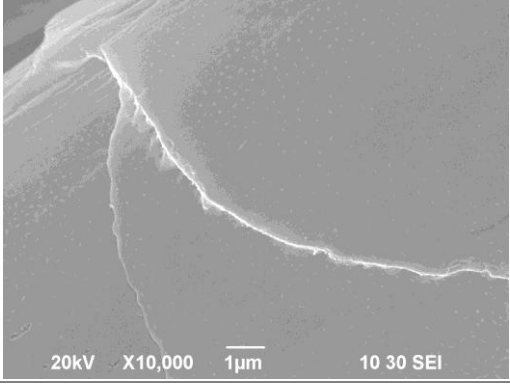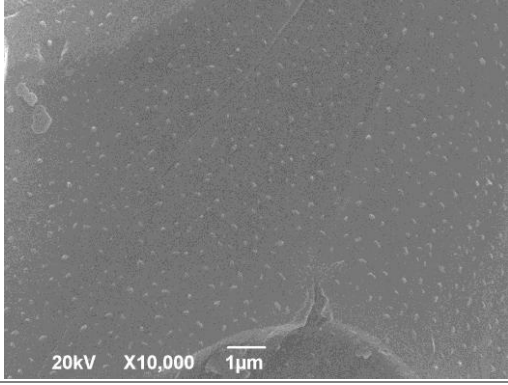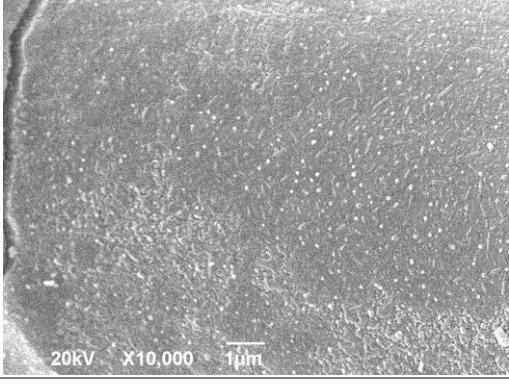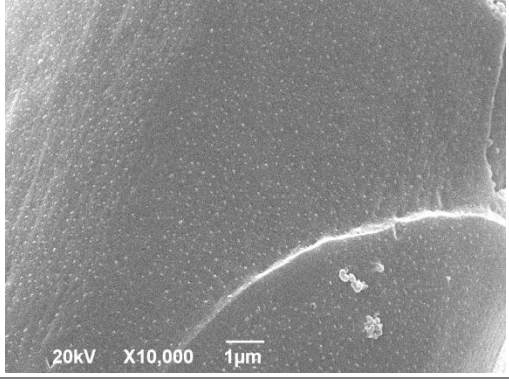
Treatment time (s/mm)	Wool A	Wool B
0 s/mm		
1 s/mm		
2 s/mm		
3 s/mm		

(To be continued)

----

4 s/mm		
5 s/mm		
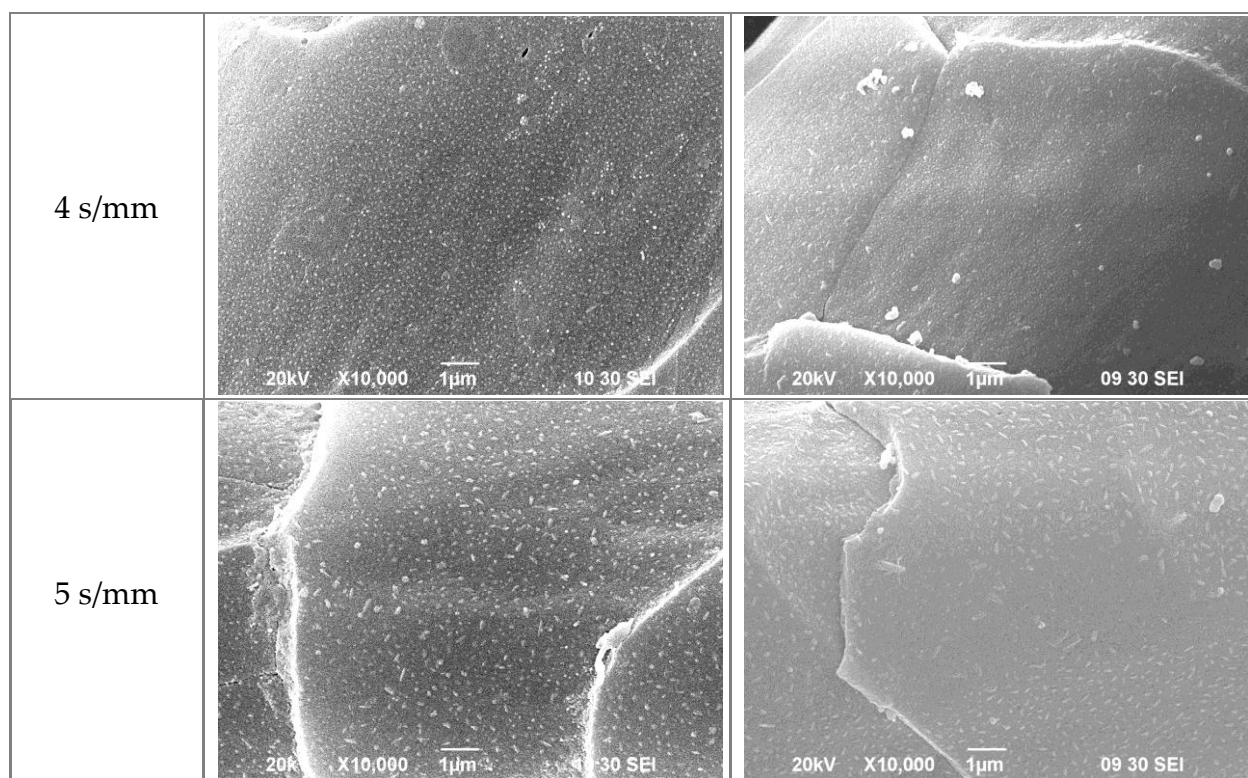
(Constant parameters: 120W, 1% O_2 and 5mm.)

Figure 4-6   Progressive topographical alteration on wool fibres exposed to atmospheric pressure plasma etching as revealed by SEM at the magnification of 10,000x.

Treatment time (s/mm)	Wool A	Wool B
0 s/mm		
1 s/mm		
2 s/mm		
3 s/mm		

(To be continued)

4 s/mm		
5 s/mm		
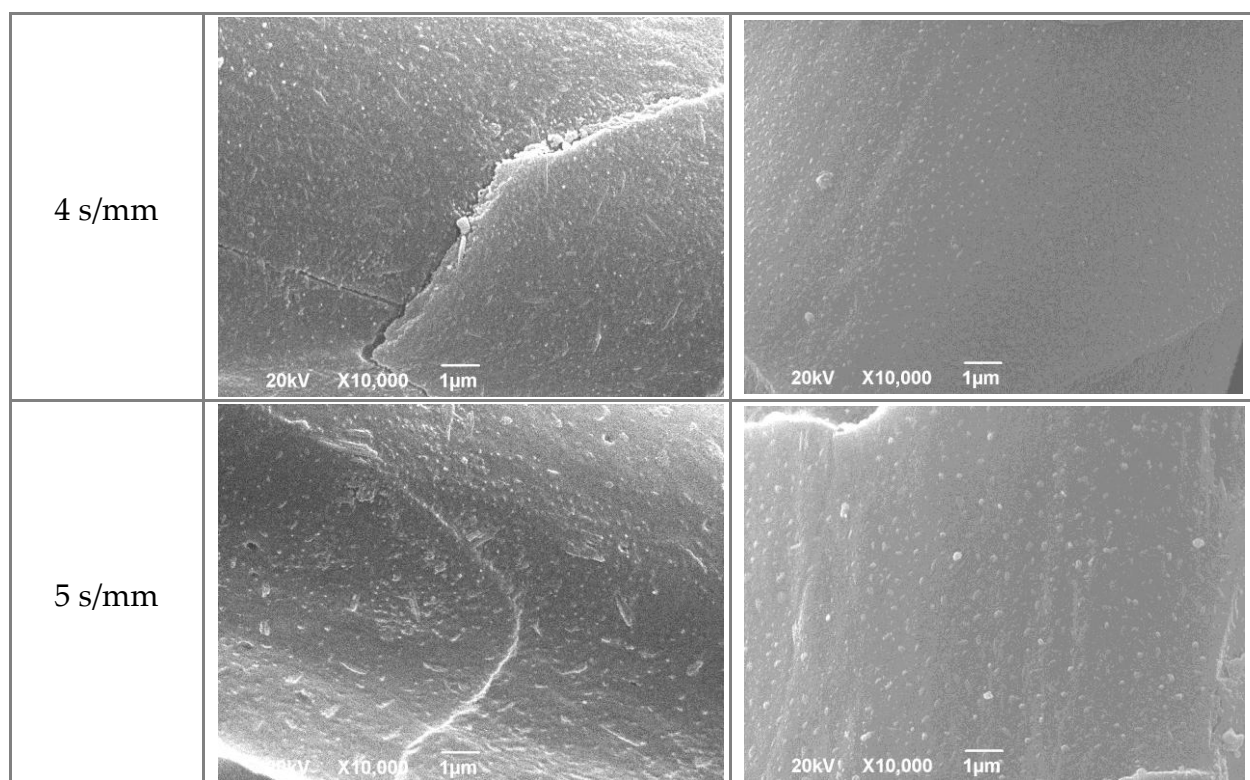
Constant parameters: 120W, 0.5% O_2 and 5mm.

Figure 4-7   Progressive topographical alteration on wool fibres exposed to atmospheric pressure plasma etching as revealed by SEM at the magnification of 10,000x.

Other than the difference in the nature of wool substrates, fabric structure also played a role in determining the optimum condition for the nano-scale etching-hydrophilisation of the substrates. Wool A represented the twill woven fabric structure while wool B represented the plain woven structure as illustrated in **Figure 4-1**. Difference in fabrics structure with various area-to-volume ratios would affect the plasma penetration and plasma bombardment, thereby affecting the efficacy of the reaction of etching-hydrophilisation.

APP hydrophilises the surface of the wool substrates via oxidation. Due to the difference in the concentration of fatty acids of the F-layer and the degree of crosslinking, there was a discrepancy observed in the optimum condition of nano-scale etching-hydrophilisation induced by atmospheric pressure plasma for different types of wool fabrics. The detailed analysis of the surface properties of the modified wool substrates in relation to the individual parameter is illustrated in **Section 4.3.3**.

4.3.1   Surface topographical modification

Preferential etching in the formation of distinctive surface topography

When the wool fabrics were subjected to the afterglow of the non-polymerising He-O_2 plasma for a few seconds, surface etching was observed using SEM at the magnification of 10,000x. Two different types of the plasma-modified wool fibres were roughened and the nano-crystalline structures were also found under different plasma condition as illustrated in

----

Figures 4-4 and 4-5. Plasma-induced physical ablation was a preferential etching. The amorphous region of wool fibres was etched away with respect to the bombardment of active species in the plasma. This kind of etching of a substrate surface attributes the development of a distinctive surface texturisation.

The modification of surface topography depended on the conditions of the plasma treatment. Detailed analysis of the development of surface structures in relation to the individual plasma operation parameter is illustrated in **Section 4.3.3**. Textile structure and chemical composition of the wool fibres were the attributes of the discrepancy of the formation of surface structure of the two different types of fabrics as observed by SEM.

4.3.2   Alternation of surface chemistry

Surface oxidation of fatty acids and disulphide crosslinks of cuticle

Subjecting the two different types of wool fabrics to the plasma afterglow for a few seconds, an alternation of the surface wetting behaviour was observed with respect to the contact angle measurement. Contact angle is defined as the tangential angle at the point of three-phase interface. The resultant angle is determined by the work of cohesion within the probing liquid and the work of adhesion at the liquid-solid interface. Water and glycerol were used as the polar probing liquids. A reduction of the contact angle with the polar liquids indicated the polar interaction at the liquid-substrate interface. Both the original wool fabrics gave large contact angles. This indicated that the liquid cohesion was predominant causing the probing liquid ball up on the fabric surface as illustrated in **Figure 4-8**. The surface energy of the substrate was significantly

---

----

smaller than that of the probing liquids as the surface cuticles of wool were

covered with covalently bound fatty acids, chiral 18-methyleicosanoic acids

(18-MEA), offering a high surface hydrophobicity are shown in **Figure 4-9**

(Negri et al., 1993). The contact angles with respect to the two probing liquids

are shown in **Table 4-2**.

	Wool A	Wool B
WCA		
GCA		
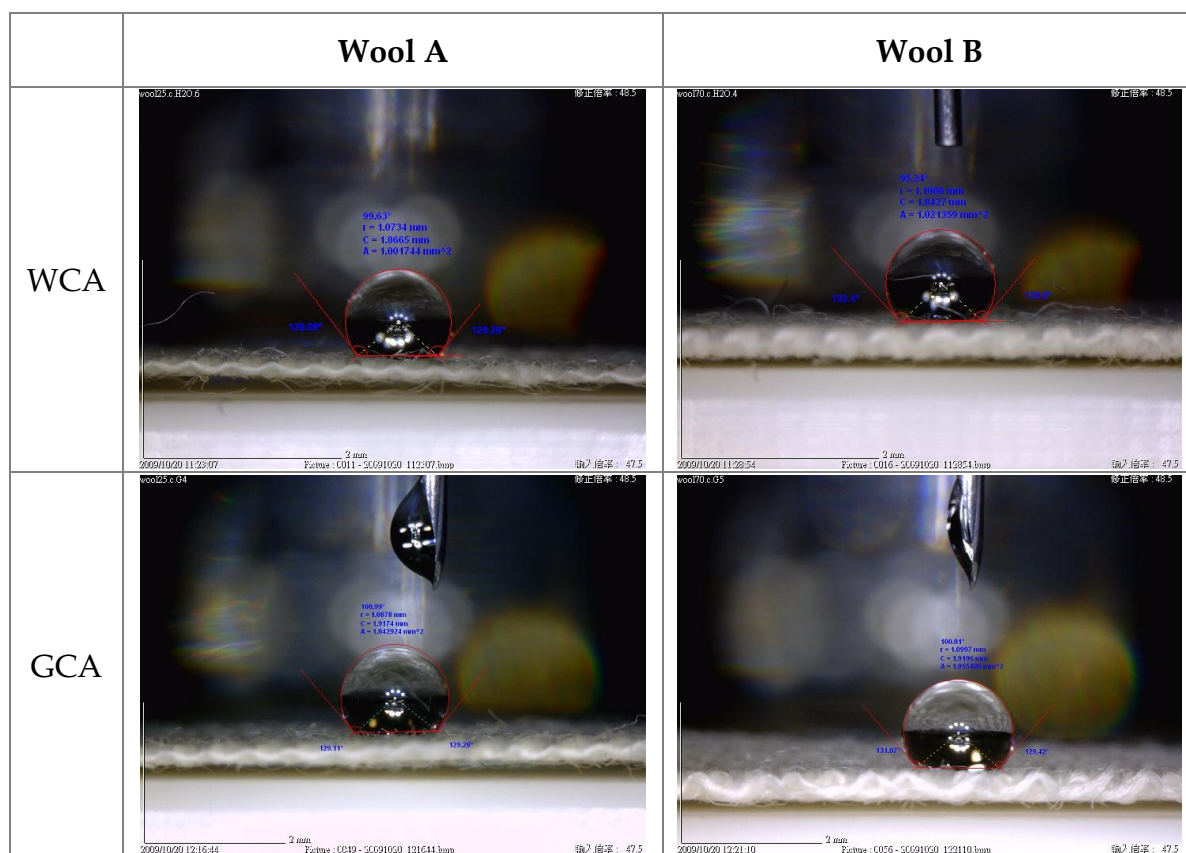
(WCA = water contact angle; GCA = glycerol contact angle)

Figure 4-8   Sessile drop images of probing liquids on the control wool fabric
samples
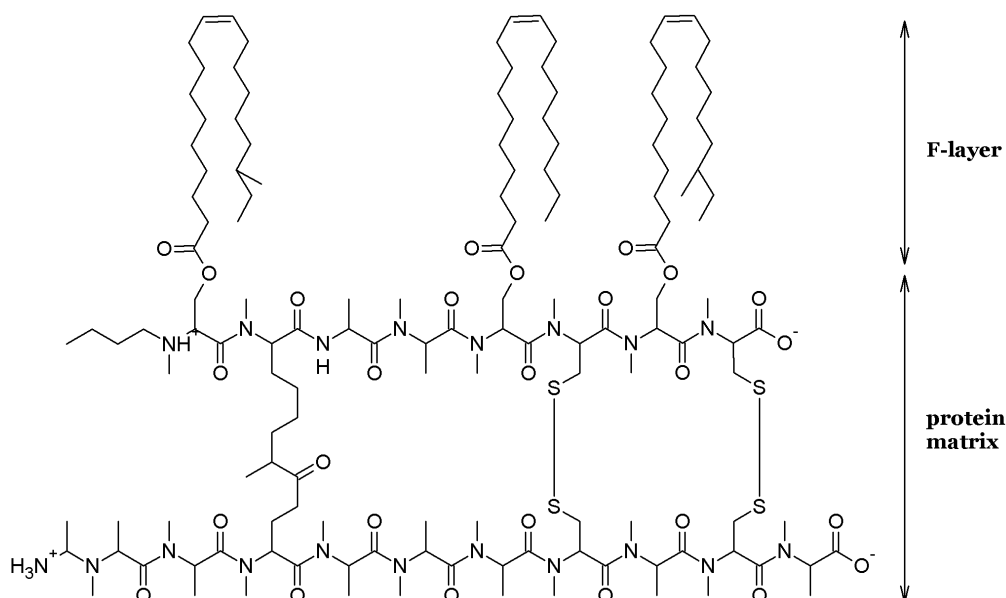
Figure 4-9   The chemical composition of wool cuticles. F-layer acts as a hydrophobic barrier of the cuticles. (Canal et al., 2007)

Table 4-2   Contact angles of original wool fabrics based on contact angle goniometry

Before plasma treatment	Wool A	Wool B
Water contact angle WCA[°]	119.2 (± 1.2)	130.8 (± 1.6)
Glycerol contact angle GCA[°]	131.5 (± 2.1)	130.8 (± 2.2)

* Values are statistically different at $P < 0.05$.

APP was capable of improving the surface wettability of the wool substrates significantly. Without any detectable change in the surface morphology of the wool cuticles, the contact angles of the probing liquids dropped to 0° upon a short exposure duration to the plasma afterglow, i.e. 1s/mm treatment. The two different types of the plasma-modified wool substrates showed a complete wetting to the probing liquids with respect to the

----

----

operation parameters being studied. Complete wetting macroscopically indicated that a remarkable boost of the surface energy of the modified fabrics was induced by the complete abrasion of the F-layer and partial abrasion of the A-layer of the wool cuticle which were corresponding to the previous studies using plasma operated in reduced pressure (Hesse, 1995; Canal et al., 2007). APP was found to be very effective in promoting the surface wettability of both types of wool fabrics.

The quantification of surface wettability of samples modified with different plasma parameters via the contact angle goniometry was not feasible with respect to the instant spreading of the probing liquids within a second. As an alternative, the wetted area measurement was employed. The wetting behaviour was quantified by the change of wetted area with respect to the control wool fabrics. The wetted area indicated by the dyestuff was measured to quantify the degree of plasma wettability modification. The relative increment was defined as $\Delta A = (A_P - A_o)/A_o$ where A_P was the wetted area of the plasma-modified wool samples and A_o represented the wetted area of the control.

In general, surface wettability of the plasma-modified wool fabrics was significantly improved for all range of operation parameters being studied. The wetted area was increased by multiple times depending on the respective operation parameters. The detailed analysis of the wetting behaviour related to the individual plasma operation parameter is illustrated in **Section 4.3.3**. Textile structure and chemical composition of the wool fibres were the attributes of the discrepancy of the wetted area of the two different types of fabrics measured.

XPS analysis confirmed the complete wetting phenomenon occurred on the wool fabrics. The XPS wide scan spectra of the wool fabrics indicated the reaction occurred on the fabric surface during the treatment as shown in **Figure 4-10 and 4-11.** A significant increase in the amount of surface polar groups on wool cuticles as listed in **Table 4-3** explained the phenomenon of complete wetting. The relative amount of polar LMWOFs containing O, N and S was found to be almost doubled. The amplification of the surface polarity made the wool fabrics to be very hydrophilic toward the polar liquids. O_{1s} while C_{1s} peak declined because of the surface oxidation of the outermost hydrophobic fatty acids, 18-methyleicosanoic acids (18-MEA) of the F-layer. Breaking down of the surface fatty acids reduced surface hydrophobicity. N_{1s} increased when the outmost fatty acid barrier layer was partially oxidised by O_2 plasma. Subsequently, the lower layer of keratinous wool fibre cells exposed resulting in the increment of N content. The detailed variation of the O and N was summarised in **Table 4-4 and 4-5**. The change of the relative concentration of polar functionalities was expressed in terms of $\Delta(O/C)$ and $\Delta(N/C)$. Detailed calculation is illustrated in **Equations 4-1 and 4-2** shown in Section **4.2.4.5.**
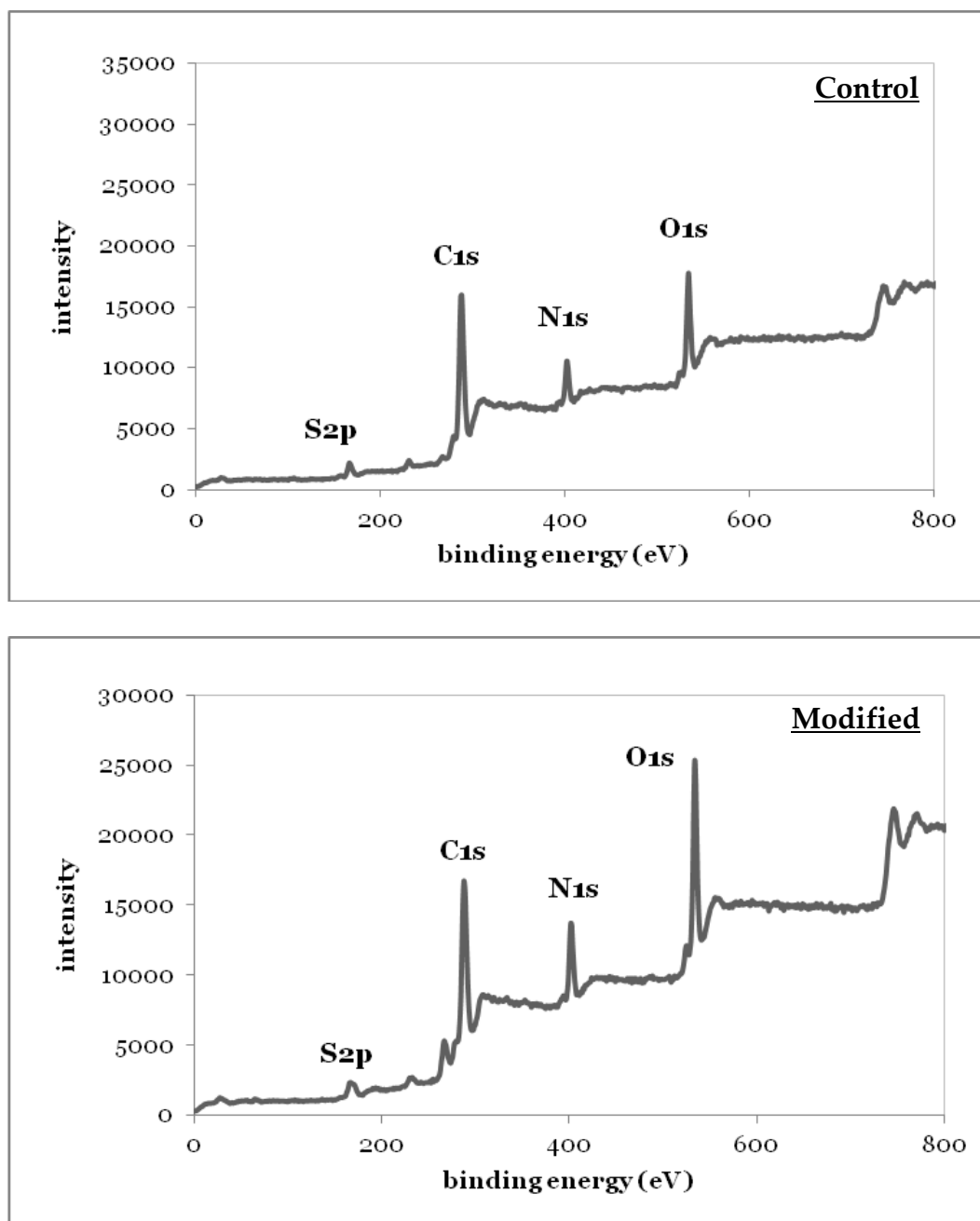
(Treatment parameters: 120W, 1%O_2, 5mm and 5s/mm)

Figure 4-10   Surface elementary composition of He-O_2 plasma-modified
wool A
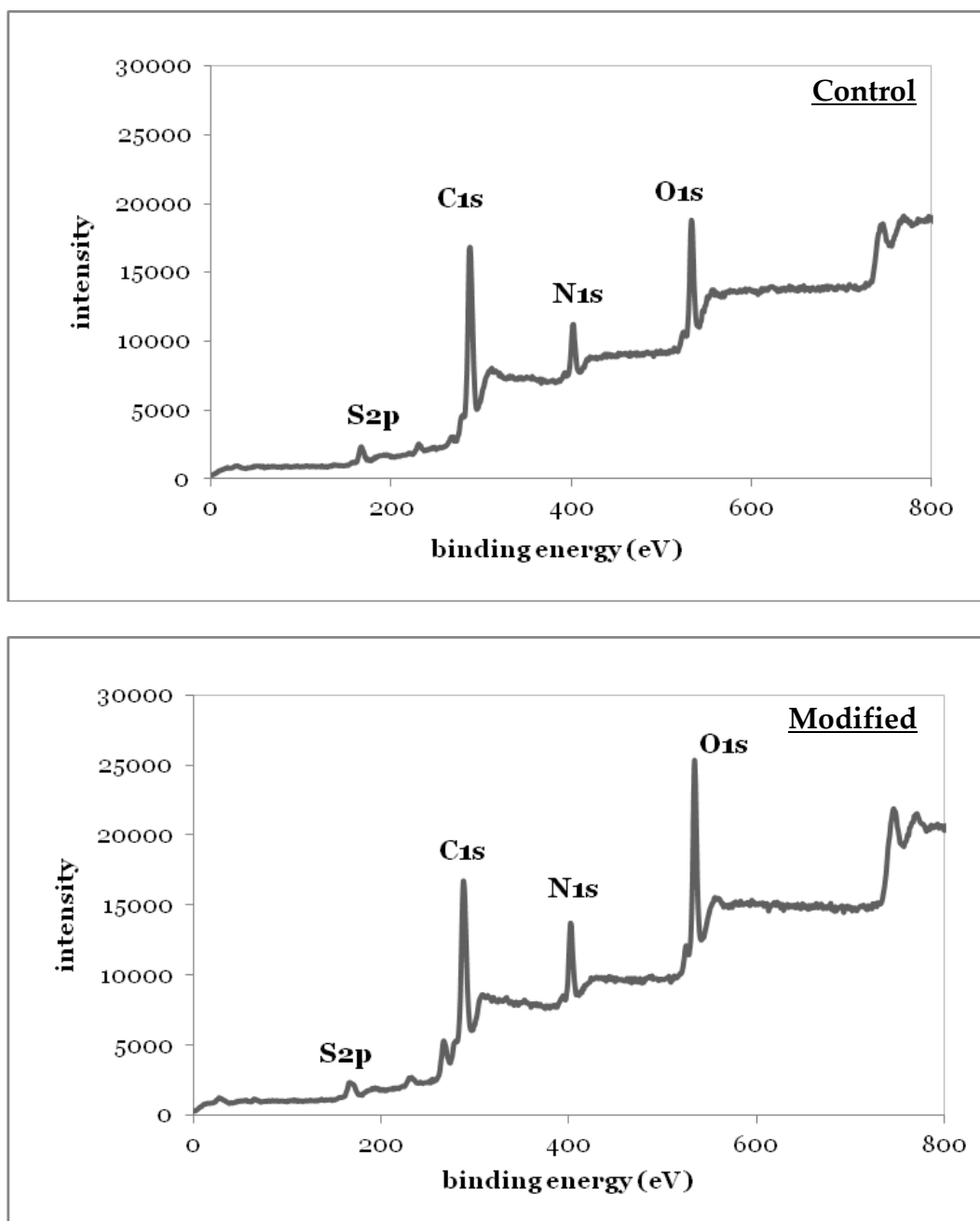
(Treatment parameters: 120W, 1%O_2, 5mm and 5s/mm)

Figure 4-11   Surface elementary composition of He-O_2 plasma-modified
wool B

Table 4-3   Overall surface polar functionalities of the modified wool fabrics revealed using XPS

	Wool A		Wool B	
	Control	Modified	Control	Modified
C	0.662	0.524	0.646	0.519
Σpolar	0.298	0.310	0.330	0.393
Σpolar/C	0.451	0.491	0.511	0.704
Δ(Σpolar/C)	N/A	+1.088	N/A	+1.377

Σpolar denoted as the sum of O, N and S(VI) representing the total surface polar elemental content (Treatment parameters: 120W, 1% O_2, 5mm, 1s/mm)

Table 4-4   XPS analysis of N and O content of the plasma-modified **wool A**

Treatment time (s/mm)	C	O	N	O/C	Δ(O/C)	N/C	Δ(N/C)
control	0.662	0.186	0.107	0.282	N/A	0.162	N/A
1	0.632	0.206	0.096	0.326	+0.159	0.152	-0.059
2	0.585	0.245	0.114	0.419	+0.486	0.195	+0.206
3	0.576	0.246	0.109	0.428	+0.519	0.190	+0.172
4	0.553	0.244	0.131	0.442	+0.569	0.236	+0.455
5	0.524	0.261	0.133	0.498	+0.770	0.254	+0.570

Positive values represent the increase of Δ(O/C) and Δ(N/C) with respect to the control sample.(Constant parameters: 120W, 1% O_2 and 5mm)

Table 4-5   XPS analysis of N and O content of the plasma-modified **wool B**

Treatment time (s/mm)	C	O	N	O/C	Δ(O/C)	N/C	Δ(N/C)
control	0.646	0.198	0.128	0.307	N/A	0.198	N/A
1	0.558	0.249	0.132	0.446	+0.456	0.236	+0.191
2	0.525	0.256	0.155	0.487	+0.588	0.294	+0.484
3	0.550	0.252	0.149	0.457	+0.491	0.271	+0.367
4	0.537	0.278	0.131	0.518	+0.691	0.244	+0.229
5	0.519	0.257	0.151	0.496	+0.618	0.290	+0.465

Positive values represent the increase of Δ(O/C) and Δ(N/C) with respect to the control sample.(Constant parameters: 120W, 1% O_2 and 5mm)

The detailed plasma-substrate interaction was shown by FTIR analysis. The FTIR analysis confirmed the abrasion reaction of the F-layer. With reference to **Figures 4-12 and 4-13**, there was a significant increase in the aliphatic -CH_3, –CH_2- and –CH- groups at **2850** to **2990 cm^{-1}** for both types of wool fabrics. The increment was contributed by the oxidation of the epicuticle fatty acids, 18-methyleicosanoic acids (18-MEA), of wool scales. Hydrophobic fatty acids gave rise to the hydrophobicity of wool fabrics. The breakdown of the surface fatty acids reduced surface hydrophobicity. Cleavage of long fatty acid chains into smaller fragments increased the aliphatic hydrocarbons of the plasma-modified wool fabrics. Simultaneously, an increment in the peak at ~**3100cm^{-1}** indicated the incorporation of polar –OH functionalities.
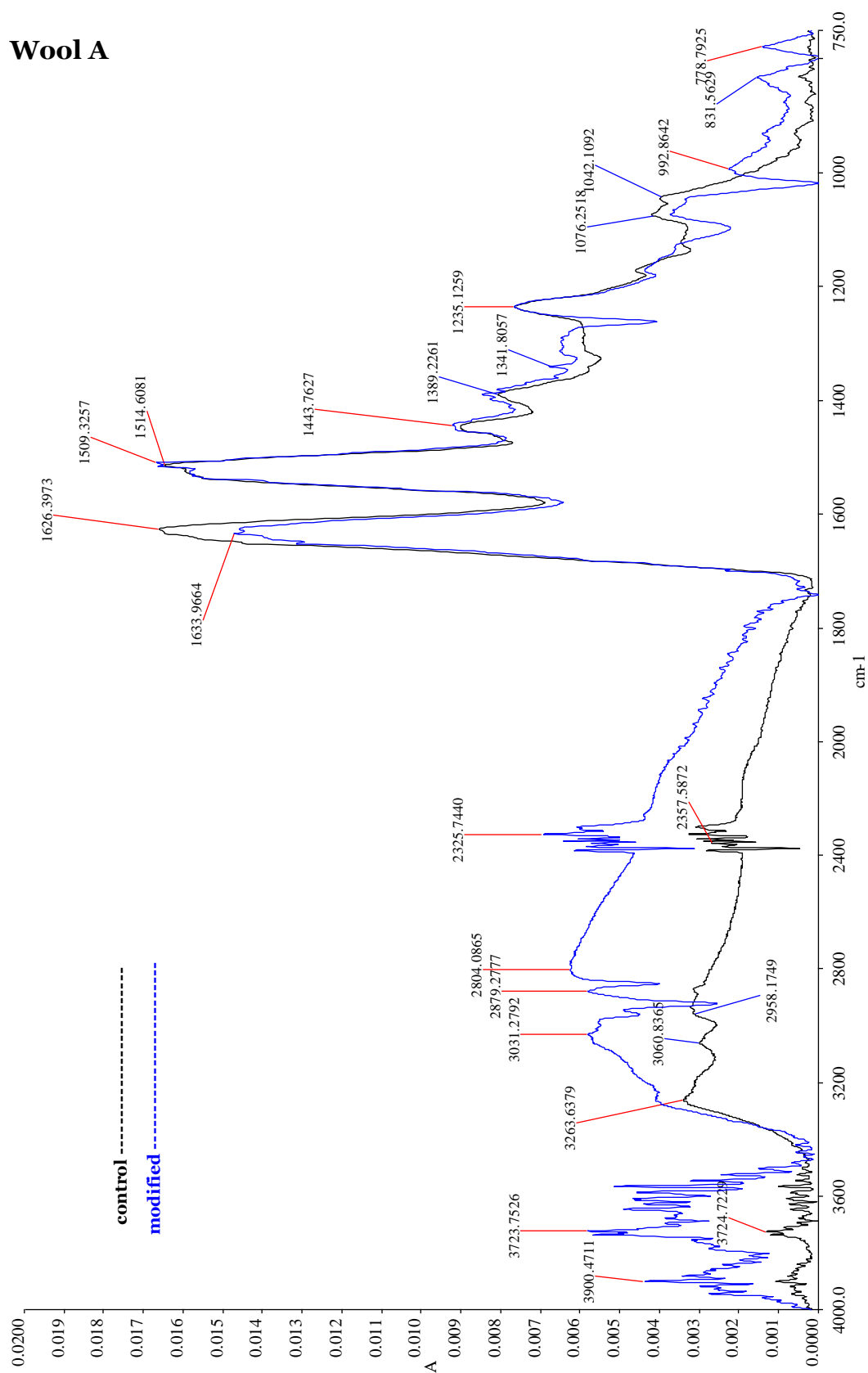
Wool A

(Treatment parameters: 140W, 1%O_2, 5mm and 5s/mm)

Figure 4-12   FTIR-ATR spectrum of the control and plasma-modified **wool A**
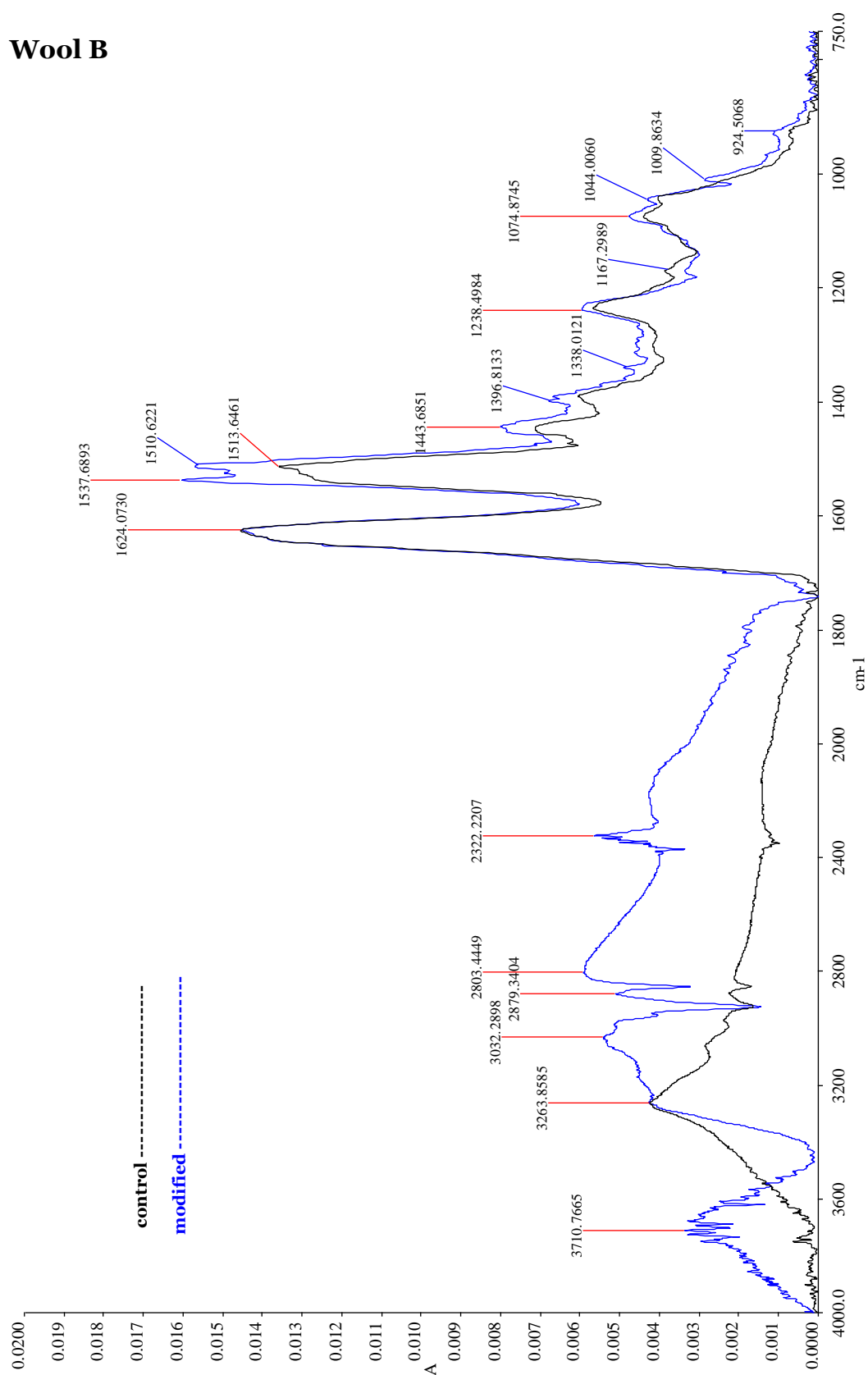
Wool B

(Treatment parameters: 140W, 1%O_2, 5mm and 5s/mm)

Figure 4-13   FTIR-ATR spectrum of the control and plasma-modified **wool B**

Chapter 4   Plasma system for wool fabrics

As a complement, the variation in S(II) and S(VI) peaks was studied to determine the degree of disulphide crosslink cleavage of the A-layer. Meanwhile, the surface chemistry of the wool substrate was altered upon the exposure to the oxidative plasma. A detailed analysis of XPS data revealed a shifting of the elemental peak area of S_{2P} from S(II) to S(VI). A growth of S(VI) peak and a drop in S(II) peak simultaneously indicated the oxidation of cysteine S(II) into the respective cystine oxides and cysteic acids S(VI). These oxidised S(VI) containing functionalities gave additional surface hydrophilicity to the wool fabrics. The change was graphically presented in **Figure 4-14**. Δ[S(VI)/S(II)] was calculated as an indicator of the reduction of disulphide crosslinks as presented in **Tables 4-6 and 4-7** respectively**.** Δ[S(VI)/S(II)] was determined as the change of the ratio of S(VI) to S(II) of the modified fabrics ([S(VI)/S(II)]$_P$) against the ratio of the control fabrics ([S(VI)/S(II)]$_o$). Detailed calculation is illustrated in **Equation 4-4** of Section **4.2.4.5**.

122
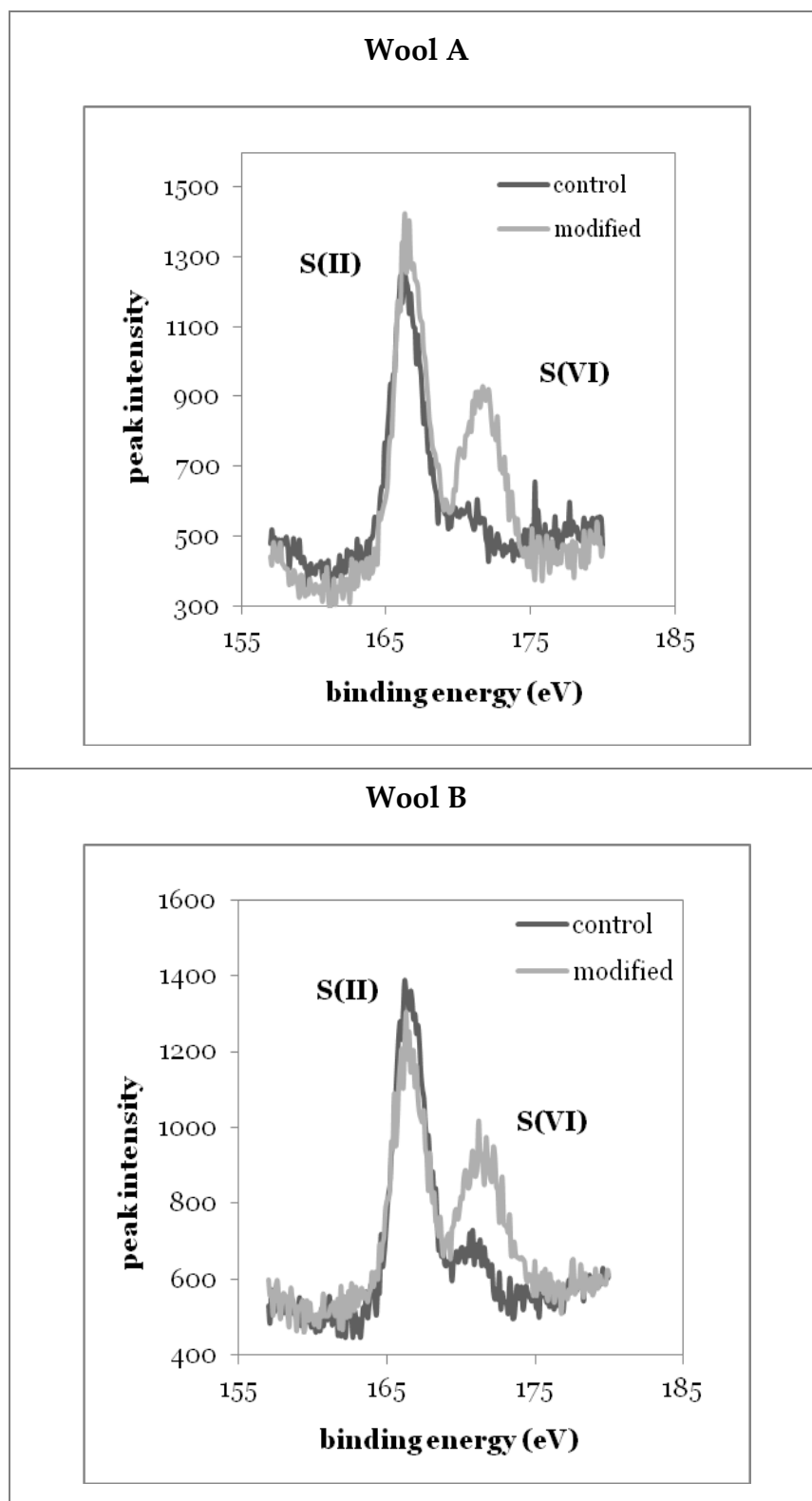
(Treatment parameters: 120W, 1%O_2, 5mm and 5s/mm)

Figure 4-14   XPS S_{2P} peaks of a) control fabrics and b) plasma-modified fabrics using XPSPeak4 software.

Table 4-6   XPS analysis of S content of the plasma-modified **wool A**

Treatment time (s/mm)	S(II)	S(VI)	[S(VI)/S(II)]	Δ [S(VI)/S(II)]
control	0.028	0.005	0.173	N/A
1	0.016	0.008	0.466	+1.693
2	0.018	0.008	0.432	+1.495
3	0.018	0.014	0.739	+3.272
4	0.021	0.012	0.563	+2.257
5	0.021	0.015	0.705	+3.077

Positive values represent the increase of Δ [S(VI)/S(II)] with respect to the control sample.(Constant parameters: 120W, 1% O_2 and 5mm)

Table 4-7   XPS analysis of the plasma-modified **wool B**

Treatment time (s/mm)	S(II)	S(VI)	[S(VI)/S(II)]	Δ [S(VI)/S(II)]
control	0.024	0.004	0.178	N/A
1	0.016	0.012	0.734	+3.119
2	0.017	0.013	0.740	+3.153
3	0.015	0.012	0.784	+3.397
4	0.016	0.012	0.795	+3.460
5	0.017	0.017	1.005	+4.641

Positive values represent the increase of Δ [S(VI)/S(II)]with respect to the control sample.(Constant parameters: 120W, 1% O_2 and 5mm)

4.3.3   Surface nano-fabrication in relation to plasma parameters

4.3.3.1   Variation of surface properties with treatment time

Surface topographical modification is time-dependent (Kan, 2007). A progressive topographical alternation is shown in **Figures 4-6 and 4-7** within 1 to 5s of study duration. W**ool A** exposing to 120W plasma with 1% O_2 at 5mm-jet distance only induced furrows parallel to the fibre axis of cuticles at the initial stage of plasma etching of 1s. Some observable nano-bumps scattered around the cuticles for 2s of exposure. In order to induce an appreciable amount of nano-crystalline structures over the whole cuticles, 3s of exposure was needed together with sufficient plasma active species accumulated on the cuticle surface. The nano-structure was found to be within a wide range of **50** to **130nm** in diameter. Upon exposing to the plasma for 4s, the nano-bumps with the diameter ranging from **70** to **90nm** were evenly distributed on the modified **wool A** fibre. Increasing the treatment time to 5s would enhance the dimension of the induced surface structure from nano-scale to micro-scale ranging from **0.19 to 0.3μm**. Thermal reaction overwhelmed the oxidation reaction resulting in melting and merging of nano-bumps into micro-bumps in the elongated rod shape.

Wool A was relatively less resistant to plasma etching. When the etching power of plasma was increased, nano-structures would melt and merge together. With reference to **Figure 4-7**, 120W plasma with 0.5%O at 5mm-jet distance possessed stronger etching power (Jeong et al., 2000; Schütze et al., 1998) which would induce a severer etching of the wool substrate. Induced surface structures were in micro-scale with a severe erosion of the cuticles.

Wool B was relatively resistant to plasma etching. 120W plasma with 1% O_2 showed no observable change of the surface cuticles under SEM at the magnification of 10,000x for all treatment times as shown in **Figure 4-6**. 120W plasma with 0.5 %O_2 at 5mm-jet distance which possessed stronger etching power (Jeong et al., 2000; Schütze et al., 1998) was employed in order to initiate the development of nano-structure on wool B fibres. 1s of exposure to plasma did not induce any observable change on the wool cuticles as shown in **Figure 4-7** at the magnification of 10,000x. As for 2s of exposure, some observable micro-bumps were developed on the surface with the diameter ranging from **0.12** to **0.21μm.** The diameter of nano-bumps formed on the plasma-modified wool fabrics was in nano-scale ranging from **50** to **90nm** after 3s of exposure with sufficient amount of plasma species accumulated on the surface. Increasing treatment time would not continuously reduce the dimension of the nano-bumps. In contrast, the dimension of the induced surface structures increased from nano-scale to micro-scale ranging from **0.12** to **0.25μm** when the treatment time was extended to 4s and 5s respectively.

The resultant macroscopic wetting behaviour of the plasma-modified wool surface was verified to be time-dependent. The aqueous liquid was spreading over the plasma modified wool surface covering an increased area subsequently with the enhancement of surface hydrophilicity after the oxidative He-O_2 plasma treatment as illustrated in **Figure 4-15**. The microscopic elemental analysis explicated the physical phenomenon. According to **Tables 4-2 and 4-3**, the increment of hydrophilic groups was progressively increasing with treatment time. The concentration of surface disulphide crosslink was reducing with treatment time.

----
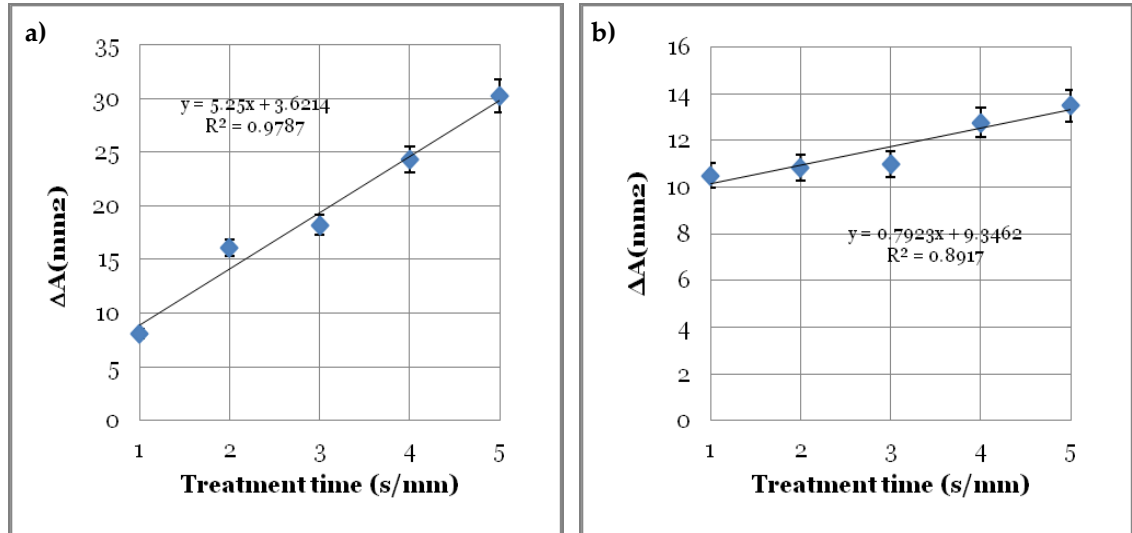
a) wool A; b) wool B. (Constant parameters: 120W, 1% O_2 and 5mm).

Figure 4-15   A time-dependent modification of wetting behaviour of wool
fibres induced by He-O_2 oxidative plasma.

Theoretically, the degree of etching-hydrophilisation increases with treatment time. Hence, the improvement of wetting behaviour would be amplified accordingly. However, when considering the actual application of the APP treatment to textile materials, it is undesirable to increase treatment time indefinitely. Firstly, increasing the treatment time will increase production cost. The He-O_2 oxidative plasma will degrade the fibres and alter the respective bulk properties, especially the mechanical properties.

The exact treatment time depended on the other three parameters, namely ignition power, O_2 concentration and jet distance. In general, 3s/mm was the optimum treatment time for the introduction of nano-crystalline structures to wool cuticles with an appreciable degree of hydrophilicity.

4.3.3.2   Variation of surface properties with ignition power and oxygen concentration

The APPJ instrument was powered by a radio frequency of 27.12MHz. Ignition power was a direct control of the plasma power in terms of etching and hydrophilisation. Plasma power was determined by the density, i.e. concentration of active species, and the kinetic energy of the plasma active species. In general, plasma power was proportional to ignition power. In the present study, three different ignition powers, i.e. 120W, 140W and 160W, were used. Ignition power was actually a direct control of the etching efficiency. It was believed that a higher ignition power would be capable of inducing crystalline structures at a faster rate as the plasma active species possessed more energy to bombard the substrate. However, thermal degradation of wool fibres would occur with the increasing ignition power. At higher powers, thermal reaction overwhelmed the oxidation reaction resulting in melt and merge of nano-structures of cuticles.

Within 1 to 5s of study duration, 120W would induce the distinct crystalline structures on the both wool A and wool B cuticles with 1% O_2 at a jet distance of 5mm for 5s/mm. When the ignition power was increased to 140W and 160W, the distinct crystalline structures disappeared. At higher ignition powers, a severe erosion of cuticles was observed as illustrated in **Figure 4-16** resulting in descaling. Other than the changing of the surface morphology, the surface chemistry was determined to be dependent on the ignition power. Though both wool A and wool B fabrics elicited similar morphological change with plasma, the surface wetting behaviour of two different wool fabrics

----

----

exhibited different manner in response to the aqueous liquid as illustrated in

Figure 4-17.

Ignition power	Wool A	Wool B
120W		
140W		
160W		
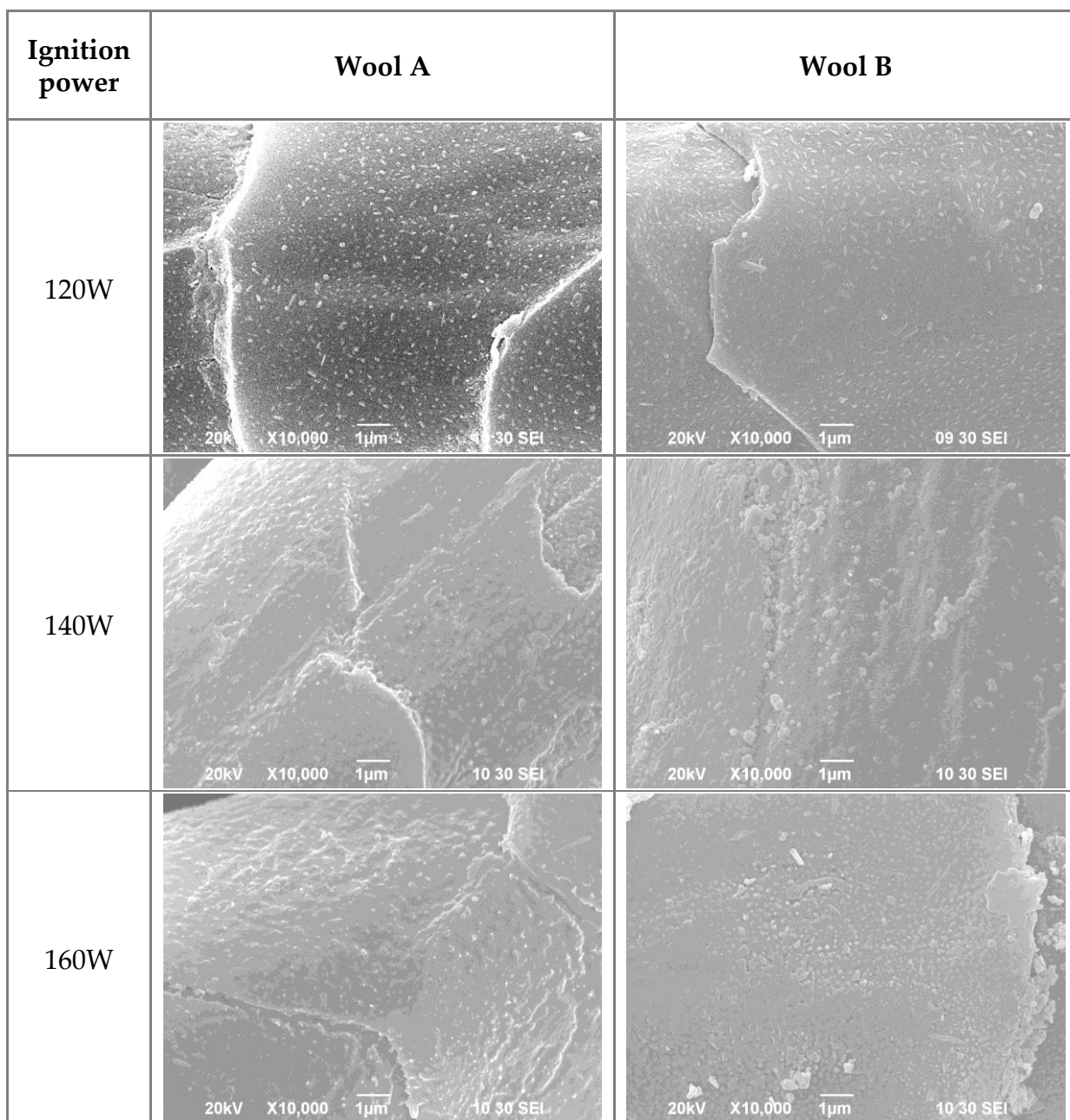
(Constant parameters: 1% O_2, 5mm and 5s/mm)

Figure 4-16   Variation of the plasma-induced surface topography of wool fabrics with respect to different RF ignition powers

----
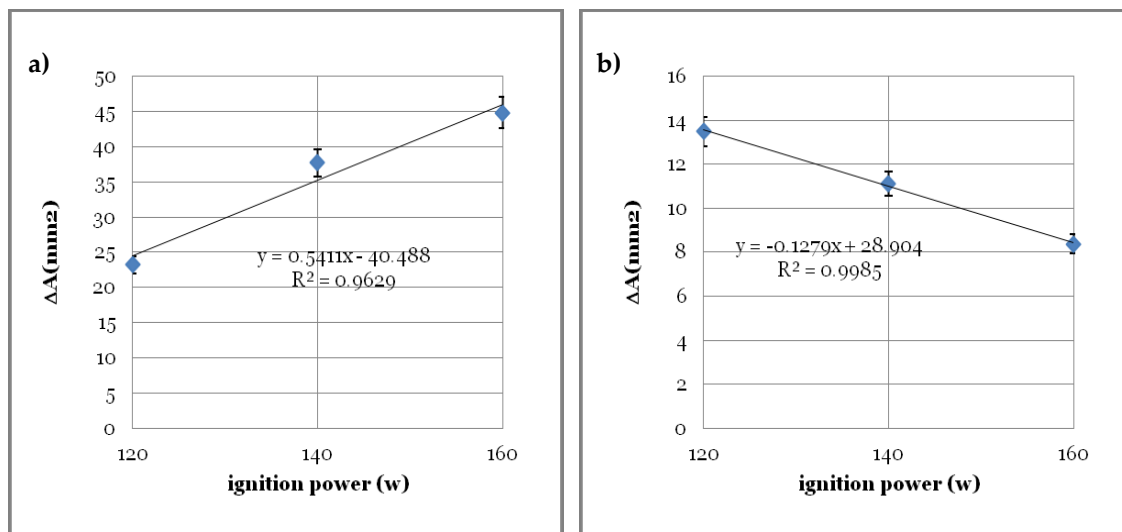
a) wool A; b) wool B. (Constant parameters: 120W, 5mm, 5s/mm)

Figure 4-17   Power-dependent plasma surface hydrophilisation of **wool substrates** shows a linear relationship revealed by the wetted area measurement.

The surface chemical composition gave some clues to the distinct trend of wettability modification of different wool substrates. With regard to **Table 4-8,** XPS analysis revealed that the C content of wool A was relatively higher than that of wool B. This indicated that the F-layer of wool A consisted of a higher concentration of fatty acids. More surface fatty acids would form a larger amount of polar LMWOF on the wool fibre surface via oxidation. The increment of total polar surface functionalities, **$\Delta(\Sigma polar/C)$,** with respect to different ignition power was presented in **Figure 4-18**.   When ignition power increased, Wool A surface formed more polar functional groups while polar groups on wool B reduced. This was a piece of important information confirming the variation of wetted area, ΔA. In **Figure 4-19** and **4-20**, FTIR revealed that the interaction newly formed polar LMWOF formed hydrogen

----

bonding represented by the sharp peak at 3725cm^{-1}. The intensity of 3725cm^{-1} of

the modified wool fabrics varied with ignition power in an opposite manner.

Table 4-8   Surface chemical composition of the control wool substrates based
on XPS analysis

Elemental content	Wool A	Wool B
C	0.662	0.646
O	0.186	0.198
N	0.107	0.128
S(II)	0.028	0.024
S(VI)	0.005	0.004
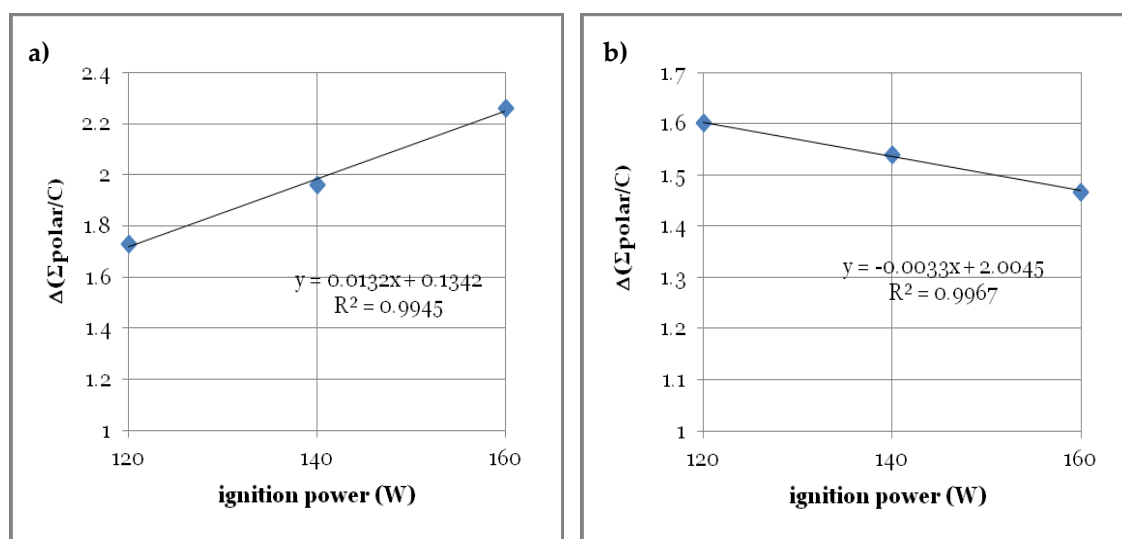
a) wool A; b) wool B. (Constant parameters: 1% O$_2$, 5mm and 5s/mm)

Figure 4-18   Power-dependent plasma surface oxidation of **wool substrates**
based on the XPS analysis of total surface polar elemental content

----
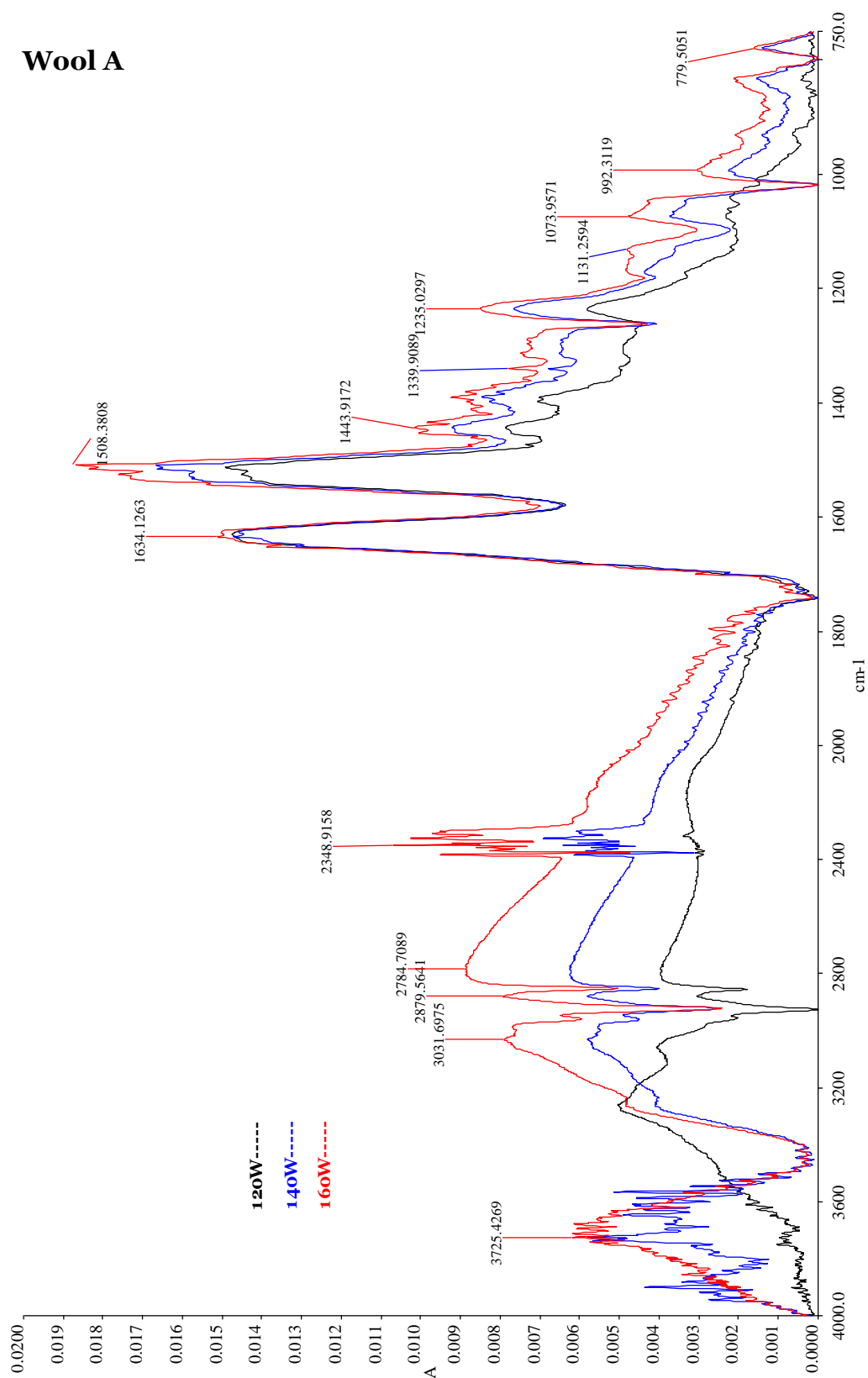
Wool A

(Constant parameters: 120W, 1%O_2, 5mm and 5s/mm)

Figure 4-19   FTIR-ATR spectrum of the plasma-modified wool A with respect to different ignition powers

Wool B
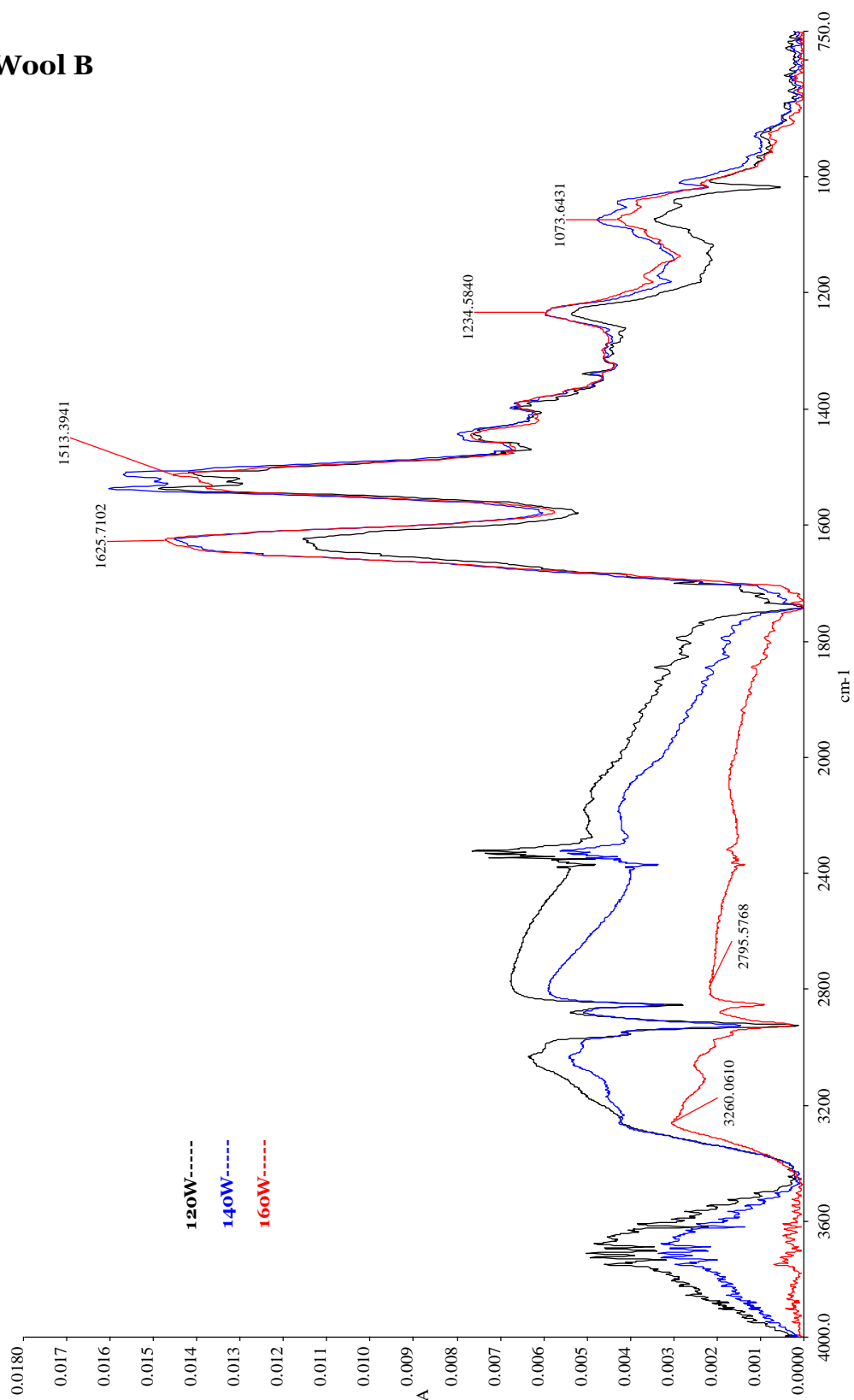
(Constant parameters: 120W, 1%O_2, 5mm and 5s/mm)

Figure 4-20   FTIR-ATR spectrum of the plasma-modified wool B with respect
to different ignition powers

For wool A, the hydrogen bonding was promoted with the increase of power. For wool A, oxidation of fatty acids was promoted with the increasing ignition power. Increased peak area at 2879 and 3031 cm^{-1} obtained from 120W to 160W indicated the increment of oxidised fragments of fatty acids and polar –OH functionalities respectively as shown in **Figure 4-19**. Consequently, a broad and sharp peak at 3725cm^{-1} grew significantly. The absorbed moisture assisted the wetting of the modified fabric surface. However, a different phenomenon occurred on wool B. Hydrogen bonding on modified wool B reduced significantly with increasing ignition power as shown in **Figure 4-20**.

In general, effectiveness of plasma is controlled by the ignition power. The higher the power, the larger amount to active species formed and hence facilitates the etching and hydrophilisation of substrate. Difference in fabric structure would be one of the possible reasons to explain the deviation of wool B from the conventional trend of surface oxidation.   Wool A was in twill form while wool B was in plain woven structure. Simultaneously, wool B was thicker and denser in fabric structure compared to wool A.   The deviation obtained was similar the study of Verschuren & Kiekens in 2005 (Verschuren & Kiekens, 2005). The pathway of plasma gas became more tortuous resulting in a longer residential time of plasma radicals within the inter fibril space of the fabric. Plasma-substrate interaction was lengthened sequentially. The degree of crosslink was reducing with the increasing power of plasma usually. Wool A followed the common trend as shown in **Figure 4-21a**. The reduction of $\Delta[S(VI)/S(II)]$ of modified wool A was proportionally increasing with ignition power. Lengthening of the plasma-substrate interaction led to the deviation of the wetting behaviour resulted in wool B.

The degree of surface crosslinks was affected by both the oxidative power and the UV intensity of the plasma. On one hand, crosslinks were cleaved by O active species via oxidation. The oxidative power of O was reducing with the residential time and distance travelled by the active species within the fabric structure, especially in ambient condition. Increasing ignition power was not able to overcame the velocity and energy lost. On the other hand, plasma is capable of inducing crosslinks. Plasma is luminous with a lots of UV photons generated in the excitation process. UV photons having a relatively longer lifetime and stronger penetration power (Holländer, et al, 1999) were able to survive and interact with wool B in the elongated pathway. As a result, induced crosslink of cleaved disulphide, i.e. crosslinks, reformed. In **Figure 4-21b** indicated the oxidation of disulphide bond was not able to be further promoted with the increase in ignition power as oxidation was being balanced by the reformation of crosslinks. The overall amount of S-containing polar LMWOFs subsequently reduced.

----
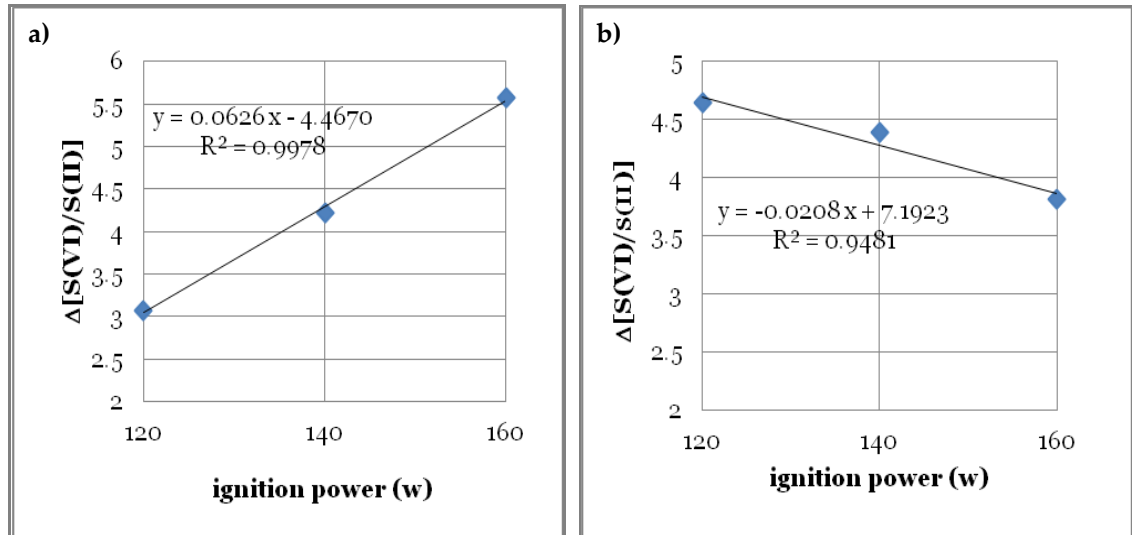
a) wool A; b) wool B. (Constant parameters: 1% O_2, 5mm and 5s/mm)

Figure 4-21   Power-dependent plasma surface oxidation of **wool substrates** shows a linear relationship as revealed by the elemental analysis of XPS of S_{2p} peaks.

As for the industrial application, a lower power input was essential to reduce energy consumption and production cost. For all powers, a complete wetting was observed within a rapid treatment of 1s/mm irrespective of the plasma variable being studied. After summarising the physical and chemical characteristics of the modified wool fabrics, 120W was considered as an appropriate ignition power for the nano-scale hydrophilisation of wool fabrics. 120W was sufficient to induce a complete wetting based on the contact angle goniometry resulting in an appreciable reduction of surface crosslinks with $\Delta[S(VI)/S(II)]$ being significantly boosted by over 3 times after plasma treatment for the two different types of fabrics presented as shown **Figure 4-21.**

The overall effective etching-hydrophilisation power of the plasma was closely related to the oxygen concentration in the APP system. Reactive O

----

species were generated in APPJ via Penning reaction (Jeong et al., 2000; Schütze et al., 1998). The dual etching and hydrophilisation reaction on the substrate surface were competing with each other. The concentration of reactive gas would determine which reaction was predominant. In general, physical ablation was predominant with low concentration of O_2 in accordance with the Penning reaction. Increasing the amount of O_2 would reduce the etching power of plasma and hence increase the dimension of the surface structures being formed. Etching power of plasma had in an inverse relationship with O_2 concentration in the system. 120W plasma operating at 5mm jet distance for 5mm/s was taken as an example. As a result, the macroscopic wetting behaviour of the wool fabrics was not linearly related to the concentration of O_2 as shown in **Figure 4-22**.
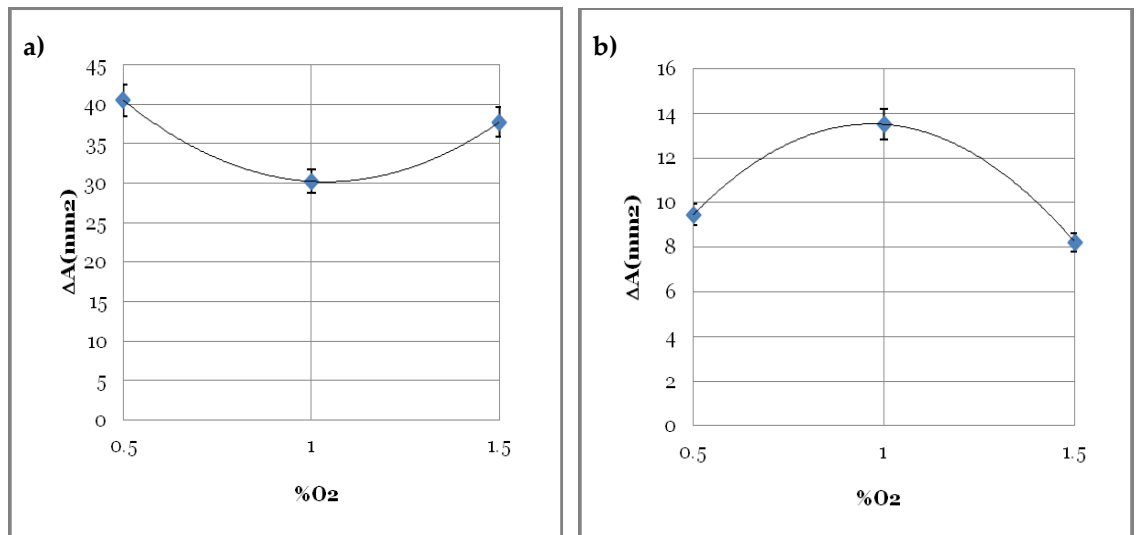
(Constant parameters: 120W, 5mm and 5s/mm)

Figure 4-22   Relative increment of the wetted area of two different types of wool fabric with respect various O_2 concentration

----

As for the consideration of achieving a minimal degree of etching, **1% O$_2$** was found to be the optimum concentration for the development of nano-crystalline structure on **wool A** cuticles as shown in **Figure 4-23**. Wool A was relatively susceptible to plasma etching. Using low concentration of O$_2$, i.e. 0.5%, would impose severe erosion on wool scale. No distinguishable scale edge was observed after exposing to 0.5% O$_2$ plasma. When the concentration was further increased to 1.5%, there is no observable surface structure detected at the magnification of 10,000x using SEM. A high concentration of O$_2$ consumed most of the He active species which were responsible for physical ablation of wool cuticle. In the case of wool B, **0.5% O$_2$** was found to be the optimum concentration for the development of nano-crystalline structure on cuticles as shown in **Figure 4-23**. With the presence of 1%O$_2$, the crystalline structures scaled up to micro-scale ranging from **0.18** to **0.47μm**. Increasing the O$_2$ concentration to 1.5% would further reduce the etching efficacy of plasma. There was a minimal amount of crystalline structure captured by the SEM at the magnification of 10,000x.

[O₂]	Wool A	Wool B
0.5%		
1%		
1.5%		
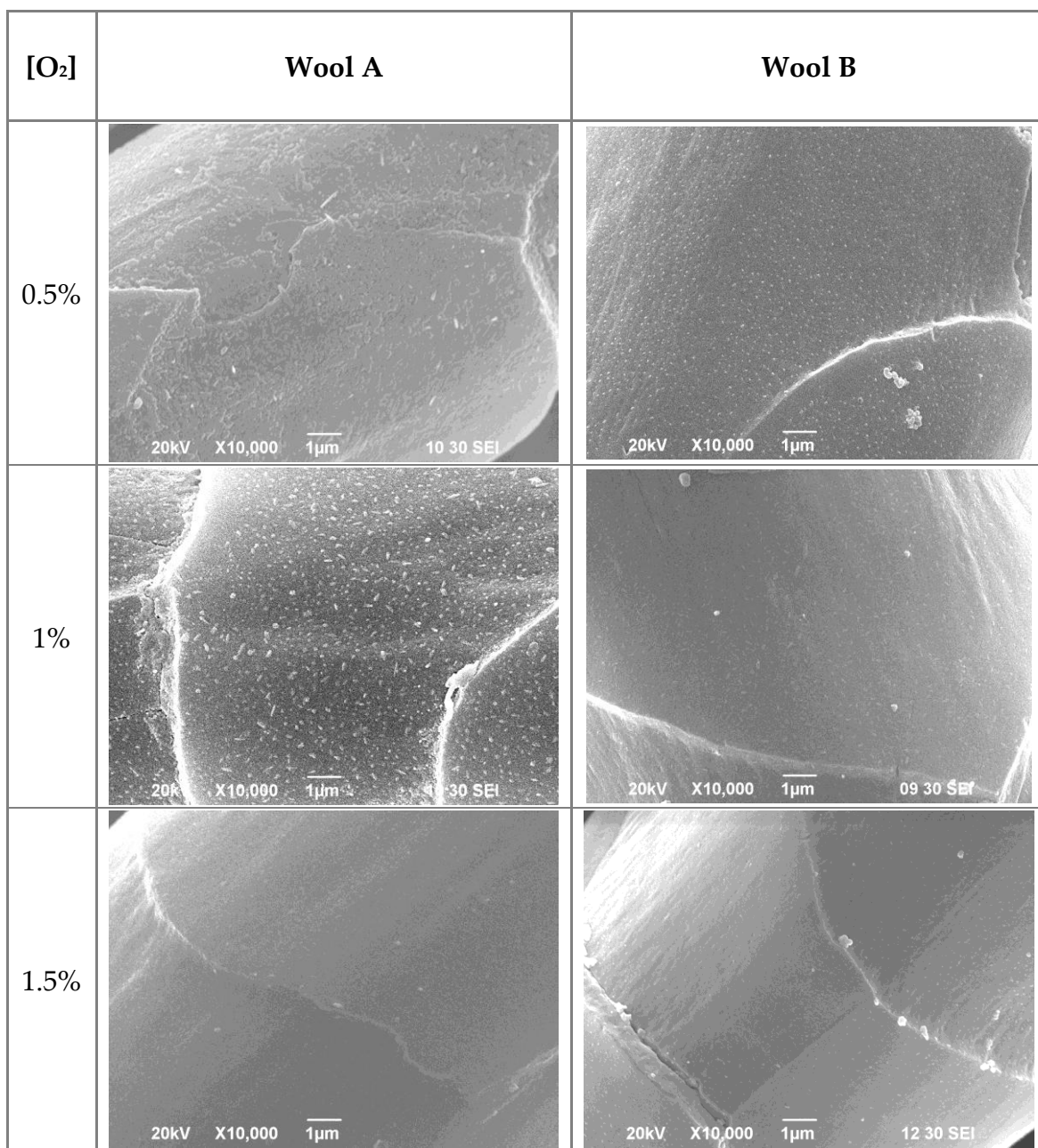
(constant parameters: 120W, 5mm and 3s/mm)

Figure 4-23   Surface atmospheric pressure plasma etching of two different types of wool fibres with respect to various O_2 concentrations at the magnification of 10,000x .

In order to achieve the greatest degree of hydrophilisation, 1.5% O_2 was found to be the optimum concentration of reactive gas for wool A as indicated by the wetted area measurement shown in **Figure 4-22**. When considering the hydrophilisation of wool B**, 1% O_2** was the optimum as shown in **Figure 4-24b and 25b**. Unlike PET film and polyester fabric, the surface of wool fibres wes multi-layered with distinct chemical composition. The prediction of the interaction between plasma and the substrate became more complicated as the plasma modified both the F-layer and the uppermost protein matrix of wool keratin.   The quantity of disulphide crosslinks was found to be the lowest with 1% O_2 plasma for the both types of wool fabrics indicated in **Figure 24a and 25a**. In order to achieve a nano-scale hydrophilisation of the wool fabrics, 1%O_2 would be considered as the optimum concentration with respect to the macroscopic observation obtained in the wetted area measurement and the SEM evaluation.

With reference to the XPS analysis of O and N content shown in **Figures 4-24 and 4-25**, 1.5%O_2 and 1%O_2 attained the largest amount of hydrophilic groups on the fibre surface of wool A and wool B respectively after APP treatment. The quantity of disulphide crosslinks was found to be the lowest with 1% O_2 plasma for the both types of wool fabrics. In order to achieve a nano-scale hydrophilisation of the wool fabrics, 1%O_2 would be considered as the optimum concentration with respect to the macroscopic observation obtained in the wetted area measurement and the SEM evaluation.
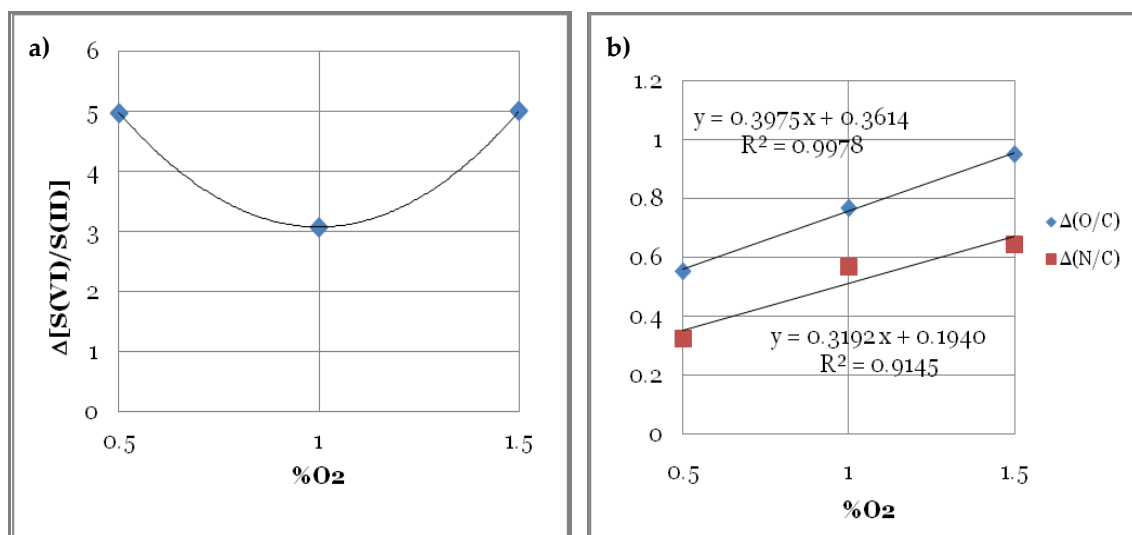
(Constant parameters: 120W, 5mm and 5s/mm)

Figure 4-24   Surface oxidation of **wool A** revealed by the XPS analysis was determined to be reactive gas-dependent
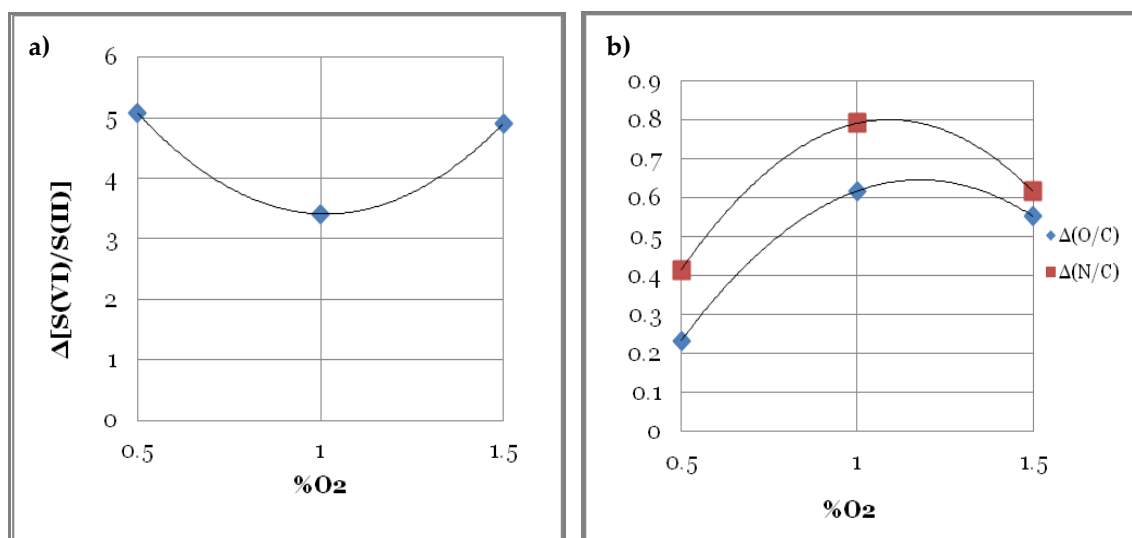
(Constant parameters: 120W, 5mm and 5s/mm)

Figure 4-25   Surface oxidation of **wool B** revealed by the XPS analysis was determined to be reactive gas-dependent

---

4.3.3.3   Variation of surface properties with jet distance

Plasma treatment utilising APPJ is a downstream treatment. Substrate is located below the nozzle as shown in **Figure 4-2**. Jet distance is defined as the perpendicular distance between the plasma nozzle and the substrate. On one hand, the active plasma species experience a severe collision with air molecules when travelling towards the substrate surface in the atmosphere. Velocity and energy content decrease with time and distance transported. On the other hand, the active species bounce off from the substrate surface with respect to a close vicinity of the plasma nozzle. Appropriate proximity between the plasma nozzle and the substrate affects the efficacy of the active species when etching a surface.

In the present study, the jet distance of 3, 5, and 7mm were studied at 120W with $1\%O_2$ for 1-5s/mm. Both types of wool fabrics responded to the jet distance in a similar manner. A close proximity to the plasma nozzle would induce thermal degradation of wool substrates, resulting in yellowing of wool fabrics. SEM revealed the importance of determining the appropriate jet distance in the plasma treatment. When the plasma nozzle was placed very close to the substrates, thermal degradation could be observed. With regard to **Figure 4-26,** the cuticles of wool were severely eroded without distinguishable cuticle cell edges when exposed to plasma at the jet distance of 3mm. With the increase in jet distance, the degradation of fibres was reduced. Distinguishable crystalline structures were also formed on the surface of wool cuticles at the jet distance of 5mm. However, no plasma-induced crystalline structures were distinguishable when the jet distance was further increased to 7mm. Cuticle surface was less eroded with the minimal surface roughness being observed by SEM at the

----

----

magnification of 5,000x. The surface morphology was found to be distance
-dependent.

Jet distance	Wool A	Wool B
3mm		
5mm		
7mm		
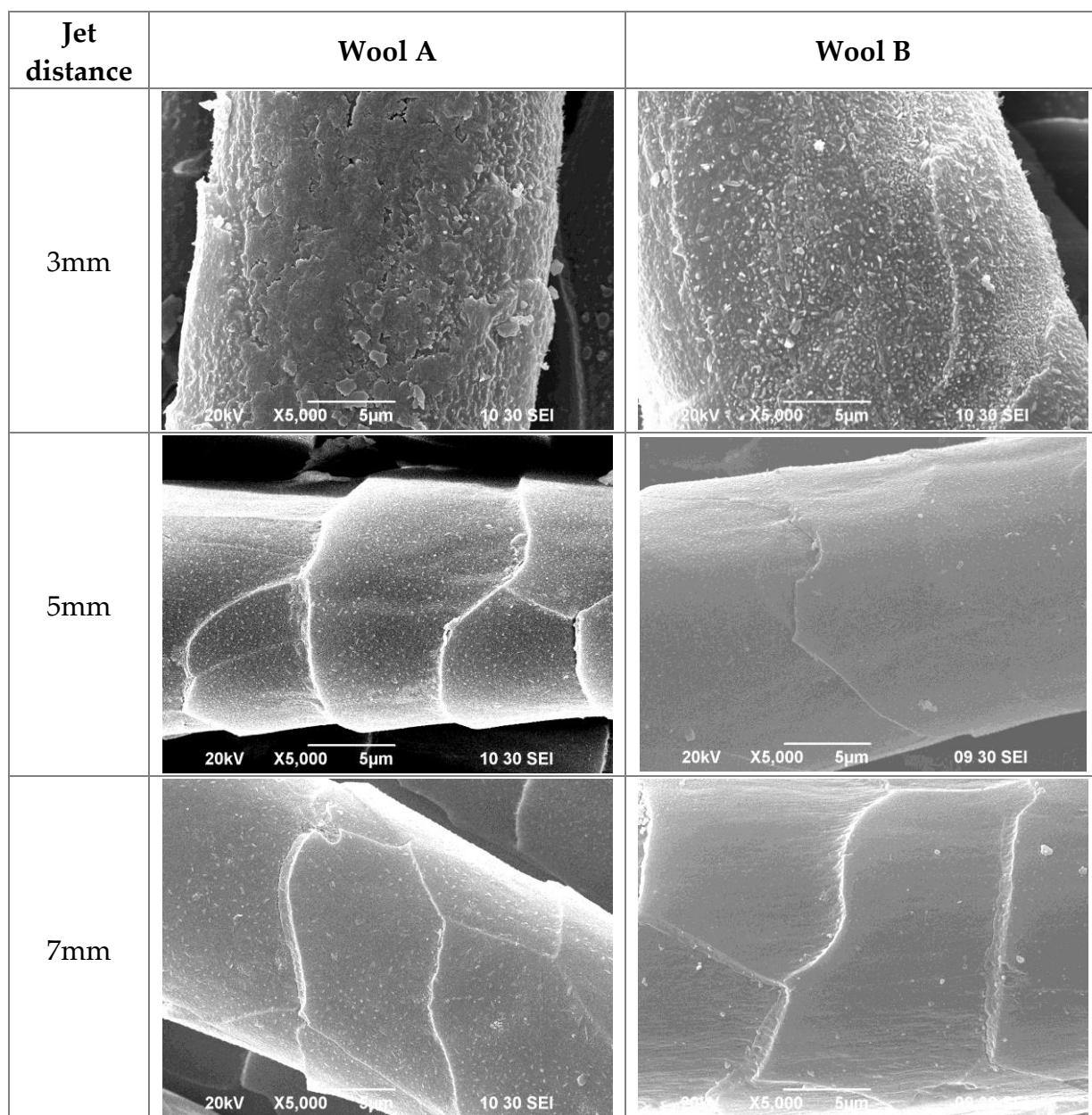
(Constant parameters: 120W, 1% O_2 and 5s/mm)

Figure 4-26   Nano-structure development of two different types of wool fibres
in relation to various jet distances revealed by SEM at the magnification of
5,000x

Other than surface morphology, surface chemistry of wool fabrics was also altered with respect to the jet distance accordingly. The relationship between the concentration of surface crosslinks and jet distance was verified to be linear as shown in **Figure 4-27.** The reduction of $\Delta[S(VI)/S(II)]$ was reducing with the increasing jet distant proportionally. This indicated that the active species in plasma did not possess sufficient energy for surface oxidation at a large jet distance. The degree of disulphide bonds showed a similar trend as the variation in the degree of surface erosion. However, the actual wetting phenomenon of the aqueous liquid was not linearly related to jet distance. Wetting behaviour of the modified fabrics was affected by both surface morphology and chemistry. In **Figure 4-28**, 3mm and 5mm were found to be the jet distance for the best improvement in the fabric wettability of wool A and B respectively. Nevertheless, 5mm jet distance would be selected to modify wool A. Close proximity of 3mm would lead to severe erosion of wool cuticles affecting the bulk properties of the fabric.

After combining the overall observation and results of wetted area, SEM and XPS of the modified wool fabric, **5mm** was the relatively effective jet distance for the APPJ etching-hydrophilisation of wool fabrics as it was capable of generating crystalline structures without severe erosion of surface cuticles with the improved surface wettability.


---
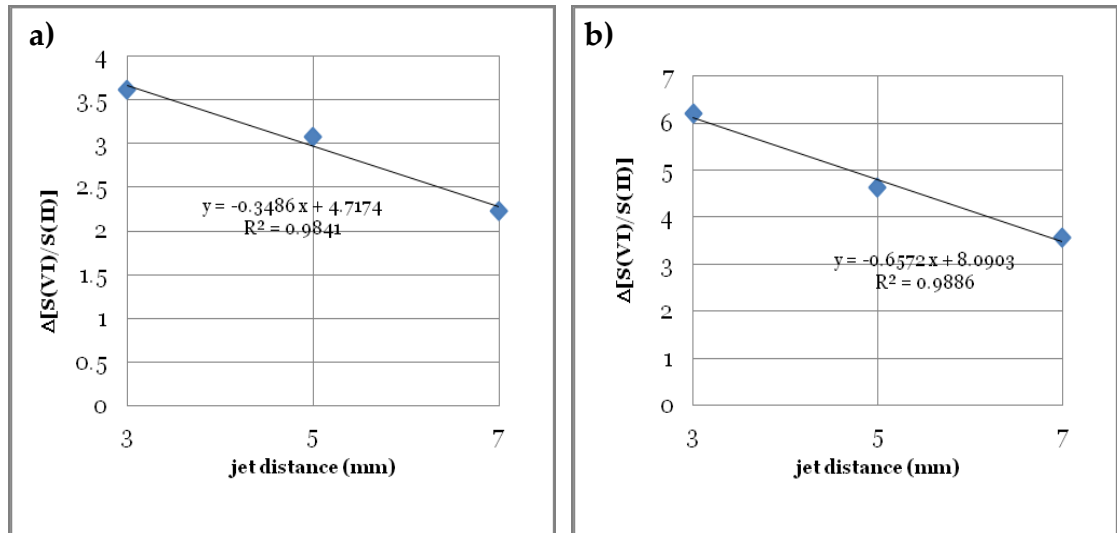
a) Wool A, b) Wool B (Constant parameters: 120W, 1% O_2 and 5s/mm)

Figure 4-27   Distance-dependent plasma surface oxidation of wool substrate shows a linear relationship as revealed by the elemental analysis of XPS of S_{2p} peaks.
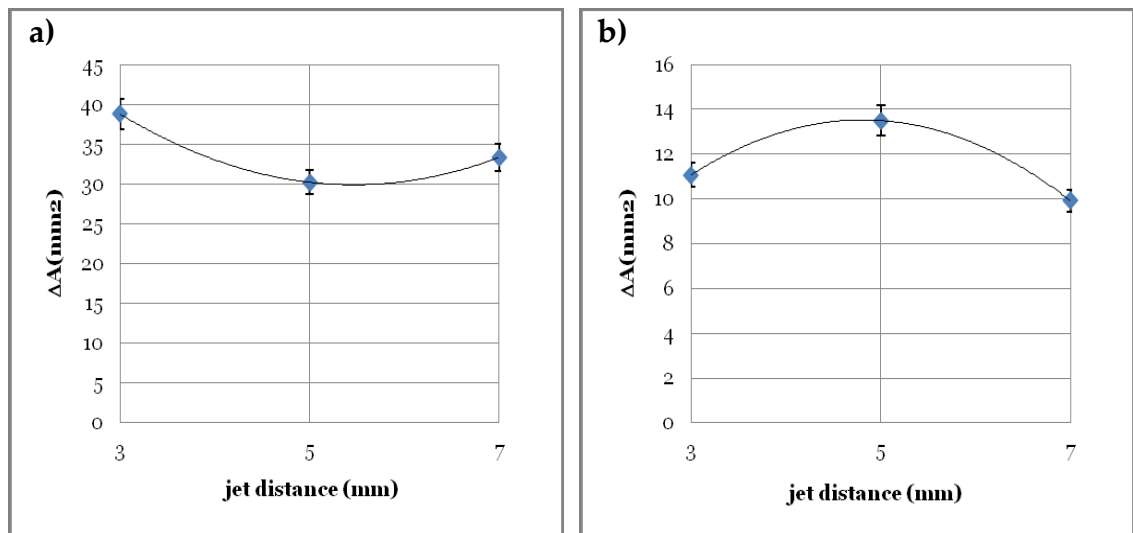
(Constant parameters: 120W, 1% O_2 and 5s/mm)

Figure 4-28   Relative increment of the wetted area of two different types of wool fabric with respect to the various jet distance

---

4.4   Conclusion

Nano-scale plasma etching-hydrophilisation on wool substrates was found to be achievable by He-O$_2$ atmospheric pressure plasma with the appropriate tuning of the plasma operation parameters. This study offers a deeper understanding of the physicochemical interaction between plasma and the textile materials.

With the assistance of advanced instrumentation for surface evaluation, a nano-scale hydrophilisation was determined to be achievable with the use of the optimum operation condition. When wool fabric A was located at 5mm with respect to the nozzle of the atmospheric pressure plasma jet operated at 120W with 1%O$_2$ for 4s/mm, the nano-scale surface roughening could be obtained with the improved surface wettability. Wool fabric B also afforded a similar but different optimum condition. Exposing wool B towards 120W plasma with 0.5% O$_2$ at a jet distance of 5mm for 3s/mm could attain the nano-crystalline structures on the cuticles with appreciable surface hydrophilisation being achieved.

Nature of the fibres, i.e. discrepancy in the susceptibility towards plasma etching, was the prime factor contributed to the deviation of the optimum condition for the plasma treatment to the same category of protein fibres. Good knowledge of the substrate was essential for the manipulation of the plasma processing of different textile materials. Plasma also showed substrate dependence in the modification.

Chapter 5 Plasma system for cotton fabric

5.1   Introduction

The depletion of non-renewable resources is leading to a resurgence of interest in the plant-derived materials in various textile sectors. Cellulosic fibre possessing attractive inherent bulk properties is widely be used in a diverse sectors with surface modifications (Allan et al., 2002; Baltazar-Y-Jimenez et al., 2007; Canal et al., 2009; Hoa et al., 2007; Karahan & Özdoğan, 2008; Mejía et al., 2009; Sinha & Panigrahi, 2009; Tsafack & Levalois-Grützmacher, 2007; Temerman & Leys, 2005). Plasma is an eco-friendly surface technique which can be used as an alternative to replace the conventional wet processing in textile industry. Atmospheric pressure plasma (APP) generates low temperature plasma flux which is suitable to modify heat fragile materials. The utilisation of plasma technique for nano-fabrication has attracted considerable attention (Matthews et al., 2004; Ren et al., 2008; Zhang & Fang, 2009).

The development of hydrophobic materials is closely related to nanotechnology which is extensively studied in recent years. Surface wettability is governed by the combination of surface roughness and chemical composition of a surface with respect to the detailed evaluation of super-hydrophobic natural materials such as lotus leaves and bird feathers (Bhushan et al., 2009; Hegemann, 2005; Liu et al., 2008; Tuteja et al., 2008). The acquisition of hydrophobic surface offering liquid repellency is exploitable for diverse applications. This section of the study examines the possibility of developing nano-scale bio-mimetic engineered materials in textile industry by employing APP technique.

The present study seeks to determine a controlled hydrophobisation of textile materials through the optimisation of the plasma nano-fabrication process. A hydrophobisation of cotton fabric was conducted with atmospheric pressure plasma jet (APPJ) using tetrafluoromethane (CF_4) and oxygen (O_2) as the reactive gases. The orthogonal experimental design technique developed by Dr. G. Taguchi (Taguchi, 1986) was employed to evaluate the four operation parameters including treatment time, ignition power, reactive gas concentration and jet distance in an attempt to control the hydrophobisation of the substrate. Detailed examination of the surface properties of the plasma-modified fabric was investigated with the use of static contact angle goniometry, wetted area measurement, mass loss measurement, scanning electron microscopy (SEM) and Fourier Transform infrared spectroscopy (FTIR-ATR).

5.2   Experimental

5.2.1   Materials

The plain woven cotton fabric of 129g/m^2 with thickness of 3.1mm supplied by Berlin Company was used as the substrate. The fabric was washed with 2% non-ionic detergent at pH 7 and 60°C for 30 min, and then rinsed with deionised water for 15 min. The scoured fabric was conditioned under the standard condition of 65 ±2% relative humidity and 21 ±1°C for at least 24 hours prior to all experiments.

Helium (He, 99.9% purity) was used as the inert carrier gas while tetrafluoromethane (CF_4, 99.9% purity) and oxygen (O_2, 99.9% purity) were used as reactive gases in the atmospheric pressure plasma treatment. Distilled water was used as the probing liquid for contact angle goniometry.

5.2.2   Instrumentation

Atmospheric pressure plasma jet (APPJ) manufactured by the Surfx Technologies LLC, CA was used as a downstream atmospheric pressure plasma treatment with substrates being exposed to the plasma afterglow. In this part of study, APPJs Atomflo™ 200 and Atomflo™ 400 were utilised for the plasma treatment of PET film and polyester fabric respectively.

5.2.3   Atmospheric pressure plasma etching

Two different reactive gases, namely CF_4 and O_2 were employed for the atmospheric pressure plasma (APP) hydrophobisation of the cotton substrate. A schematic diagram of the plasma treatment is shown in **Figure 5-1**.

R represents reactive gas, i.e. CF_4 and O_2

Figure 5-1   Schematic diagram of $He-O_2$ plasma treatment of cotton substrate

CF_4 plasma treatment was conducted by an APPJ, Atomflo™ 200 using a rectangular nozzle (AH-250L, Surfx Technologies LLC, CA)) which covered an active area of $25 \times 1 mm^2$. The nozzle mounted vertically above the substrate was moving at a constant speed of 2mm/s while exposing to the afterglow plasma generated from the radio frequency of 13.56MHz. He was used as the inert carrier gas. In parallel, O_2 plasma treatment was conducted by an APPJ, Atomflo™ 400 using a rectangular nozzle (AH-500L, Surfx Technologies LLC, CA) which covered an active area of $50 \times 1 mm^2$ vertically mounted above the substrate. The substrate was moving at a constant speed of 2mm/s exposing to the afterglow plasma generated by a radiofrequency of 27.12MHz. He was used as the inert carrier gas. After the APP treatment, the modified fabrics were conditioned at the relative humidity of 65 ±2% and 21 ±1°C prior to further evaluations. The CF_4 plasma-modified cotton samples were conditioned for at least 24 hours. In the case of O_2 plasma, the modified cotton samples were subjected to ageing for 720hrs.

The optimum condition of the hydrophobisation of the substrate in each system was determined through the orthogonal optimisation (Ye, et al, 2000; Yin & Jillie, 1987). The flow rate of the carrier gas, He, was fixed at 15 L/min and 30L/min in the systems of CF_4 and O_2 plasma respectively. The other four plasma variables including treatment time (T), ignition power (P), reactive gas concentration (R) and jet distance (d) were optimised based on the selected values of variables as shown in **Table 5-1**.

Table 5-1   The input factors and level settings assigned for the plasma etching optimisation

level	T(s/mm)	P(W)	R(%)	d(mm)
I	3	120	0.5	3
II	5	140	1	5
III	7	160	1.5	7

T is the treatment time; P is the plasma power; **R representing tetrafluoromethane, F or oxygen, O, which** is expressed as the percent of reactive gas; and d is the jet distance between the substrate and the jet nozzle.

5.2.4   Characterisation

5.2.4.1   Scanning electron microscopy (SEM)

Surface topographical feature of the plasma-modified fabrics was analysed using a scanning electron microscope (SEM, Model JSM-6490, JEOL Ltd., Japan). Samples were gold-coated with a sputter coater (Model SCD005, BAL-TEC, Liechtenstein) prior to SEM analysis. Images of plasma-modified fabrics were captured at the magnification of 5,000x, 10,000x and 15,000x with 20kV accelerating voltage for the investigation of nano-structures formed in the course of the treatment.

5.2.4.2   Contact angle goniometry

The change of surface wettability of the plasma-modified fabrics was characterised by the contact angle goniometry using the sessile drop technique with the aid of a micro-litre dispenser (GS-1200, Gilmont, Barnant Company, US). The contact angle defined as the tangential angle at the three-phase contact

----

point was evaluated based on the image was captured by a digital microscope (AM413T- DinoLite Pro, ANMO Electronics Corp., Taiwan). Two probing liquids including distilled water (72.8mN/m) and glycerol (63.4mN/m) were used and the drop size was 3μL. The recorded contact angle was reported as the average of 10 measurements of an individual sample. The paired comparison t-test was employed to confirm the significant difference of the reported data to be within a confidence level of 95%.

5.2.4.3   Wetted area measurement

Unlike the polymer film, cotton fabric is non-isotropic and porous. In order to quantify the surface wettability of the plasma-modified cotton fabric, the wetted area with a dye solution was recorded (Wardman and Abdrabbo, 2010). All the experiments were carried out in a conditioned room at a temperature of 22°C and relative humidity of 65%. The dye solution was an aqueous solution of 0.1g/L Solophenyl Blue FGL-01 165% and the drop size was 10μL approximately. The wetted area was defined as the area within the liquid boundary after complete drying. The wetted area recorded was reported as the average of 3 measurements of individual sample. The paired comparison t-test was employed to confirm the significant difference of the reported data to be within a confidence level of 95%. The wetting behaviour was quantified through the change of the dimension of the wetted area with the dye solution with respect to the control fabrics. The change was calculated as the relative increment of the wetted area, $\Delta A = (A_P - A_o)/A_o$ where A_P is the wetted area of the plasma-modified cotton fabric, and A_o represents the wetted area of the control fabric respectively.

5.2.4.4   Mass loss measurement

To quantify the degree of etching by plasma, the etching rate was calculated based on the mass loss measurement (Gao, et al, 2009). The mass of fabric sample was weighed by an electronic semi-micro balance (CPA225, Sartorius AG, Germany). The mass loss ΔM was calculated as $(M_P - M_o)/M_o$ where M_P and M_o are the mass of plasma-modified sample and the mass of the original samples respectively. The mass measurement recorded was reported as the average of 3 measurements of individual sample. The paired comparison t-test was employed to confirm the significant difference of the reported data to be within a confidence level of 95%. The etching rate E (nm/s) was derived from the mass loss based on the density of the cotton fabric.

5.2.4.5   Fourier transform infrared spectroscopy (FTIR-ATR)

Perkin Elmer spectrophotometer (Spectrum 100, Perkin Elmer Ltd.) equipped with a horizontal attenuated total internal reflectance (HATR) accessory was used to analyse the surface chemical composition of the plasma-modified cotton fabric. ZnSe was employed as the ATR crystal. Each FTIR spectrum obtained was an average of 128 scans with a resolution of $4cm^{-1}$. A semi-quantitative analysis of the surface chemical modification was based on the peak area of the spectra recorded.

5.3   Results and discussion

Orthogonal design for process optimisation is useful for the design of experiments widely employed by scientists, researchers and engineers. The theory was developed by a Japanese engineer, Dr. G. Taguchi (Ross, 1996; Taguchi, 1995). A complete set of factorial experiments was applied to the system of with different reactive gases, namely He-CF_4 and He-O_2 respectively to condense the expenditure of tests and time. Four plasma variables investigated are treatment time (T), ignition power (P), reactive gas concentration (R) and jet distance (d) within the selected range as shown in **Table 5-1**. A fractional factorial experimental design of four factors at three levels for each system was generated accordingly for plasma hydrophobisation of the cotton fabric. In the design, the correlation among various parameters was assumed to be negligible. The detailed arrangement of experiments is shown in **Table 5-2** helped reduce the total number of experimental trials to 9 runs.

Table 5-2   The orthogonal table with the designated $L_9 3^4$ of fractional factorial experimental design of four factors at three level settings used in the plasma etching optimisation.

	Variables			
run	T	P	R	d
1	I	I	I	I
2	I	II	II	II
3	I	III	III	III
4	II	I	II	III
5	II	II	III	I
6	II	III	I	II
7	III	I	III	II
8	III	II	I	III
9	III	III	II	I

Wetting behaviour of the liquids over the fabric surface is a complex phenomenon affected by the surface morphology, surface roughness and surface chemical composition of the substrate. The surface characteristics of the plasma-modified substrate depend strongly on the nature of plasma gas and the etching condition. In the present study, the cotton fabrics modified with both reactive gases, CF_4 and O_2, were found to be hydrophobic.

With the aid of the contact angle goniometry, the water contact angle (WCA) of original cotton fabric was determined to be **62.28°**. The droplets of distilled water stayed on the fabric surface modified by both the CF_4 and O_2 plasma. In general, water contact angles of CF_4 and O_2 modified cotton fabrics were boosted by at least **85% and 100%** respectively as illustrated in **Table 5-3**.

In parallel, the wetted area measurement revealed the rise of the hydrophobicity of the modified fabrics after plasma treatment as shown in **Table 5-4.** The wetted area of original fabric (A_o) was found to be **310mm²**. On the other hand, the wetted area of the modified fabrics (A_P) using CF_4 and O_2 was reduced significantly by at least **90% and 50%** respectively. It seemed that, both CF_4 and O_2 plasma have salient effect on the hydrophobicity of the cotton substrate. However, these two types of gas could induce surface hydrophobisation via different mechanisms.

Table 5-3   Surface hydrophobicity of the CF_4 and O_2 plasma-modified cotton revealed based on the contact angle goniometry with distilled water.

(* Values are statistically different at P < 0.05.)

Control Run	CF₄-modified cotton		O₂-modofied cotton	
	WCA	ΔWCA	WCA	ΔWCA
Control Run	62.28	N/A	62.28	N/A
1	113.54	+0.82	125.51	+1.02
2	115.5	+0.85	124.62	+1.00
3	119.12	+0.91	124.50	+1.00
4	115.19	+0.85	123.69	+0.99
5	108.32	+0.74	127.42	+1.05
6	118.81	+0.91	128.48	+1.06
7	120.51	+0.93	130.55	+1.10
8	123.42	+0.98	129.96	+1.09
9	116.44	+0.87	132.95	+1.13

WCA (º) represents water contact angles; ΔWCA (º) represents the changes of water contact angle with respect to the control fabric. Positive values of ΔWCA indicate the increment of hydrophobicity with respect to the control sample.

Table 5-4   Surface hydrophobicity of the CF_4 and O_2 plasma-modified cotton revealed based on the wetted area measurement with an aqueous dye liquid.

(* Values are statistically different at $P < 0.05$.)

Run	CF_4-modified cotton		O_2-modofied cotton	
	A_P	ΔA	A_P	ΔA
A_o	310	N/A	310	N/A
1	15	-0.953	242	-0.221
2	114	-0.855	82	-0.737
3	21	-0.931	271	-0.126
4	43	-0.882	211	-0.320
5	18	-0.928	35	-0.887
6	13	-0.959	151	-0.515
7	18	-0.943	97	-0.686
8	23	-0.926	277	-0.107
9	25	-0.912	10	-0.969

A_o (mm^2) represents wetted area of control fabric while A_P (mm^2) represents wetted area of modified fabrics. ΔA (mm^2) represents the changes of wetted area with respect to the control fabric. Negative values of ΔA indicate the improvement of hydrophobicity with respect to the control sample.

5.3.1   Hydrophobisation with CF$_4$ plasma

FTIR analysis was employed to verify the surface chemistry of the plasma-modified fabrics. Firstly, there was an increment of in plane –OH bending at 1420-1390cm^{-1}. The O-C-O and C-OH stretching at 1400cm^{-1} shown in **Figure 5-2** indicated the cleavage of cellulose molecules by hydroxyl abstraction and the bond scission by electrons and ions (Sahin, 2007). Simultaneously, plasma radicals also cleaved the chains of cellulose resulting in generating the short chains of unsaturated hydrocarbons. Neutral fluorine species present in the afterglow were proposed to be grafted on the active sites sequentially thereby generating an appreciable amount of fluorinated ketones (-CF$_2$COCH$_2$), carboxylic acids (-CF$_2$-COOH) and unsaturated hydrocarbons (F$_2$C=CF and F$_2$C=C) on the cellulose polymer chains eliciting characteristic frequency at 1800-1770cm^{-1}, 1780-1740cm^{-1}, 1870-1800cm^{-1} and 1760-1730cm^{-1} (Chalmers & Griffiths, 2002) as shown in **Figure 5-3**.

FTIR-ATR analysis confirmed that the plasma-substrate interaction was a free-radical fluorination process.

159
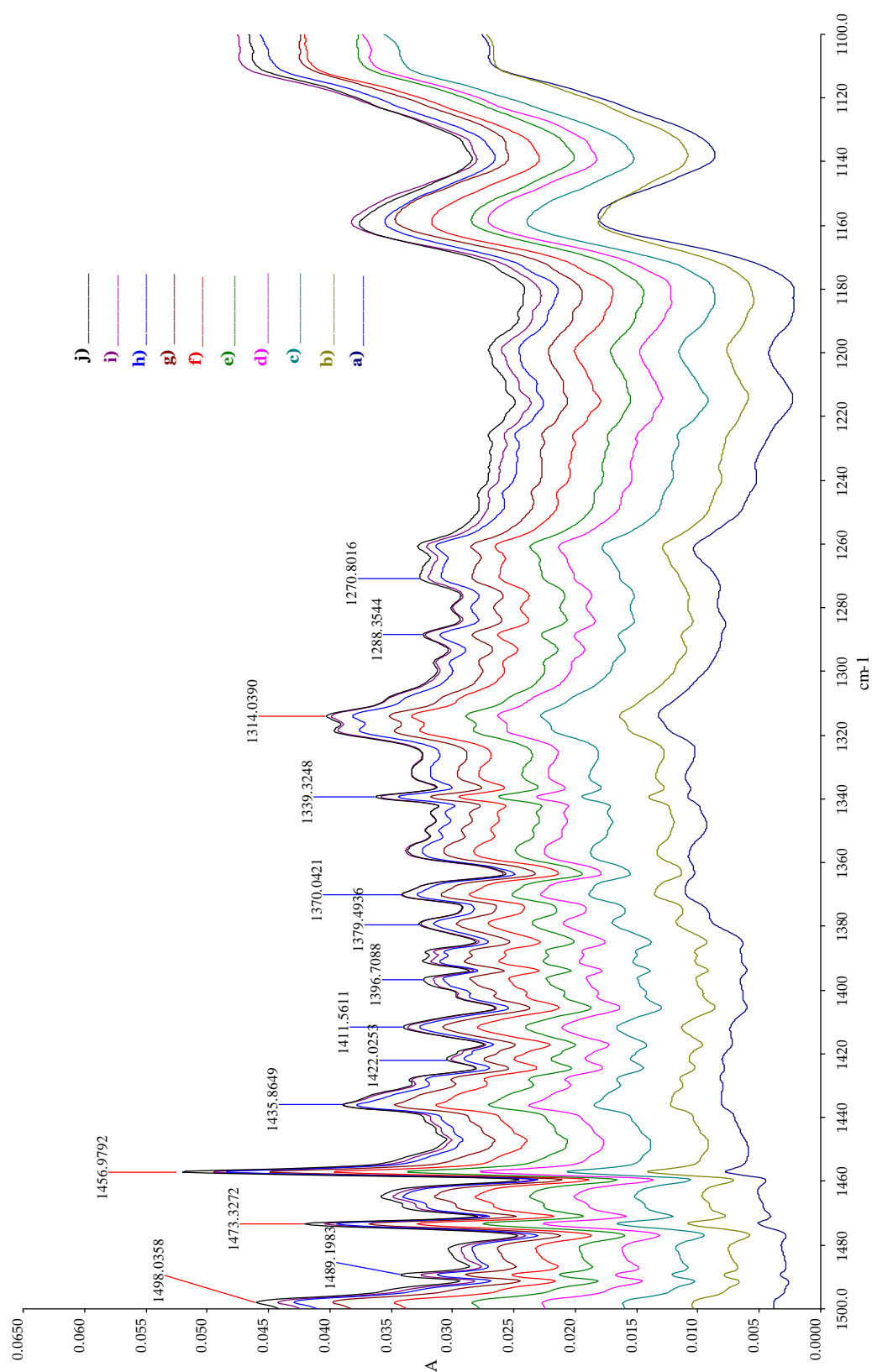
Spectrum (a) represents the control fabric and spectra (b)-(j) represent and optimisation runs 1-9 respectively.

Figure 5-2   FTIR spectra of the CF_4 modified cotton fabrics in the region of 1500-1000cm^{-1}.
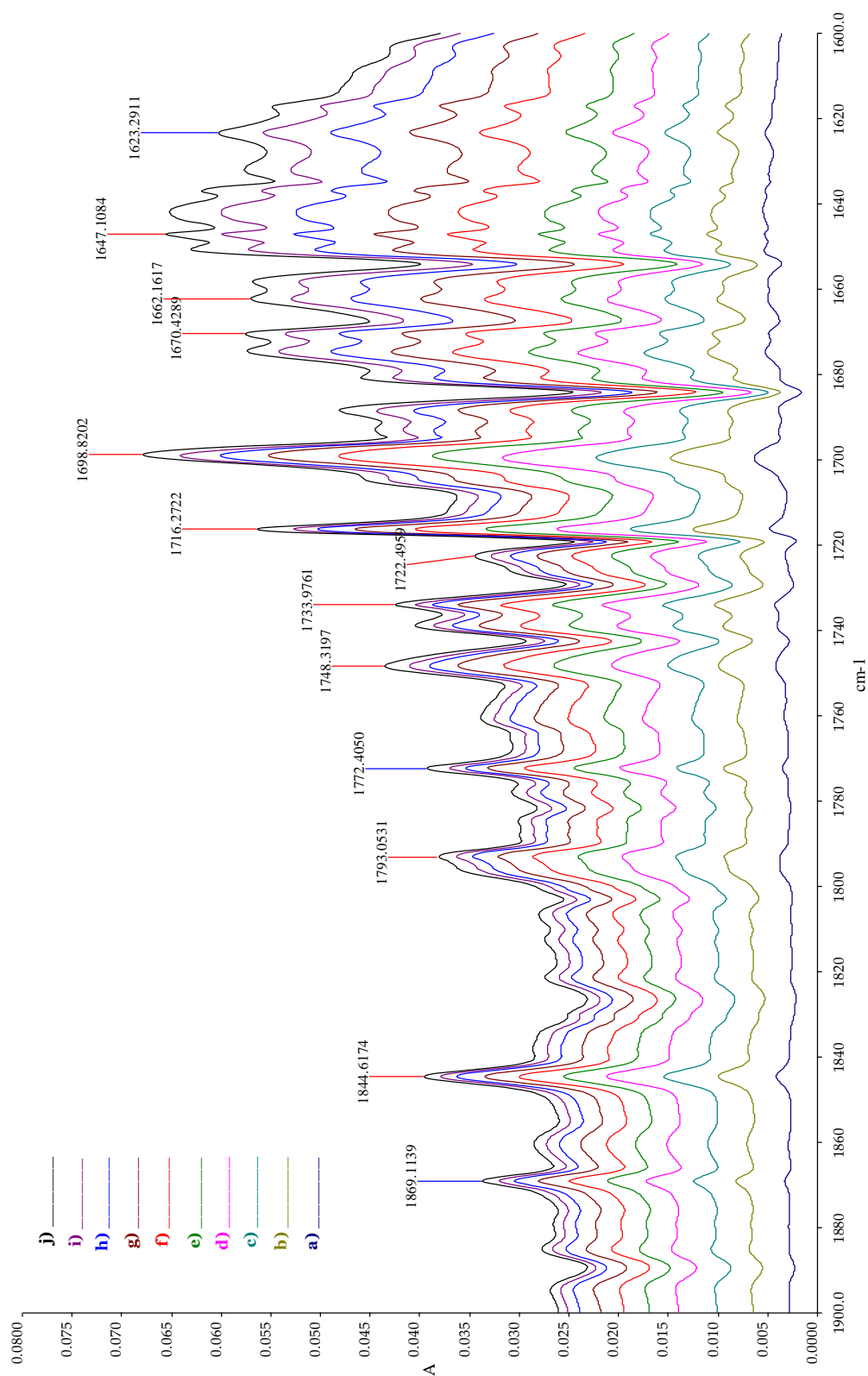
Spectrum (a) represents the control fabric and spectra (b)-(j) represent the optimisation runs 1-9 respectively.

Figure 5-3　　FTIR spectra of the CF_4 modified cotton fabrics in the region of 1900-1600cm^{-1}.

5.3.2 Hydrophobisation with O$_2$ plasma

In general, O$_2$ was used as the reactive gas for hydrophilic modification of hydrophobic surfaces. However, O$_2$ plasma was formed to be capable of eliciting etching-hydrophobisation of cotton fabrics by utilising the ageing effect of the plasma-modified surface.

FTIR analysis was also employed to reveal the surface chemistry of the O$_2$-plasma-modified fabrics. Firstly, there was an increment of O-H stretching at 2400-2270cm^{-1} as shown in **Figure 5-4,** indicating the formation of carboxylic acids via oxidation of the primary hydroxyl sites as proposed by Vaideki and his colleagues (Vaideki et al., 2007). Upon ageing, the surface polarity would be reverse. Masses of volatile LMWHFs are mobile moieties. The thermodynamic reorientation towards the bulk and sublimation in the open system of these polar moieties the modified cotton surface converted to be hydrophobic. The residual radicals continuously reacting with the ambient upon storage would be another factor contributing to the transformation of surface polarity and hence the wettability (Molina, et al, 2002; Nakamatsu et al., 1999; Wertheimer et al., 1999). Ageing of the modified fabric was detected by FTIR as shown in **Figure 5-5**. The increment of peaks at 2990-2850cm^{-1} and 2850-2700 cm^{-1} represented (-CH$_3$ and –CH$_2$-) and (-CH$_3$ attached to O) respectively (Chalmers & Griffiths, 2002; Vaideki et al., 2007). This indicated the formation of hydrophobic aliphatic hydrocarbons leading to the surface hydrophobisation of cotton fabrics. FTIR-ATR analysis also confirmed that the plasma-substrate interaction was an oxidative process.

As a result, the wetted area of the O_2 plasma-modified cotton fabrics listed in **Table 5-4** was reduced significantly after storage in the conditioned room in air at the relative humidity of 65 ±2% and 21 ±1°C for 720hrs.
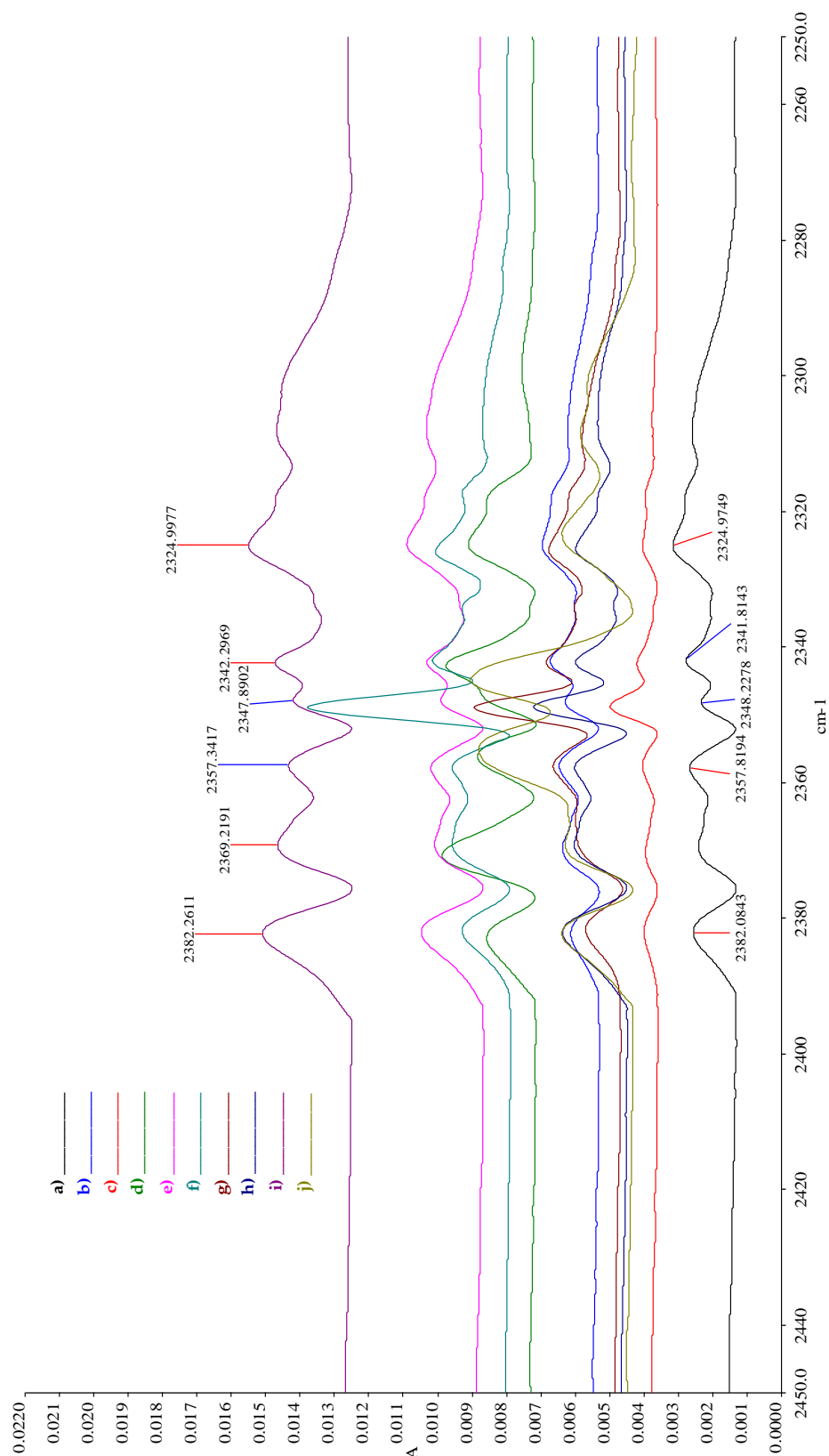
Spectrum (a) represents the control fabric and spectra (b)-(j) represent the optimisation runs 1-9 respectively.

Figure 5-4   FTIR spectra of the O_2 modified cotton fabrics in the region of 2400-2280cm^{-1}.
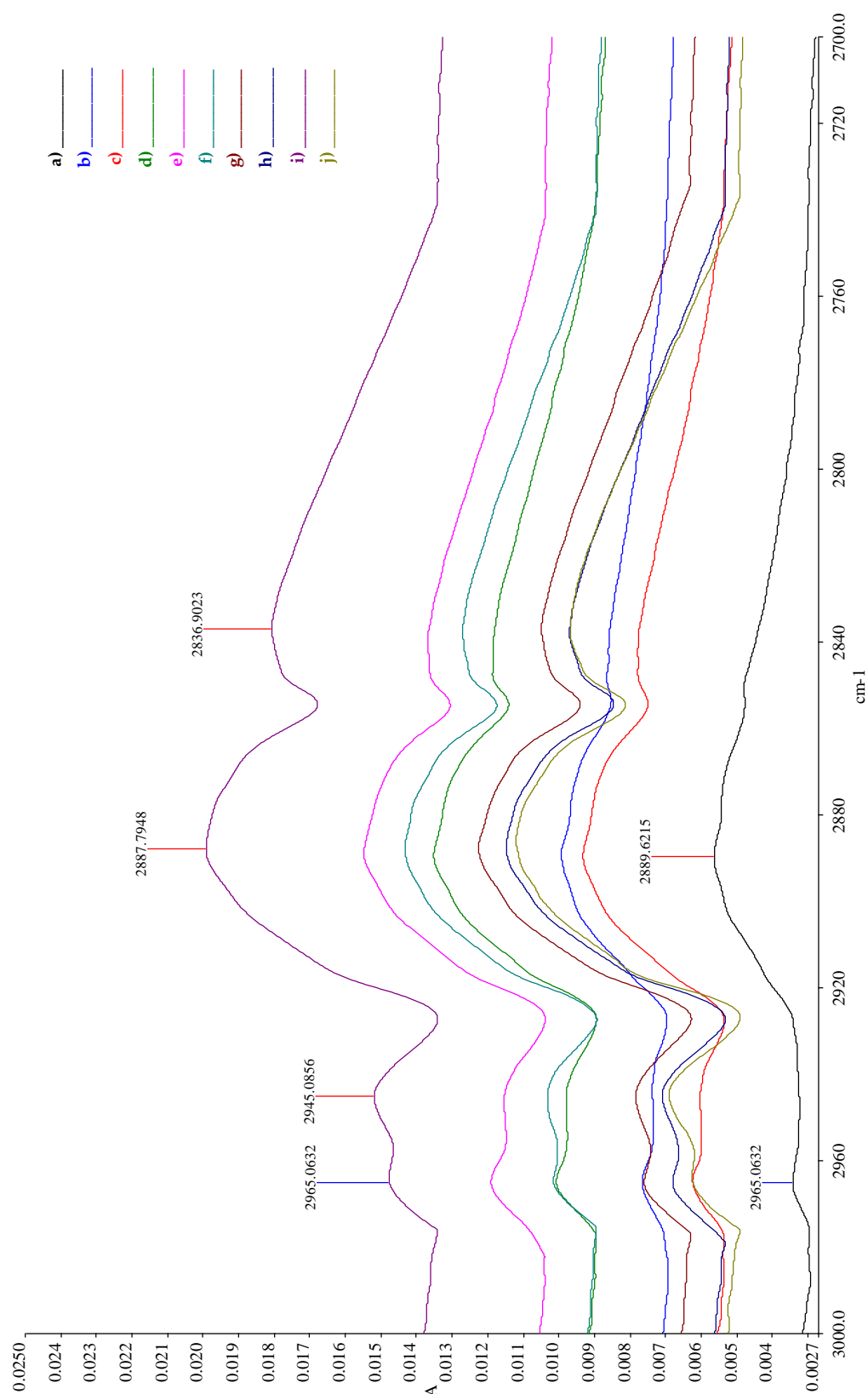
Spectrum (a) represents the control fabric and spectra (b)-(j) represent the optimisation runs 1-9 respectively.

Figure 5-5   FTIR spectra of the O_2 modified cotton fabrics in the region of 3000-2700cm^{-1}.

Chapter 5   Plasma system for cotton fabric

5.3.3   Surface texturisation by CF$_4$ and O$_2$

In spite of the nature of reactive gas in the plasma system, both CF$_4$ and O$_2$ would reduce the surface wettability of cotton fabric. Surface etching was proposed to be the prime factor contributing to the surface hydrophobicity. In accordance with the SEM images captured as shown in **Figures 5-6, 5-7, 5-8 and 5-9**, surface roughening was clearly observed. In addition, a reduction of fabric thickness was found to be in nano-scale with the depth of etching being limited within 100nm/s as illustrated in **Table 5-5**. Surface roughening introduced surface hydrophobicity to cotton fabrics overrode the effect of the surface chemical composition.
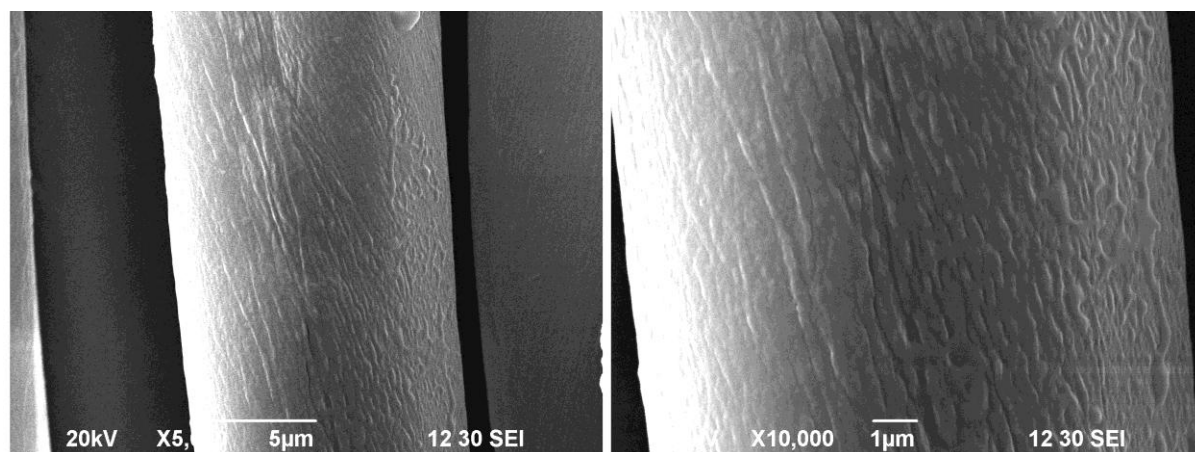
Figure 5-6   SEM micrographs of the original cotton fibres captured at the magnification of 5,000x and 10,000x
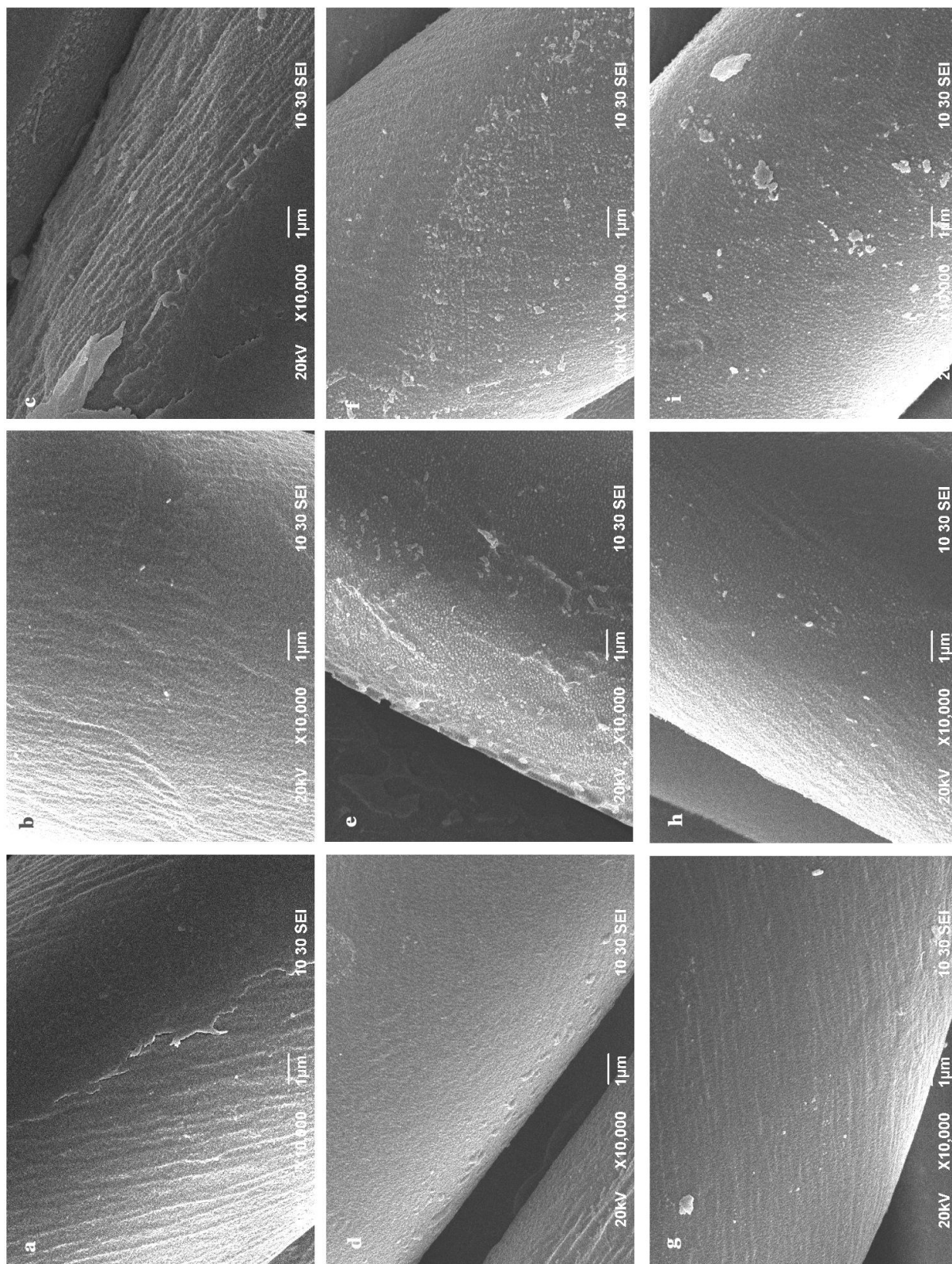
----

Micrographs (a)-(i) represent the optimisation runs 1-9 respectively at the magnification of 10,000x

Figure 5-7   SEM micrographs illustrating the surface morphology of cotton fibres exposed to the He-CF$_4$ atmospheric pressure plasma
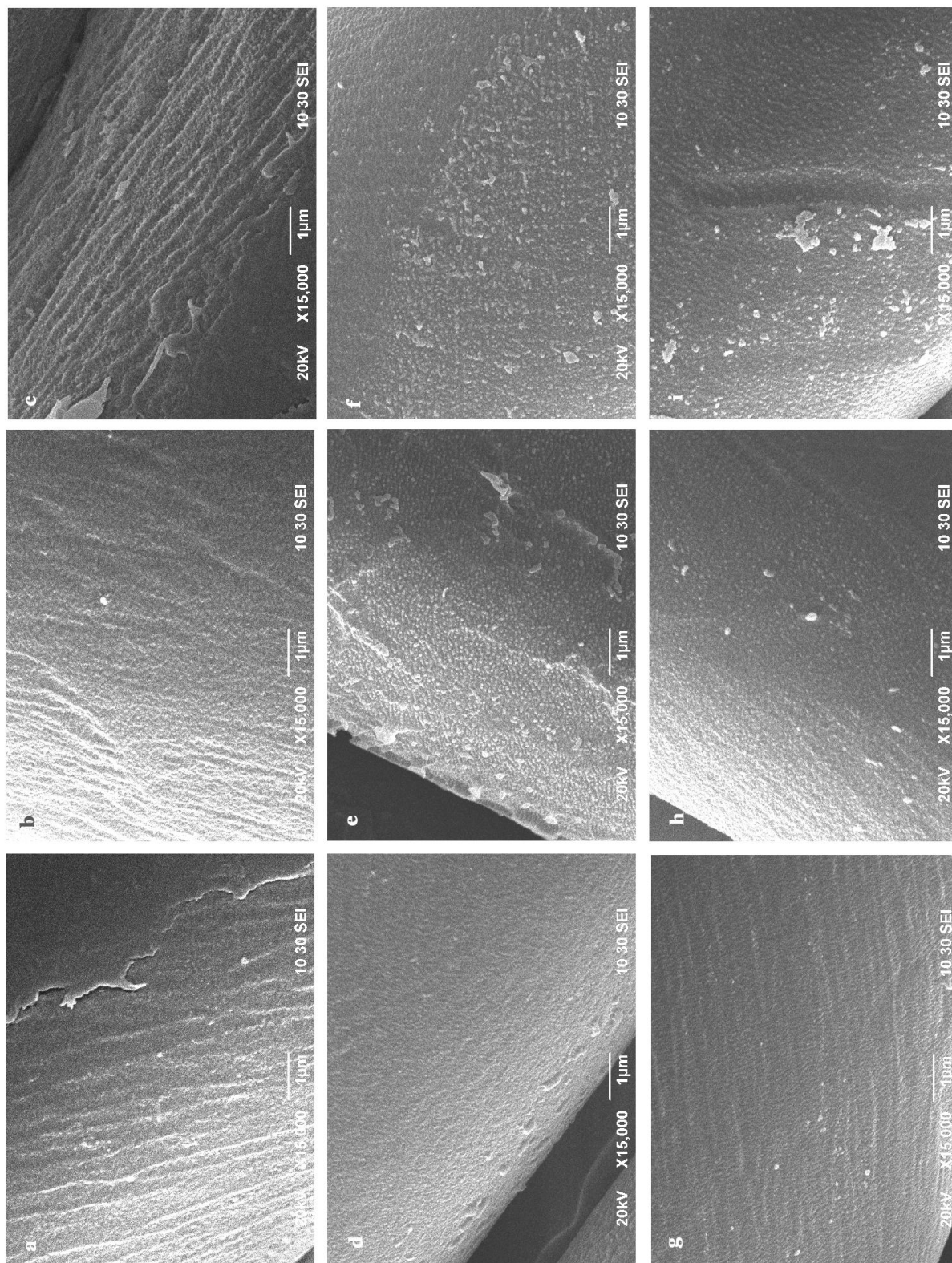
----

Micrographs (a)-(i) represent the optimisation runs 1-9 respectively at the magnification of 15,000x

Figure 5-8   SEM micrographs revealing the nano-scale surface modification of cotton fibres exposed to plasma using CF_4 as the reactive gas
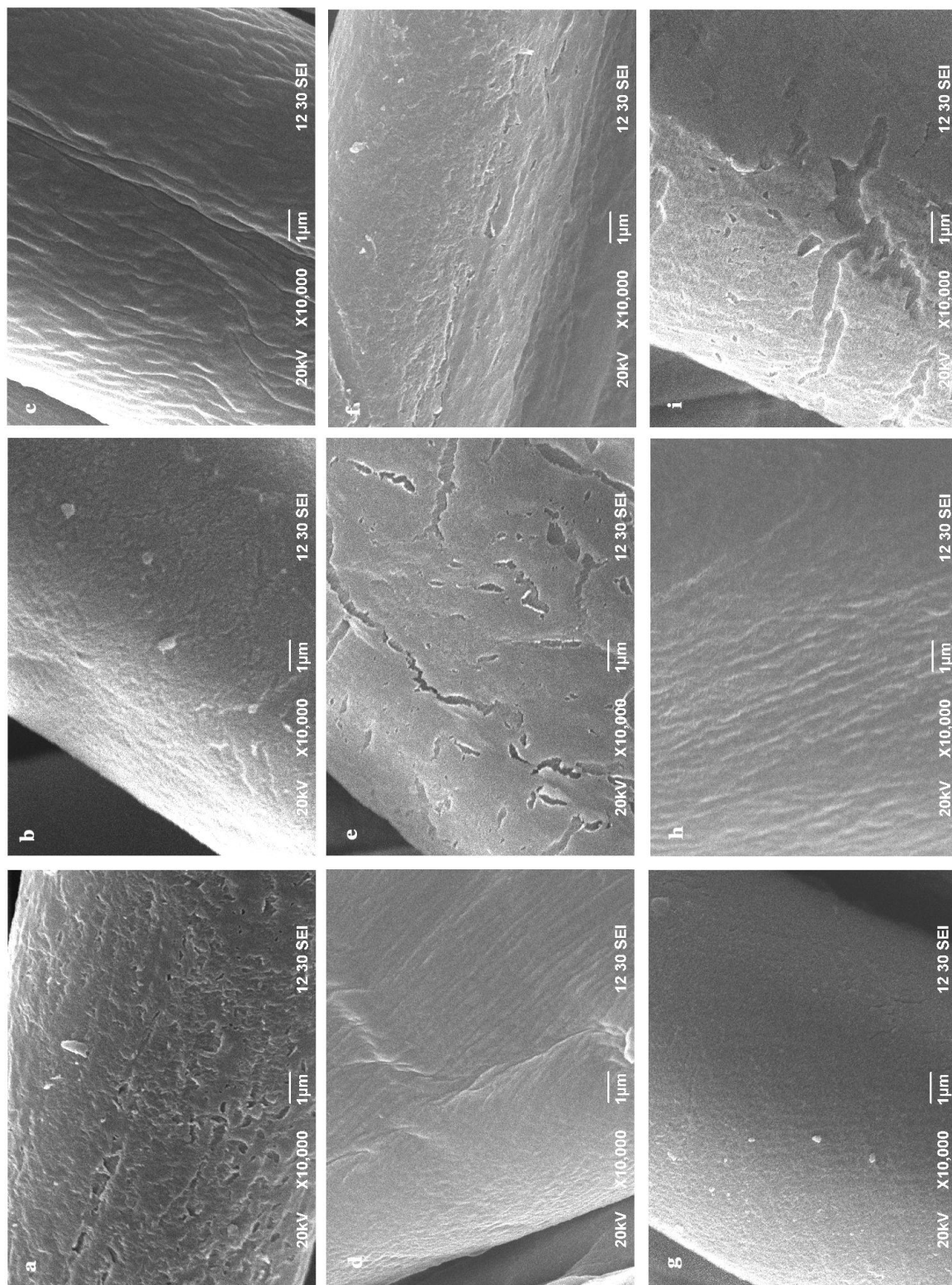
----

Micrographs (a)-(i) represent the optimisation runs 1-9 respectively at the magnification of 10,000 x

Figure 5-9   SEM micrographs illustrating the surface morphology of cotton fibres exposed to the He-O$_2$ atmospheric pressure plasma

----

Table 5-5   Nano-scale surface roughening was induced by the CF_4 and O_2 plasma-modified cotton as determined by mass loss measurement.

(* Values are statistically different at $P < 0.05$.)

Run	Etching rate, E (nm/s)	
	CF_4-modified	O_2-modofied
1	-25.42	-7.40
2	-24.32	-21.91
3	-28.69	-4.54
4	-15.01	-1.92
5	-18.57	-9.85
6	-12.13	-11.41
7	-6.73	-0.99
8	-11.45	-2.09
9	-13.47	-12.05

The etching rate, E (nm/s) represents the changes of fabric thickness per unit of treatment time. Negative values of E indicate the reduction of fabric thickness with respect to the control sample.

The original cotton fibres are ribbon-like with micro-ridges and grooves being formed on the surface as shown in **Figure 5-6**. These micro-structures forming extensive network of channel on the fibre surface assist horizontal wicking of liquids.

After the cotton fabrics were exposed to the CF_4 plasma, some nano-cones were formed on the ridges and grooves of the fibre surface in all selected experimental runs as shown in **Figures 5-7 and 5-8**. When using CF_4 as the reactive gas, a lotus-leaf like surface morphology on cotton fibres was achieved resulting in non-wetting behaviour. Horizontal wicking was inhibited with

----

respect to the high density of nano-structures formed on the ridges and grooves thereby increasing the surface roughness dramatically. As a result, all the CF_4-modified cotton samples showed a reduction of wetted area at least by 60%.

When the cotton fabrics were exposed to the O_2 plasma, some ridges present on the fibres were removed in most of the experimental runs, except those which were modified at the jet distance of 7mm, namely **runs 3, 4 and 8.** The modified fibre appeared to be similar to the duck feather (Liu et al., 2008). The reduction of surface roughness minimised the horizontal wicking of the dye liquid. The dye liquid retained at the point of first contact without spreading observed. In the case of **runs 1, 5 and 9**, a close proximity to the jet nozzle at 3mm eroded the fibre surface severely thereby developing the micro-pits as illustrated in **Figure 5-9**. It was observed that the dye liquid diffused in radial direction through the pits. As a result, the dye liquid was localised in a small area. Macroscopically, the wetted area of the modified cotton fabric was reduced.

Physical ablation was the predominant reaction which elicited a distinctive surface morphology of the substrate. In both systems, He carrier participated in the ablation. However, with the use of the different reactive gases, different surface morphology would be induced by CF_4 and O_2 consequently. O_2 reacted with the substrate causing the oxidation and hydrolysis of cellulosic fibres. O_2 plasma generated a great deal of volatile low molecular weight hydrolysed fragments (LMWHFs) which were easily removed from the substrate surface via sublimation in the open system. Simultaneously, thermal degradation of the cotton fibres induced by O_2 was more severe than that by CF_4 with respect to the thermal conductivity λ of the gases. λ of O_2 was 1.6 times higher than that of

----

CF$_4$ with reference to **Table 5-6** . Unlike O$_2$, CF$_4$ acted on the surface mainly via physical bombardment of F species without thermal degradation of the modified cotton fibres. Thermal degradation and physical ablation simultaneously acting on the substrate in the O$_2$ system could differentiate the surface morphology of the plasma-modified cotton fibres obtained from that in the CF$_4$ system. Micro-scaled to nano-scaled structures were generated on the cotton fibres were revealed using a SEM at the magnification of 10,000x and 15,000x as illustrated in **Figures 5-7 and 5-8.** The cotton fibres were texturised by both types of plasma with different characteristics.

Inhibition of horizontal wicking by both reduction and increment of surface roughness introduced surface hydrophobity on plasma-modified cotton fabrics.

Table 5-6   General physical properties of the reactive gases, CF$_4$ and O$_2$

	CF$_4$	O$_2$	Air
Thermal conductivity λ (mW/mK at 300K)	16	26.3	23.94
Density ρ (kg/m^3 under 1.0130bar at 21°C)	3.636	1.325	1.200
Specific volume (m^3/kg under 1.0130bar at 21°C)	0.275	0.755	0.833
Van der Waals' constant (L/mol)	0.0633	0.0319	N/A

(Lide, 2010-2011; Medard, 2009)

Detailed evaluation of the orthogonal optimisation of surface hydrophobisation of the two different plasma systems using He-CF$_4$ plasma and He-O$_2$ plasma will be discussed in Sections of **5.3.1 and 5.3.2** respectively.

5.3.4. Orthogonal control of hydrophobisation using He-CF$_4$ plasma

CF$_4$ was used as the reactive gas for the plasma-induced hydrophobisation of the hydrophilic cotton fabric. Surface morphology and surface chemical composition were the main attributes contributing to the surface hydrophobicity of a substrate. The reduction of wetted area, i.e. ΔA which acted as the indicator of the wetting behaviour, was tabulated in accordance with the etching conditions as shown in **Table 5-7**. Statistical analysis of the experimental data was employed to evaluate each input factor. In Table 5-7, Ai is the arithmetic mean of the change of wetted area (ΔA) at level i and ΔAi is the maximal difference of Ai indicating the significance of the variable on ΔA. The analysis revealed that the significance of dominating factors that controlled the surface hydrophobicity was in the order of **F, P, T and d**.

Table 5-7   The orthogonal table designated $L_9 3^4$ with tetrafluoromethane (F) was used as the reactive gas.

(* Values are statistically different at $P < 0.05$.)

Variables					
run	**T**	**P**	**F**	**d**	**ΔA**
1	I	I	I	I	-0.953
2	I	II	II	II	-0.855
3	I	III	III	III	-0.931
4	II	I	II	III	-0.882
5	II	II	III	I	-0.928
6	II	III	I	II	-0.959
7	III	I	III	II	-0.943
8	III	II	I	III	-0.926
9	III	III	II	I	-0.912
A$_I$	-0.913	-0.926	**-0.946**	**-0.931**	
A$_{II}$	-0.923	-0.903	-0.884	-0.919	
A$_{III}$	**-0.927**	**-0.934**	-0.934	-0.913	
ΔA$_i$	0.01	0.03	**0.06**	0.01	sd =0.03

Negative values of ΔA indicate the improvement of hydrophobicity with respect to the control sample.

First of all, the surface hydrophobicity was most sensitive to F, i.e. the concentration of CF_4. With respect to the plasma chemistry, the decomposition of CF_4 in the plasma depended on the relative ratio of the carrier gas (Frenais et al., 2009, Hicks & Herrmann, 2003; Okuda, 2008; Vinogradov et al., 2004; Vinogradov & Lunk, 2005). The relative concentration of CF_4 and He determined the reactions shifting in between ablation and fluorination. In other words, i.e. the concentration of CF_4 determined which reaction would be predominant in the afterglow region with the flow rate of He being kept constant. The statistical trend analysis revealed that 0.5% CF_4 had the most profound effect on the wetted area of the modified fabric as shown in **Figure 5-10a**. 0.5% CF_4 attained the highest CF_4 decomposition rate to form the largest amount of F-containing active species leading to the smallest wetted area, i.e. the largest reduction of ΔA. The flow rate of reactive gas was proposed to be another factor affecting the decomposition of CF_4 (Frenais et al., 2009; Kim & Park, 2008). Increasing CF_4 flow rate would reduce the residence time of reactive gas in the plasma glow region thereby reducing the time of interaction with the electrons and He*. As a result, the amount of F active species present in the afterglow would be reduced accordingly. **Table 5-8** shows the increasing concentration of CF_4 reduced the degree of fluorination.

----
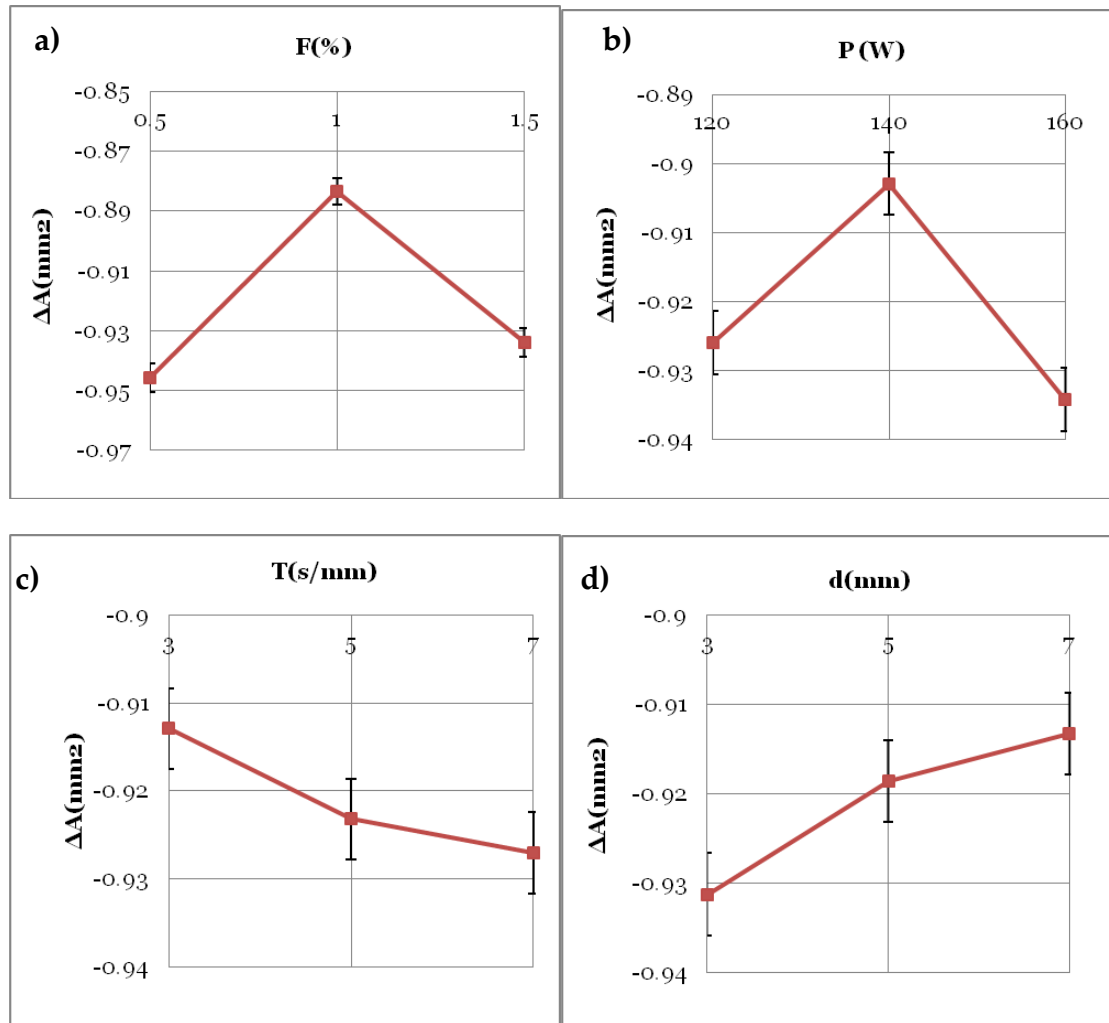
a) Concentration of CF₄ (F), b) ignition power (P), c) treatment time (s/mm) and d) jet distance (d).

Figure 5-10   Statistical trend analysis of the reduction of wetted area against the He-CF₄ etching parameters

----

Table 5-8   Correlation between the concentration of CF$_4$ (**F**) and hydrophobisation was evaluated by FTIR analysis and mass loss measurement.

F	FC (A·cm^{-1})	E (nm/s)
0.5%	17.57	-16.33
1%	15.91	-17.60
1.5%	15.84	-17.99

The peak area at the range of **1730-1800cm^{-1}**, **FC** represents the fluorinated functionalities. The etching rate, **E** represents the changes of fabric thickness per unit of treatment time. Negative values of E indicate the reduction of fabric thickness with respect to the control sample.

However, the overall surface hydrophobisation did not decline with the increasing CF$_4$ concentration. ΔA induced by 1% CF$_4$ could fit the proposed correlation with the concentration of CF$_4$. In contrast, 1.5% CF$_4$ induced surface hydrophobisation similar to 0.5% CF$_4$. Hydrophobisation was not only controlled by the reactive gas concentration, but also controlled by surface roughness. Surface roughness was attributed to the significant increment of hydrophobisation of cotton fabric of 1.5% CF$_4$ as shown in **Table 5-8.** Nano-bumps observed by using SEM as shown in **Figures 5-7 and 5-8** were proposed to be one of the attributes to promote surface hydrophobicity (Tuteja et al., 2008). Air sacs in between them bumps that could trap air locally were able to further promote the hydrophobisation of the substrate.

The ignition power was found to be the second essential parameter influencing surface hydrophobisation. In general, increasing ignition power promotes electrical discharge and hence the decomposition rate of plasma gases. However, FTIR analysis revealed an opposite correlation between the amount

----

---

of fluorinated hydrocarbons formed and the surface hydrophobisation in **Table 5-9**. Electron bombardment was proposed to be prevalent at a high ignition power. Fluorination of substrate surface modified by APP mainly underwent radical-initiated grafting via UV excitation and hydroxyl abstraction of neutral fluorine species (Fanelli et al., 2008). Electron bombardment essentially generated F ions and atoms which were acting as etching agent in addition to He species. Consequentially, increasing ignition power promoted ablation but inhibited fluorination as illustrated in **Table 5-9**.

Table 5-9   Correlation between ignition power (**P**) and hydrophobisation was evaluated by FTIR analysis and mass loss measurement.

P	FC_i (A·cm^{-1})	E_i (nm/s)
120W	17.25	-15.72
140W	15.61	-18.22
160W	16.46	-18.10

The peak area at **1700cm^{-1}**, **FC** represents the fluorinated unsaturated hydrocarbons. The etching rate, **E** represents the changes of fabric thickness per unit of treatment time. Negative values of E indicate the reduction of fabric thickness with respect to the control sample.

According to the statistical trend analysis in shown **Figure 5-10b,** 160W plasma was found to be the most profound ignition power for the surface hydrophobisation with an appreciable amount of F-containing functionalities grafted with sufficient surface roughness to trap air sacs. However, the trend deviated from the normal postulation. 140W plasma being a higher ignition power as compared to 120W did not induce hydrophobicity on the cotton

----

substrate. Plasma chemistry of He-CF$_4$ was proposed to be the cause of the deviation. Fluorination and ablation were dependent on the concentration of CF$_4$ present in the plasma.

Ignition power determined the prevalence of electron bombardment and penning reaction. Bond dissociation energy was taken as the reference of the energy required for the activation of the plasma gases. The excitation energy of He was much lower that than of CF$_4$ as shown in **Table 5-10**. The surface characteristics of the modified fabrics revealed the distinct trend in relation to ignition power. At a low ignition, i.e. at 120W, penning reaction was predominant without sufficient energy for direct excitation of CF$_4$. A high degree of fluorination was caused by the He-induced free radical grafting of neutral F-containing species. At a high ignition, i.e. at 160W, electric excitation became predominant. F ions and atoms were dominant in the plasma leading to physical ablation. As a result, etching rate was the highest while fluorination was the lowest as shown in **Table 5-9**. At 140W, both reactions balanced with each other leading to the least degree of fluorination among the three different ignition powers. Simultaneously, the etching rate at 140W was found to be similar to that induced at 120W. As a result, the degree of hydrophobisation was found to be the least among the three different powers.

The orthogonal optimisation based on the degree of hydrophobicity with respect to the ignition power revealed that the alteration of the surface morphology overrode the effect of chemical modification. Though 160W induced the least degree of fluorination, ΔA was determined to be the maximum among the three ignition power. According to SEM micrographs in Figure 5-8, 160W generated the most significant amount of nano-bumps on the

----

----

fibre surface as shown in micrographs (c), (f), and (i). This fits the postulation that physical modification of the substrate surface is the dominating factor in controlling the degree of hydrophobisation.

Table 5-10   Thermochemical properties of the reactive gases, CF_4 and O_2, as well as the carrier gas, He

	CF₄	O₂	He
Standard enthalpy formation ($\Delta_f H^o$(g)/kJ mol⁻¹ at 298.15 K)	-933.6	0	0
Standard entrolpy (S^o(g)/J mol⁻¹ K⁻¹ at 298.15 K)	261.6	205.2	126.2
Heat capacity (C_P(g)/J mol⁻¹ K⁻¹ at 298.15 K)	61.1	29.4	20.8
Bond dissociation energy (D^o_{298} kJ mol⁻¹ at 298.15 K)	546.8	498.4	3.809*

*D^o_{298} of He referred as D^o_{298} of He-He (Lide, 2010-2011)

Treatment time and jet distance were the least influential parameters on the hydrophobisation of cotton fabric.

Time was required to accumulate sufficient amount of active species on the substrate for the reaction. With reference to the statistical trend analysis illustrated in **Figure 5-10c,** the degree of hydrophobisation was found to be increasing with treatment time. 7s/mm induced the greatest reduction of wetted area thereby exhibiting the best hydrophobisation of the cotton fabric among the three different duration of treatment employed. Treatment time was closely

----

----

related to the concentration of active plasma species accumulated on a modified surface.

APPJ is a downstream treatment. Jet distance was the perpendicular distance between the plasma nozzle and the substrate located below as shown in **Figure 5-1**. An appropriate proximity between the plasma source and the substrate affected the efficacy of the active species when etching a surface. In the atmospheric pressure plasma treatment, the active plasma species experienced a severe collision with air molecules when travelling towards the substrate surface. Both velocity and energy content decreased with respect to the time and distance transported. Hydrophobisation was found to be reducing with the increase of jet distance as illustrated in **Figure 5-10d**. The reduction of wetted area induced by 3mm was found to be the largest while 7mm elicited the least reduction.

The control of hydrophobisation by both treatment time and jet distance was proposed to be affected by gas density of the plasma gas. In accordance with **Table 5-6**, CF_4 was 3 times denser with the air being easily displaced. CF_4 occupied most of the volume of space between the substrate and the plasma nozzle. Velocity and effective energy content of the CF_4 plasma active species could maintain at a constant value. As a result, the CF_4 was found to be efficient in hydrophobisation in all the treatment time and jet distances with the reduction of wetted area over 90%.

In order to verify the optimal condition of hydrophobisation of cotton fabric using He-CF_4 plasma, the postulated condition of the plasma treatment was put into actual experimental trials. Using CF_4 plasma excited by 160W of

----

----

radio frequency with 0.5% CF$_4$ being used to modify the cotton fabric for 7s/mm at 3mm jet distance, the greatest hydrophobisation was determined. The reduction of ΔA was found to be -0.972. Surface ablation induced by CF$_4$ was found to be in nano-scale as shown in **Figure 5-11**. With a great deal of nano-bumps being generated, numerous air sacs trapped in the surface of the fibre elicited the prominent effect of hydrophobisation of cotton.
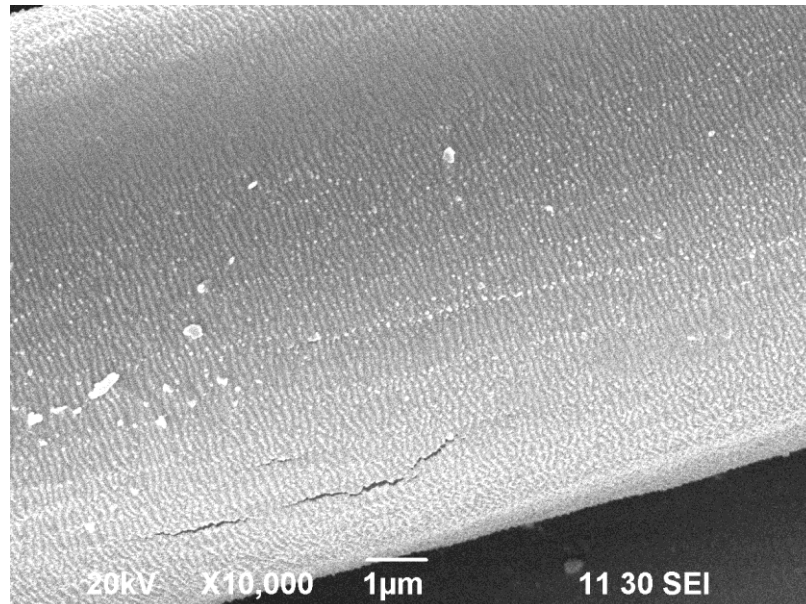
(Operation parameters: 3mm, 0.5% CF$_4$, 7s/mm and 160W. SEM micrograph was captured at a magnification of 10,000x.)

Figure 5-11   Surface morphology of cotton fibres modified under the optimal condition as determined by the orthogonal optimisation

----

182

5.3.5   Orthogonal control of hydrophobisation using He-O$_2$ plasma

O$_2$ plasma was used for surface hydrophobisation of cotton fabrics with ageing effect. Both surface morphology and surface chemical composition were the attributes contributed to the hydrophobicity of a modified substrate. The change of wetted area, i.e. ΔA being the indicator of the wetting behaviour, was tabulated in accordance with the etching conditions as shown in **Table 5-11**. Statistical trend analysis revealed that the significance of dominating factors to control the surface hydrophobicity was in the order of **d, O, T and P**.

Table 5-11   The orthogonal table designated $L_9 3^4$ with oxygen (O) being used as
the reactive gas.

(* Values are statistically different at $P < 0.05$.)

		Variables			
run	**T**	**P**	**O**	**d**	**ΔA**
1	I	I	I	I	-0.221
2	I	II	II	II	-0.737
3	I	III	III	III	-0.126
4	II	I	II	III	-0.320
5	II	II	III	I	-0.887
6	II	III	I	II	-0.515
7	III	I	III	II	-0.686
8	III	II	I	III	-0.107
9	III	III	II	I	-0.969
A$_I$	-0.361	-0.409	-0.280	**-0.693**	
A$_{II}$	-0.574	**-0.577**	**-0.676**	-0.646	
A$_{III}$	**-0.587**	-0.537	-0.566	-0.184	
ΔA$_i$	0.23	0.17	0.39	**0.51**	sd = 0.16

Negative values of ΔA indicate the improvement of hydrophobicity with
respect to the control sample.

To begin with, the surface hydrophobicity was considered to be most sensitive to d, the jet distance. The control of hydrophobisation by jet distance was proposed to be greatly affected by the gas density of the plasma gas. In accordance with **Table 5-6**, the density of O_2 was similar as that of air which was not able to occupy the whole volume of space between the substrate and plasma nozzle. As a result, the O_2 was found to be sensitive to the change of jet distance in terms of hydrophobisation as illustrated in **Table 5-12**. The etching rate dramatically dropped to less than 3nm/s at 7mm jet distance. The resultant ΔA was only 20% as illustrated in **Figure 5-12a**.

Table 5-12   Correlation between jet distance and hydrophobisation was evaluated by FTIR analysis and mass loss measurement.

	OC (A·cm^{-1})	E (nm/s)
Control	0.24	N/A
3mm	**1.38**	-9.77
5mm	1.34	-11.43
7mm	1.17	-2.85

The peak area in the range of **3000-2300cm^{-1}**, **OC** represents the aliphatic hydrocarbons (Vaideki et al., 2007). The etching rate, **E** represents the changes of fabric thickness per unit of treatment time. Negative values of E indicate the reduction of fabric thickness with respect to the control sample.

---
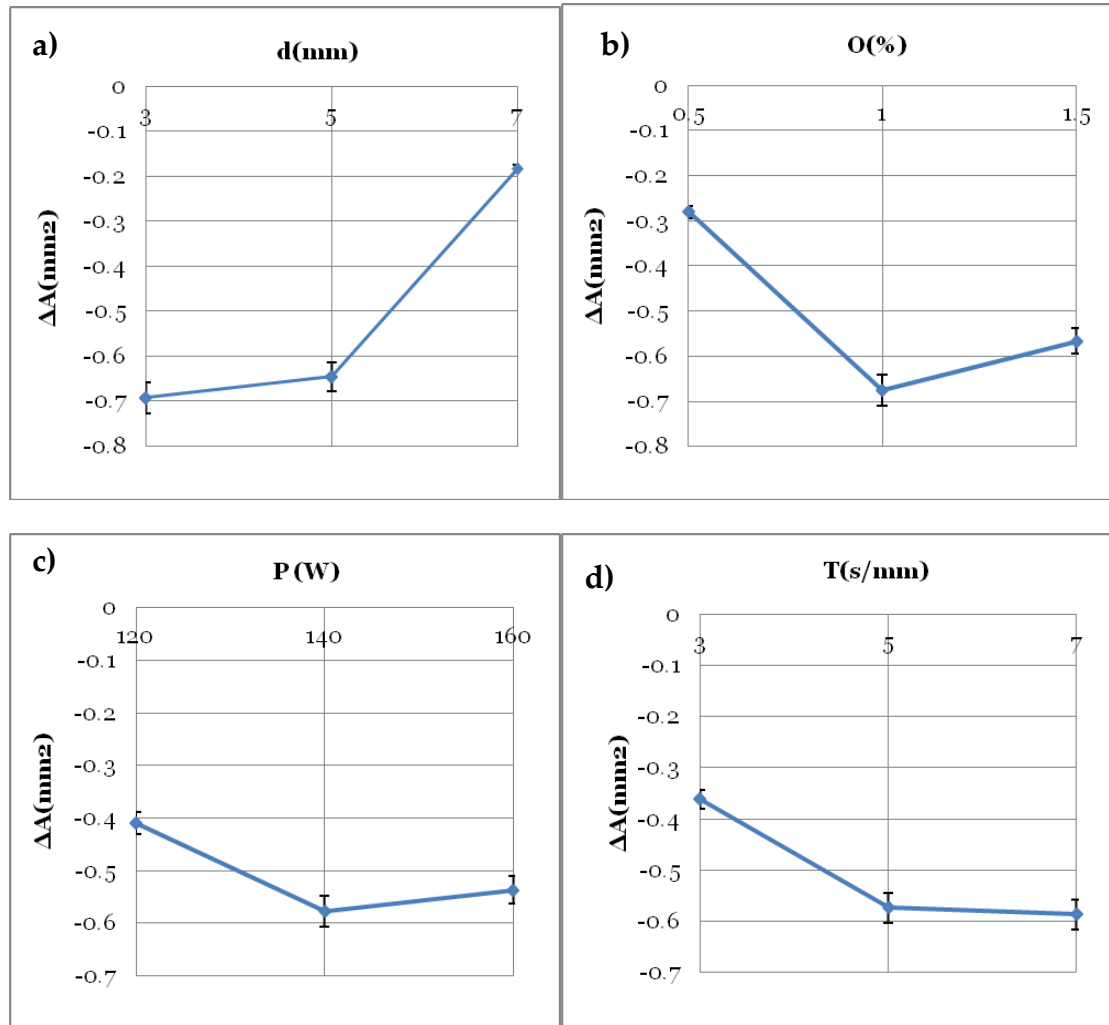
a) Jet distance (d), b) concentration of O₂ (O), c) ignition power (P) and d) treatment time (s/mm).

Figure 5-12   Statistical trend analysis of the reduction of wetted area against the He-O₂ etching parameters

Hydrophobisation was found to be reducing with the increase of jet distance as illustrated in **Figure 5-12a**. The reduction of wetted area induced by 3mm was found to be the largest while 7mm elicited the least reduction.

APPJ is a downstream treatment. Jet distance was the perpendicular distance between the plasma nozzle and the substrate located below as shown in **Figure 5-1**. In general, an appropriate proximity between the plasma source

----

and the substrate affected the efficacy of the active species when etching a surface. In the APP treatment, the active plasma species experienced a severe collision with air molecules when travelling towards the substrate surface. Both the velocity and energy content decreased with respect to the time and distance transported. 3mm jet distance essentially minimised the side effect of ambient collision with the air molecules reserving most of the energy for physical ablation of the substrate fibres.

With regard to the SEM micrographs shown in **Figures 5-9a), e) and i)**, the change of surface morphology induced a significant improvement of hydrophobicity. Surface features of the O_2 plasma-modified fibre were etched away and appeared alike polyester fibres which was able to reduce the wicking of dye liquids. The micro-voids formed on the fibre surface facilitated the penetration of dye particles into the fibre leading to the localisation of wetted area for the dye present on the modified fabric. Physical observation did compile with the detailed FTIR analysis and the mass-loss measurement as shown in **Table 5-12**. Chain scission and sublimation of volatile low molecular weight oxidised fragments (LMWOF) were determined to be the most severe at 3mm. Further increasing the jet distance would reduce the efficacy of the two reactions accordingly.

A small jet distance of 3mm jet was found to be the most effective proximity for the O_2 plasma hydrophobisation of cotton substrate.

The reactive concentration of O_2, **O** was found to be the second crucial factor manipulating the degree of hydrophobisation. O_2 plasma which was oxidative in nature could induce surface hydrophilisation. In general, a higher

----

----

degree of hydrophilisation was more prone to ageing of the modified surface

(Molina et al., 2002; Nakamatsu et al., 1999; Wertheimer et al., 1999).

Manipulation of the degree of hydrophilisation of the substrate controlled the

hydrophobisation of the aged substrates. Similar to the film model mentioned

in Section **3.3.3** of Chapter 3, 1% O_2 led to the highest hydrophobisation of the

cotton substrate with respect to the greatest degree of hydrophilisation. The

reduction of ΔA changed with the concentration of O_2 according to **Figure 5-12b**.

The reversal of surface polarity was confirmed by the FTIR analysis as shown in

Table 5-13.

Table 5-13   Correlation between concentration of O_2 and hydrophobisation was evaluated by FTIR analysis.

	OC (A·cm^{-1})
Control	0.24
0.5%	0.65
1%	**0.68**
1.5%	0.67

The peak area in the range of **3000-2300cm^{-1}**, **OC** represents the aliphatic hydrocarbons (Vaideki et al., 2007).

0.5% O_2 attained the least hydrophobisation as it induced physical ablation

predominantly with the least surface oxidation. The amount of hydrophilic

groups available for ageing sequentially was found to be the least. The

reduction of ΔA induced by 0.5% O_2 was not very dramatic. Although 1.5% O_2

did not induce much oxidation as that of using 1% O_2, the surface

----

----

morphological modification was still proposed to be the attribute of the significant increase in the hydrophobicity of the modified fabric. With reference to **Figure 5-9**, the SEM micrographs **a), f) and g)** show that the cotton fibres were analogous to the fibres of polyester with the micro-ridges and grooves being removed by the 1.5% O_2 plasma. Smooth surface with hydrophobic hydrocarbons on the modified substrate surface elicited hydrophobisation.

A moderate concentration of the O_2 gas was found to be the most effective proximity for O_2 plasma hydrophobisation of cotton substrate.

Ignition power was the third essential parameter controlling hydrophoibisation of cotton fabric. In general, increasing ignition power promotes electrical discharge and hence the excitation of plasma gases. In **Table 5-14**, the degree of oxidation was increasing with ignition power. However the etching rate did not following the same trend. There was a sudden drop of etching rate at high ignition, i.e. 160W. Oxidation and thermal degradation were the two surface reactions imposed by O_2 plasma leading to the deviation from the conventional postulation. Thermal conductivity, λ, of O_2 of 26.3mW/mK was higher than that of air with reference to **Table 5-6**.

The higher the ignition power, the more profound of the thermal degradation of the substrate would be with respect to the higher concentration of O-containing species in the plasma, i.e. thermal degradation became more prominent with the increasing ignition power. At 160W, thermal degradation would induce the melting of micro-bumps and nano-bumps formed by physical ablation. As a result, thermal degradation overwhelmed ablation leading to the reduction of surface roughness.

The statistical trend analysis indicated that a moderate ignition power of 140W could induce the highest degree of hydrophobisation as shown in **Figure 5-12c**. 140W plasma offered the largest etching rate and hence generated the greatest surface roughness. Surface roughness is essential in trapping air to further promote surface hydrophobicity.

Table 5-14   Correlation between ignition power and hydrophobisation was evaluated by FTIR analysis and mass loss measurement.

	OC (A·cm^{-1})	E (nm/s)
Control	0.24	N/A
120W	1.07	-3.44
140W	1.29	**-11.28**
160W	1.53	-9.33

The peak area in the range of **3000-2300cm^{-1}**, **OC** represents the aliphatic hydrocarbons (Vaideki et al., 2007). The etching rate, **E** represents the changes of fabric thickness per unit of treatment time. Negative values of E indicate the reduction of fabric thickness with respect to the control sample.

Treatment time was the least effective parameter influencing the hydrophoibisation of cotton fabric. The statistical trend analysis illustrated in **Figure 5-12d** revealed that the degree of hydrophobisation was found to be increasing with treatment time. Time was required to accumulate sufficient amount of active species on the substrate for the reaction. For example, 3s/mm only induced a low level of oxidation. Hence, increasing treatment time to 5s/mm and 7s/mm progressively could promote the oxidation and etching of cotton fibres as shown in **Table 5-15**.

7s/mm induced the greatest reduction of wetted area exhibiting the best hydrophobisation of the cotton fabric among the three different duration of treatment employed.

Table 5-15   Correlation between treatment time and hydrophobisation was evaluated by FTIR analysis and mass loss measurement.

	OC (A·cm^{-1})	E (nm/s)
Control	0.24	N/A
3s/mm	0.53	-0.36
5s/mm	1.41	-0.57
7s/mm	1.95	-0.59

The peak area in the range of **3000-2300cm^{-1}**, **OC (A·cm^{-1})** represents the aliphatic hydrocarbons (Vaideki et al., 2007). The etching rate, **E** represents the changes of fabric thickness per unit of treatment time. Negative values of E indicate the reduction of fabric thickness with respect to the control sample.

In order to verify the optimal condition of hydrophobisation of cotton fabric using He-O$_2$ plasma, the postulated condition of the plasma treatment was put into the actual experimental trials. Using O$_2$ plasma excited by 140W of radio frequency with 1% O$_2$ to modify the cotton fabric for 7s/mm at 3mm jet distance, the greatest hydrophobisation was determined after subjected to ageing for 720hrs. The reduction of ΔA was found to be -0.983. The same optimal condition of hydrophobisation of cotton fabric using He-O$_2$ plasma was also put into actual experimental trials. In this case, the plasma-modified sample was not subjected to ageing. The evaluations were taken after 24hrs

----

----

conditioning. Surface morphology was being the same as that with ageing. However, the degree of hydrophobisation was relatively insignificant. The reduction of ΔA was found to be -0.341 with minimal ageing effect being taken into account.

Surface voids induced by O_2 plasma as shown in **Figure 5-13** was determined to be the prime factor of dyestuff penetration leading to apparent hydrophobisation of cotton.
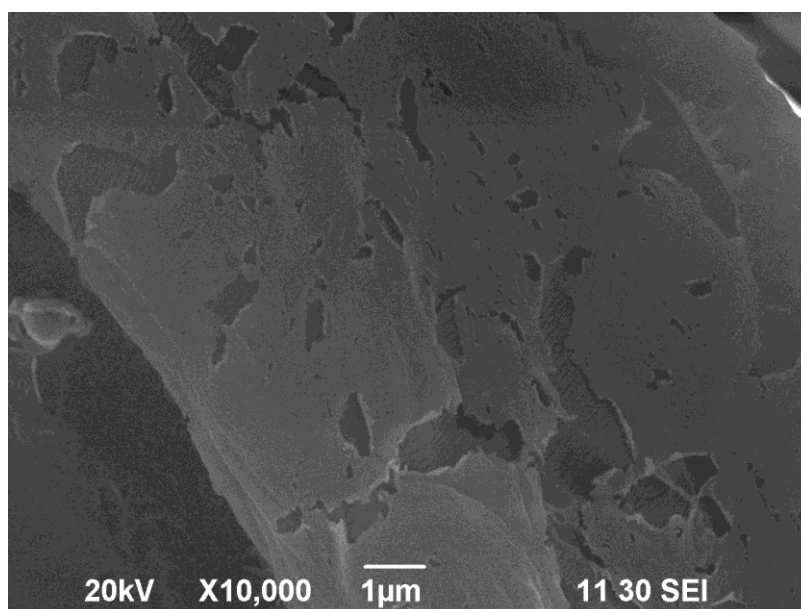
(Operation parameters: 3mm, 1% O_2, 7s/mm and 140W. SEM micrograph was captured at a magnification of 10,000x)

Figure 5-13   Surface morphology of cotton fibres modified under the optimal condition as determined by the orthogonal optimisation

----

5.4   Conclusion

A hydrophobic modification of the hydrophilic cotton fabric through atmospheric pressure plasma using CF_4 and O_2 reactive gases was conducted. Irrespective of the nature of reactive gas, both CF_4 and O_2 were found to be capable of hydrophobisation of cotton substrate. Although CF_4 and O_2 elicited hydrophobisation via different mechanisms, both gases induced surface roughening which was proposed to be the prime factor attributing to the reduction of wetted area over the plasma-modified fabric surface. The roughening was found to be in nano-scale.

The orthogonal optimisation illustrated the sensitivity of individual parameters for the plasma hydrophobisation of cotton was reactive gas dependent. Parameter dependence and operation condition for achieving the optimal hydrophobisation were found to be different in the two systems studied. In the He-CF_4 system, the parameter of (1) low CF_4 concentration, (2) high plasma power, (3) short jet distance and (4) long treatment duration were necessary for the hydrophobisation of cotton substrate. The optimal condition was determined as 0.5% CF_4, 160W, 3mm and 7s/mm. In the He-O_2 system, the parameter of (1) short jet distance, (2) moderate O_2 concentration, (3) long treatment duration and (4) moderate ignition power were essential for the hydrophobisation of the hyhydrophilic substrate. The optimal condition was determined as 3mm, 1% O_2, 7s/mm and 140W with 720hrs of ageing.

193

Chapter 6   Conclusion and recommendation

6.1   Conclusion

Atmospheric pressure plasma (APP) was employed to modify the surface wettability of different textile materials, namely polyester, wool and cotton. Prior to the actual applications to the textile materials, the plasma was applied tentatively to a thin polymeric film to study the basic plasma-substrate interaction. The modification was found to be dependent on the four main operation parameters, namely (1) treatment time, (2) ignition power, (3) reactive gas concentration and (4) jet distance. After summarising the effect of individual parameter imposed on the etching-functionalisation of the substrates, ignition power and jet distance factors were found to be the prime driving force for the distinctive topographical development and functaionlisation of a substrate surface. On the other hand, reactive gas concentration and treatment time factors determined the equilibrium between etching and hydrophilisation reactions. The simulation of plasma-substrate interaction using a polymeric film demonstrated an empirical framework of atmospheric pressure plasma treatment by offering a deeper understanding of the physicochemical interaction between plasma and textile materials.

An empirical model of plasma-substrate etching interaction was successfully developed based on the SEM-MATLAB image processing. The image processing was proposed to be a potential tool for fast prediction of the etching reaction in a plasma treatment.

Nano-scale surface wettability modification of textile materials utilising APP was found to be achievable with the appropriate manipulation of the operation parameters. The optimal condition of etching-functionalisation showed the factor of substrate dependence. The condition was discovered to be sensitive to the nature of reactive gas utilised in the plasma treatment.

6.1.1   Simulation of reaction

PET film was used to develop the empirical model for the industrialisation and realisation of plasma in textile industry. Nano-scale He-O_2 APP etching-hydrophilisation on PET thin film was achievable under the controlled condition. Both the density of nano-surface structure and surface energy were found to be varied with the treatment time in a quadratic relationship using stable plasma. Oxygen concentration contributed to the coherence factor in the treatment. Ignition power and jet distance related to structure density and surface hydrophilicity in a linear manner respectively. 3s/mm was determined to be the optimum plasma treatment time achieving the development of nano-spot in the range of 60 to 99nm diameter on the PET substrate. The highest surface energy of 84mN/m was required for the APPJ operating at 80W within 5mm jet distance by feeding 1% O_2/He gaseous admixture.

SEM-MATLAB image processing was found to be the potential tool for predicting the surface etching of plasma of the film model. This technique allowed a quick prediction but required skillful technologists for processing manipulation.

6.1.2   Plasma system for polyester substrates

He-O$_2$ APP etching-hydrophilisation treatment was successfully applied to polyester fabric with reference to the film model. High ignition power plasma of 180W at a jet distance of 3mm with 2.2% O$_2$ was required for the optimal nano-scale etching-hydrophilisation of the polyester fabric. Surface wettability of the fabric modified under the optimum condition was improved significantly allowing a complete wetting after 2.5s/mm treatment. The effect of ignition power overrode the effect of O$_2$ concentration at a high level.

Nano-grooves generated on the fibre surface under the optimal condition essentially facilitated the wicking of wetting liquids. The change of surface morphology of the polyester fibres deviated from that of the film model. The discrepancy was caused by the difference of the internal stress field existed between the biaxially—drawn film and the unidirectionally-drawn fibre.

6.1.3   Plasma system for wool substrates

He-O$_2$ APP etching-hydrophilisation was successfully applied to two different types of wool substrates. Wool twill fabric, namely wool A, was located at 5mm with respect to the nozzle of the atmospheric pressure plasma jet which was operated at 120W with 1%O$_2$ for 4s/mm. The nano-scale surface roughening was obtained with the improved surface wettability. Wool plain woven fabric, namely wool B, was also processed under a similar but different optimum condition. Exposing wool B towards 120W plasma with 0.5% O$_2$ at a jet distance of 5mm for 3s/mm could attain nano-crystalline structures on the cuticles with the appreciable surface hydrophilisation being achieved.

Nature of the fibres was the prime factor contributed to the deviation of the optimum condition for the plasma treatment to with respect to the same category of protein fibres. Good knowledge of the substrate was essential for the manipulation of the plasma processing of different textile materials. Plasma also showed substrate dependence in the modification.

6.1.4   Plasma system for cotton substrates

An etching-hydrophobic modification of hydrophilic cotton fabric through APP using different reactive gases, CF_4 and O_2, was conducted. Irrespective of the nature of reactive gas, both CF_4 and O_2 gases were found to be capable of hydrophobisation of cotton substrate. Although both CF_4 and O_2 gases elicited hydrophobisation via different mechanisms, they still induced surface roughening which was proposed to be the prime factor attributing to the reduction of wetted area over the plasma-modified fabric surface. The surface roughening was found to be in nano-scale. The change of surface morphology was also found to be reactive gas dependent.

In significant, orthogonal optimisation illustrated that the sensitivity of individual parameters for the plasma hydrophobisation of cotton was reactive gas dependent. Parameter dependence and operation condition for achieving the optimal hydrophobisation were found to be different in the two various systems being studied. In the He-CF_4 system, the parameters of (1) low CF_4 concentration, (2) high plasma power, (3) short jet distance and (4) long treatment duration are necessary for the hydrophobisation of cotton substrate. The optimal condition was determined as 0.5% CF_4, 160W, 3mm and 7s/mm. In the He-O_2 system, the parameters of (1) short jet distance, (2) moderate O_2

----

concentration, (3) long treatment duration and (4) moderate ignition power are essential for the hydrophobisation of the hydrophilic substrate. The optimal condition was determined as 3mm, 1% O_2, 7s/mm and 140W.

6.2   Recommendation and future works

The objectives of the research project have been achieved. In order to further improve and manipulate the plasma process, some future works are recommended with details as follows.

6.2.1   Simulation of reaction

Plasma treatment is progressive. With respect to the film model, plasma-substrate interaction is not essentially in a linear relationship. Hence, using advanced *in-situ* analysis of the modified substrates will facilitate the determination of the optimal operation condition and easily control the degree of plasma-substrate interaction.

Plasma treatment is a physicochemical modification. SEM-MATLAB image processing only attains a 2-dimension etching prediction but plasma-substrate interaction is actually 3-dimensional. Hence, advanced instrumentation technique, for example atomic force microscopy, might be taken into account for the evaluation of the penetration of plasma, i.e. the quantification of the induced height of roughness. This is important to manipulate the modification at surface to sub-surface level without altering the bulk properties of the substrates.

In addition, the simulation of the model should not be limited to physical change only. In order to yield a better understanding of the chemistry of plasma-substrate interaction, some advanced instrumentations such as *in-situ* FTIR or *in-situ* NMR may be employed for the characterisation of the course of the treatment.

6.2.2   Plasma system for polyester substrates

In the study of the PET film model, stress field was found to be the intrinsic factor attribute to the shape and dimension of the plasma-induced surface structure. Moreover, stress field was found to be also affecting the plasma parameter studied. Polyester fibres manufacture in various drawn ratios could be utilised in the future studies so as to obtain more information about the relationship between the stress field and the plasma parameters. This would be essential for the plasma processing of synthetic fibres.

6.2.3   Plasma system for wool substrates

For the modification of wool substrates, two different types of wool fabric of different fabric structure were used. Both the crystallinity of the fibres and the structure of the fabric affect the plasma-substrate interaction as gaseous collision was the prime factor of the modification. In order to reveal the individual factors, we should be the other factors to be constant. The two different wool fabrics should be in the same fabric structure. Or fabrics of different fabric structures made up of the same kind of wool fibres could also be studied in the future.

Nevertheless, the degree of crystallinity of the wool fibres should evaluated in order to obtain more information about the effect of substrate crystallinity upon APP treatments. Thermal analysis such as DSC, TGA and XRD could be employed to monitor the change in crystallinity.

6.2.4   Plasma system for cotton substrates

Plasma treatment is not permanent. Ageing effect has to be carefully taken into account with respect to the hydrophobisation of cotton using He-O_2 plasma. In order to have a better manipulation of the surface properties of the modified substrates, the choice of reactive gas and the ageing duration affecting the resultant properties should be thoroughly studied. Based on the inclusion of the ageing effect of O_2-modified cotton fabrics in the present study, it would be prosperous to further investigate the possibility of developing a dry water-repellent treatment using plasma technique for cotton fabrics.

.

Chapter 7   References

1.   Allan, G., Fotheringham, A., and Weedall, P. (2002) "The use of plasma and neural modeling to optimise the application of a repellent coating to disposable surgical garments", *AUTEX Research Journal*, 2(2), 64-68

2.   Almetwally, A. (2007) "Technology of nanofibres: An overview", *The Indian Textile Journal*, 117, 25-31

3.   Appleyard, H.M. (1960) Guide to the Identification of Animal Fibres, Wool Industries Research Association, Great Britain

4.   Bahners, T., Kesting, W. and Schollmeyer, E. (1993) "Designing surface properties of textile fibers by UV-laser irradiation", *Applied Surface Science.*, 69, 12-15

5.   Baltazar-Y-Jimenez, A. and Bismarck, A. (2007) "Surface modification of ligocellulosic fibres in atmospheric air pressure plasma", *Green Chemistry*, 9, 1057-1066

6.   Beake, B.D., Ling, J.S.G. and Leggett, G.J. (1998) "Correlation of friction, adhesion, wettability and surface chemistry after argon plasma treatment of poly(ethylene terephthalate)", *Journal of Materials Chemistry*, 8, 2845-2854

7.   Beake, B.D., Ling, J.S.G. and Leggett, G.J. (1998) "Scanning force microscopy investigation of poly(ethylene terephthalate) modified by argon plasma treatment", *Journal of Materials Chemistry*, 8(8), 1735-1742

8.   Bhushan, B., Jung, Y.C. and Koch, K. (2009) "Micro-, nano- and hierarchical structures for superhydrophobicity, self-cleaning and low adhesion", *Philosophical Transactions of the Royal Society A*, 7, 1631-1672

9.   Borcia, C., Borcia, G., Dumitrascu, N. (2008)"Relating plasma surface modification to polymer characteristics", *Applied Physics A*, 90, 507-515

10. Cai, Z.S. and Qiu, Y.P. (2006) "The Mechanism of Air/Oxygen/Helium Atmospheric Plasma Action on PVA", *Journal of Applied Polymer Science*, 99, 2233-2237

11. Canal, C., Gaboriau, F., Ricard, A., Mozetic, M., Cvelbar, U. and Drenik, A. (2007) "Density of O-atoms in an Afterglow Reactor During Treatment of Wool", *Plasma Chemistry and Plasma Processing,* 27, 403-413

12. Canal, C., Gaboriau, F., Villeger, S., Cvelbar, U. and Ricard, A. (2009) "Studies on antibacterial dressings obtained by fluorinated post-discharge plasma", *International Journal of Pharmaceutics,* 367, 155-161

13. Carneiro, N., Souto, A.P., Marimba, A., and Tena, B. (2001) "Dyeability of corona-treated fabrics", *Coloration Technology*, 117, 298-302

14. Černákorá, Ľ., Kováčik, D., Zahoránová, A., Černák, M. and Mazúr, M. (2005) "Surface Modification of Polypropylene Non-Woven Fabrics by Atmospheric-Pressure Plasma Activation Followed by Acrylic Acid Grafting", *Plasma Chemistry and Plasma Processing*, 25(4), 427-437

15. Chalmers, J. and Griffiths, P. (Eds.) (2002) "Spectra-Structure Correlations in the Mid and Far Infrared", Handbook of Vibrational Spectroscopy, Vol. 3, pp. 1783-1816

16. Champion, Y. and Fecht, H-J. (2004), *Nano-Architectured and Nanostructured Materials*, Weinheim, Wiley-VCH

17. Fanelli, F., Fracassi, F. and d'Agostino, R. (2008) "Fluorination of Polymers by Means of He/ CF4-Fed Atmospheric Pressure Glow Dielectric Barrier Discharges", *Plasma Processes and Polymers*, 5, 424–432

18. Fiala, A., Simor, M. and Wypkema, A. (2006) "Plasma Technology for Multifunctional Textiles", *International Dyer*, 191(5), 14-16

19. Foltin, V., Leštinská, L. and Machala, Z. (2006) "Spectroscopic investigations of atmospheric pressure microwave torch nitrogen plasma jet", *Czechoslovak Journal of Physics,* 56, Supplement 2, B712-720

20. Fresnais, J., Chapel, J.P., Benyahia, L. and Poncin-Epaillard, F. (2009) "Plasma-Treated Superhydrophobic Polyethylene Surfaces: Fabrication, Wetting and Dewetting Properties", *Journal of Adhesion Science and Technology*, 23, 447–467

21. Gao, Z., Sun, J., Peng, S., Yao, L. and Qiu, Y. (2009) "Surface modification of a polyamide 6 film by He/CF$_4$ plasma using atmospheric pressure plasma jet", *Applied Surface Science*, 256, 1496–1501

22. Gheorghiu, M., Arefi, F., Amouroux, J., Placinta, G., Popa, G. and Tatoulian, M. (1997) "Surface cross linking and functionalization of poly(ethylene terephthalate) in a helium discharge", *Plasma Sources Science and Technology*, 6, 8-19

23. Grill, A. (1994), *Cold Plasma in Materials Fabrication, from. Fundamentals to Applications*; IEEE Press: New York

24. Gupta, B., Hilborn, J., Hollenstein, CH., Plummer, C.J.G., Houriet, R. and Xanthopoulos, N. (2000), "Surface Modification of Polyester Films by RF Plasma", *Journal of Applied Polymer Science*, 78, 1083-1091

25. Hegemann, D. (2005) "Stain Repellent Finishing on Fabrics", *Advanced Engineering Materials*, 7(5), 401-404

26. Hegemann, D., Hossain, M.M., Balazs, D.J. (2007), "Nanostructured plasma coatings to obtain multifunctional textile surfaces", *Progress in Organic Coatings*, 58, 237–240

27. Herbert, T.(2003) "Atmospheric Pressure Plasma Liquid Deposition", *International Dyer*, 188(5), 11-13

28. Herbert, T.(2006) "Atmospheric Pressure Plasma Liquid Deposition", *International Dyer*, 191(5), 12-13

29. Hesse, A., Thomas, H. and Höcker, H. (1995). Zero-AOX Shrinkproofing Treatment for Wool Top and Fabric Part I: Glow Discharge Treatment, *Textile Research. Journal*, 65, 355-361

30. Hicks, R.F. and Herrmann, A.W. (2003) "Atmospheric Pressure Plasma Cleaning of Contaminated Surfaces", Technical Report, U.S. Department of Energy,
http://www.osti.gov/energycitations/servlets/purl/820519-F7yzPx/native/
(Retrieved November 20, 2010)

31. Hoa, T.T.P., Binh, N.T.T., and Giang, N.C. (2007) "Effect of Atmospheric Plasma Treatment on Mechanical Properties of Jute Fiber and Interface adhesion between Fiber and Resin", *Journal of Chemistry*, 45, 201-206

32. Holländer, A., Wilken, R. and Behnisch, J. (1999) "Subsurface chemistry in the plasma treatment of polymers", *Surface & Coatings Technology*, 116-119, 788-791

33. Jang, J.H. and. Jeong, Y.J. (2006) "Nano-roughening of PET and PTT fabrics visa continuous UV/O$_3$ irradiation", *Dyes and Pigments*, 69, 137-143

34. Jeong, J.Y., Park, J., Henins, I., Babayan, S.E., Tu, V.J., Selwyn, G.S., Ding, G. and Hicks, R.F. (2000) "Reaction Chemistry in the Afterglow of an Oxygen-Helium, Atmospheric-Pressure Plasma", *Journal of Physical Chemistry* A, 104, 8027-8032

35. Kaelble, D.H. (1970) "Dispersion-Polar Surface Tension Properties of Organic Solids", *Journal of Adhesion*, 2, 66-81

36. Kan, C.W. (2007) "Surface Morphological Study of Low Temperature Plasma Treated Wool – A Time Dependence Study", Méndez-Vilas, A. and Díaz, J., eds., *Modern Research and Educational Topics in Microscopy*, Spain, Formatex, Badajoz, 683-689

37. Kan, C.W., Chan, K., Yuen, C.W.M. and Miao, M.H. (1999) "Low Temperature Plasma on Wool Substrates: The Effect of the Nature of the Gas", *Textile Research. Journal*, 69, 407-416

38. Kan, C.W. and Yuen, C.W.M. (2007) "Plasma technology in wool", *Textile Progress*, 39(3), 122-187

39. Kan, C.W. and Yuen, C.W.M. (2008) "Static properties and moisture content properties of polyester fabrics modified by plasma treatment and chemical finishing", *Nuclear Instruments and Methods in Physics Research Section B*, 266, 127-132

40. Karahan, H.A. and Özdoğan, E. (2008) "Improvements of Surface Functionality of Cotton Fibers by Atmospheric Plasma Treatment", *Fibers and Polymers*, 9(1), 21-26

----

41. Kim, D. and Park D.W. (2008) "Decomposition of PFCs by steam plasma at atmospheric pressure", *Surface and Coatings Technology,* 202, 5280-5283

42. Kim, J.H., Liu, G.M, and Kim, S.H. (2006) "Deposition of stable hydrophobic coatings with in-line CH_4 atmospheric rf plasma", *Journal of Materials Chemistry*, 16, 977-982

43. Kostić, M., Radić, N., Obradović, B.M., Dimitrjević, S., Kuraica, M.M. and Škundrić, P. (2008) "Antimicrobial textile prepared by silver deposition on dielectric barrier discharge treated cotton/polyester fabric", *Chemical Industry & Chemical Engineering Quarterly*, 14(4), 219-222

44. Lee, H.R., Kim, D.J. and Lee, K.H. (2001) "Anti-reflective coating for the deep coloring of PET fabrics using an atmospheric pressure plasma technique", *Surface & Coatings Technology*, 142-144, 468-473

45. Lei, J.X., Shi, M.W. and Zhang, J.C. (2000) "The investigation of argon plasma surface modification to polyethylene: Quantitative ATR-FTIR spectroscopic analysis", *European Polymer Journal*, 36, 1277-1281

46. Leroux, F., Perwuelz, A., Campagne, C. and Behary, N. (2006) "Atmospheric air-plasma treatments of polyester textile structures", *Journal of Adhesion Science and Technology*, 20(9), 939-957

47. Lide, D.R.(Ed.) (2010-2011) CRC Handbook of Chemistry and Physics, 91st Edition, internet version 2011, Chapman and Hall/CRCnetBASE, http://www.hbcpnetbase.com/ (Retrieved November 20, 2010)

48. Liu, Y., Chen, X. and Xin, J.H. (2008), "Hydrophobic duck feathers and their simulation on textile substrates for water repellent treatment", *Bioinspiration & Biomimmetics*, 3, 046007 (8pp)

49. Mariottia, D. (2008) "Nonequilibrium and effect of gas mixtures in an atmospheric microplasma", *Applied Physics Letters*, , 92, 151505 (3pp)

50. Masaaki, O., Noboru, S. and Toshiaki, Y. (2008) "Development of functional sportswear for controlling moisture and odor prepared by atmospheric pressure nonthermal plasma graft polymerization induced by RF glow discharge", *Journal of Electrostatics*, 66, 381-387

---

51. Matthews, S.R., Hwang, Y.J., McCord, M.G. and Bourham, M.A. (2004) "Investigation into Etching Mechanism of Polyethylene Terephthalate (PET) Films Treated in Helium and Oxygenated-Helium Atmospheric Plasmas", *Journal of Applied Polymer Science*, 94, 2383-2389

52. McCord, M.G., Hwang, Y.J., Hughes, L.K. and Bourham, M.A. (2003) "Surface Analysis of Cotton Fabrics Fluorinated in Radio-Frequency Plasma", J*ournal of Applied Polymer Science*, 88, 2038-2047

53. Meade, S.J., Dyer, J.M., Caldwell, J. and Bryson, W.G. (2008) "Covalent Modification of the Wool Fiber Surface: Removal of the Outer Lipid Layer", *Textile Research Journal*, 78(11), 934-957

54. Medard, L. (Ed.) (2009) *Gas Encyclopaedia*, Air Liquide, Elsevier, online version
http://encyclopedia.airliquide.com/list.asp?LanguageID=11&CountryID=19
(Retrieved November 20, 2010)

55. Mejía, M.I., Marín, J.M., Restrepo, G., Pulgarín, C., Mielczarski, E., Mielczarski, J., Arroyo, Y., Lavanchy, J.-C and Kiwi, J. (2009) "Self-cleaning modified TiO$_2$–cotton pretreated by UVC-light (185 nm) and RF-plasma in vacuum and also under atmospheric pressure", *Applied Catalysis B: Environmental*, 91, 481-488

56. Molina, R., Jovančić, P., Comelles, F., Bertran, E. and Erra, P. (2002) Shrink-resistance and wetting properties of keratin fibres treated by glow discharge, *Journal of Adhesion Science and Technology*, 16 (11), 1469- 1485

57. Molina, R., Jovančić, P., Jocić, D., Bertran, E. and Erra, P. (2003) "Surface characterization of keratin fibres treated by water vapour plasma", *Surface and Interface Analysi*s, 35 (2), 128-135

58. Morent, R., De Geyter, N. and Leys, C. (2007) "Surface Modification of Nonwoven Textiles using a Dielectric Barrier Discharge Operating in Air, Helium and Argon at Medium Pressure", *Textile Research Journal*, 77(7), 471-488

----

59. Nakamatsu, J., Delgaso-Aoarico, L.F., De Silva, R. and Soberón, F. (1999) "Ageing of plasma-treated poly(tetrafluoroethylene) surfaces", Journal of Adhesion Science and Tehcnolohy, 13 (7), 753-761

60. Negri, A.P., Cornell, H.J. and Rivett, D.E., (1993) "A Model for the Surface of Keratin Fibers", *Textile Research. Journal*. 63, 109– 115.

61. Niemi, K., Reuter, St., Schaper, L., Knake, N., Schulz-von der Gather, V. and Gans, T. (2007) "Diagnostics on an atmospheric pressure plasma jet", *Journal of Physics: Conference Series*, 71, 012012

62. Okuda, I., Takahashi, E., Kato, S. and Matsumoto, Y. (2008) "Decomposition of CF_4 Using Pulsed-Electron-Beam-Generated Atmospheric-Pressure Low-Temperature Plasmas", *Japanese Journal of Applied Physics*, 47 (7), 5681-2683

63. Park, J., Henins, I., Herrmann, H.W., Selwyn, G.S., Jeong, J.Y., Hicks, R.F., Shim, D. and Chang, C.S. (2000) "An atmospheric pressure plasma source", *Applied Physics Letters*, 276(3), 288-290

64. Placinta, G., Arefi-Khonsari, A., Gheorghiu, M., Amouroux, J. and Popa, G. (1997) "Surface Properties and the Stability of Poly(ethylene Terephtalate) Films Treated in Plasmas of Helium–Oxygen Mixtures", *Journal of Applied Polymer Science*, 66, 1367-1375

65. Raffaele-Addamo, A., Selli, E., Barni, R., Riccardi, C., Orsini, F., Poletti, G., Meda, L., Massafra, M.R. and Marcandalli B. (2006) "Cold plasma-induced modification of the dyeing properties of poly(ethylene terephthalate) fibers", *Applied Surface Science*, 252, 2265-2275

66. Ren, Y., Wang, C.X. and Qiu, Y.P. (2008) "Aging of surface properties of ultra high modulus polyethylene fibers treated with He/O_2 atmospheric pressure plasma jet", *Surface and Coatings Technology*, 202, 2670-2767

67. Rombaldoni, F., Mosotti, R., Montarsolo, A., Demichelis, R., Innocenti, R. and Mazzuchetti, G. (2008) "The effects of HMDSO plasma polymerization on physical, low-stress mechanical and surface properties of wool fabrics", *AUTEX Research Journal*, 8(3), 77-83

----

68. Ross P.J. (1996) *Taguchi Techniques for Quality Engineering*, McGraw-Hill, New York, United States

69. Ryu, J., Wakida, T. and Takagishi, T. (1991) "Effect of Corona Discharge on the Surface of Wool and Its Application to Printing," *Textile Research. Journal*, 61(10), 595-601

70. Samanta, K.K., Jassal, M. and Agrawal, A.K. (2009) "Improvement in water and oil absorbency of textile substrate by atmospheric pressure cold plasma treatment", *Surface and Coatings Technology*, 203, 1336–1342

71. Sasaki, K. and Kadota, K. (1999) "Diagnostics-Plasma Flow by Laser-Induced Fluorescence Spectroscopy Decay Processes of Electrons in the Afterglow of High-Density CF_4, c-C_4F_8 and CF_4-H_2 Plasmas", *Japanese Journal of Applied Physics*, 28 (7), 4383-4388

72. Sahin, H.T. (2007) "RF-CF_4 plasma surface modification of paper: Chemical evaluation of two sidedness with XPS/ATR-FTIR", *Applied Surface Science*, 253, 4367-4373

73. Schütze, A., Jeong, J.Y., Babayan, S.E., Park, J., Selwyn, G.S. and Hicks, R.F. (1998) "The Atmospheric-Pressure Plasma Jet: A Review and Comparison to Other Plasma Sources", *IEEE Transaction on Plasma Science*, 26(6), 1685-1693

74. Selwyn, G.S., Herrmann, H.W., Park, J. and Henins, I. (1999-2000) "Materials Processing using an Atmospheric-Pressure Plasma Jet", *Physics Division Progress Report: Research Highlights*, 189-197

75. Shenton, M.J. and Stevens, G.C. (2001) "Adhesion enhancement of polymer surfaces by atmospheric plasma treatment", *Journal of Physics D: Applied Physics*, 34, 2761-2768

76. Shenton, M.J., Stevens, G.C., Wright, N.P. and Duan, X. (2002) "Chemical-Surface Modification of Polymers Using Atmospheric Pressure Nonequilibrium Plasmas and Comparisons with Vacuum Plasmas", *Journal of Polymer Science: Part A: Polymer Chemistry*, 40, 95-109

77. Shibata, M., Nakano, N. and Makabe, T. (1996) "Effect of $O_2(a^1\Delta_g)$ on plasma structures in oxygen radio frequency discharges", *Journal of Applied Physics*, 80(11), 6142-6147

78. Shin, Y. and Yoo, D.I. (2008) "Surface Characterization of PET Nonwoven Fabric Treated by He/O_2 Atmospheric Pressure Plasma", *Journal of Applied Polymer Science*, 108, 785–790

79. Sinha, E. and Panigrahi, S. (2009) "Effect of Plasma Treatment on Structure, Wettability of Jute Fiber and Flexural Strength of its Composite", *Journal of Composite Materials*, 34, 1791-1802

80. Sigurdsson, S. and Shishoo, R. (1997) "Surface properties of polymers treated with tetrafluoromethane plasma", *Journal of Applied Polymer Science*, 66 (8), 1591-1601

81. Šimor, M., Ráhel, J., Černák, M., Imahori, Y., Štefečka, M. and Kando, M. (2003) "Atmospheric-pressure plasma treatment of polyester nonwoven fabrics for electroless plating", *Surface and Coatings Technology*, 172, 1-6

82. Sinha, E. and Panigrahi, S. (2009) "Effect of Plasma Treatment on Structure, Wettability of Jute Fiber and Flexural Strength of its Composite", *Journal of Composite Materials*, 34, 1791-1802

83. Song, X.B. and Wang, C.X. (2006) "Effect of atmospheric pressure plasma jet on wettability of fibers and fabrics", *Wool Textile Journal*, 8, 22-26

84. Sung-Spitzl, H. (2003) "Plasma Pre-treatment of Textile for Improvement of Dyeing Processes", *International Dyer*, 188(5), 20-24

85. Szabová, R., Černáková, L., Wolfová, M. and Černák, M. (2009) "Coating of TiO_2 nanoparticles on the plasma activated polypropylene fibers", *Acta Chimica Slovaca*, 2(1), 70-76

86. Taguchi, G. (1986) *Introduction to Quality Engineering*, Asian Productivity Organization, Tokyo, Japan.

----

87. Taguchi, G (1995) "Quality engineering (Taguchi methods) for the development of electronic circuit technology". *IEEE Transactions on Reliability,* 44 (2), 225–229

88. Temmerman, E. and Leys, C. (2005) "Surface modification of cotton yarn with a DC glow discharge in ambient air", *Surface & Coatings Technology*, 200, 686– 689

89. Tendero, C., Tixier, C., Tristant, P., Desmaison, J. and Leprince, P. (2006) "Atmospheric pressure plasmas: A review", *Spectrochimica Acta Part B*, 61, 2-30

90. Tichý, M., Hubička, Z., Šícha, M., Čada, M., Olejníček, J., Churpita, O., Jastrabík, L., Virostko, P., Adámek, P., Kudrna, P., Leshkov, S., Chichina, M. and Kment, Š. (2009) "Langmuir probe diagnostics of a plasma jet system", *Plasma Sources Science and Technology*, 18, 014009 (11pp)

91. Tokino, S., Wakida, T., Uchiyama, H. and Lee, M. (1993) "Laundering shrinkage of wool fabric treated with low-temperature plasmas under atmospheric pressure", *Journal of Society of Dyers and Colourists*, 109(10), 334-335

92. Tsafack, M.J. and Levalois-Grützmacher, J. (2007) "Towards multifunctional surfaces using the plasma-induced graft-polymerization (PIGP) process: Flame and waterproof cotton textiles", *Surface and Coatings Technology*, 201, 5789-5795

93. Tsai, P.P., Roth, J.R. and Chen, W.W. (2005) "Strength, Surface Energy, and Ageing of Meltblown and Electrospun Nylon and Polyurethane (PU) Fabrics Treated by a One Atmosphere Uniform Glow Discharge Plasma (OAUGDP™)", *Textile Research Journal*, 75(12), 819-825

94. Tuteja, A., Choi, W., McKinley, G.H., Cohen, R.E. and Rubner, M.F. (2008) "Design Parameters for Superhydrophobicity and Superoleophobicity", *Materials Research Society Bulletin*, 33(8), 752-758

95. Tyner, D.W. (2007) "Evaluation of Repellent Finishes Applied by Atmospheric Plasma", MSc Thesis, North Carolina State University, Textile Engineering,

----

----

96. Vaideki, K., Jayakumar, S., Thilagavathi, G. and, Rajendran, R. (2007) "A study on the antimicrobial efficacy of RF oxygen plasma and neem extract treated cotton fabrics", *Applied Surface Science*, 253 7323–7329

97. Verschuren, J. and Kiekens, P. (2005) "Gas Flow Around and Through Textile Structures during Plasma Treatment", *AUTEX Research Journal*, 5 (3), 154-161

98. Vesel, A., Junkar, I., Cvelbar, U., Korac, J. and Mozetic, M. (2008) "Surface modification of polyester by oxygen and nitrogen-plasma treatment", *Surface and Interface Analysis*, 20, 1444-1453

99. Vince, J., Orel, B., Vilčnik, A., Fir, M., Vuk, A.Š., Jovanovski, V. and Simončič, B. (2006) "Structural and Water-Repellent Properties of a Urea/Poly(dimethylsiloxane) Sol-Gel Hybrid and Its Bonding to Cotton Fabric", *Langmuir*, 22(15), 6489-6497

100. Vinogradov, I.P., Dinkelmann, A. and Lunk, A. (2003) "Deposition of fluorocarbon polymer films in a dielectric barrier discharge (DBD)", *Surface and Coatings Technology*, 174-175, 509-514

101. Vinogradov, I.P., Dinkelmann, A. and Lunk, A. (2004) "Measurement of the absolute CF_2 concentration in a dielectric barrier discharge running in argon/fluorocarbon mixtures", *Journal of Physics D: Applied Physics*, 37, 3000-3008

102. Vinogradov, I.P. and Lunk, A. (2005) "Spectroscopic Diagnostics of DBD in Ar/Fluorocarbon Mixtures – Correlation between Plasma Parameters and Properties of Deposited Polymer Films", *Plasma Processes and Polymers*, 2, 201-208

103. Virk, R.K., Ramaswamy, G.N., Bourham, M. and Bures, B.L. (2004) "Plasma and Antimicrobial Treatment of Nonwoven Fabrics for Surgical Gowns", *Textile Research Journal*, 74(12), 1073-1079

104. Vohrer, U., Müller, M. and Oehr, C. (1998) "Glow-discharge treatment for the modification of textiles", *Surface and Coatings Technology*, 98(1-3), 1128-1131

----

105. Wardman, R.H. and Abdrabbo, A. (2010) "Effect of Plasma Treatment on the Spreading of Micro Drops Through Polylactic Acid (PLA) and Polyester (PET) Fabrics", *AUTEX Research Journal*, 10 (1), 1-7

106. Wang, C.X. and Qiu, Y.P.(2007a) "Effect of atmospheric pressure plasma jet treatment on wettability of two sides of wool fabric", *Wool Textile Journal*, 1, 23-27

107. Wang, C.X. and Qiu, Y.P. (2007b) "Two sided modification of wool fabrics by atmospheric pressure plasma jet: Influence of processing parameters on plasma penetration", *Surface and Coatings Technology*, 201, 6273-6277

108. Wang, C.X., Ren, Y. and Qiu, Y.P. (2007) "Penetration depth of atmospheric pressure plasma surface modification into multiple layers of polyester fabrics", *Surface and Coatings Technology*, 202, 77-83

109. Wang, C.X., Liu, Y., Xu, H.L., Ren, Y. and Qiu, Y.P. (2008a) "Influence of atmospheric pressure plasma treatment time on penetration depth of surface modification into fabric", *Applied Surface Science*, 254, 2499-2505

110. Wang, C.X., Xu, H.L., Liu, Y. and Qiu, Y.P. (2008b) "Influence of twist and filament location in a yarn on effectiveness of atmospheric pressure plasma jet treatment of filament yarns", *Surface and Coatings Technology*, 202, 2775-2782

111. Wang T., Wang C., and Qiu, Y., (2008) "Surface Modification of Ultra High Modulus Polyethylene Fibers by an Atmospheric Pressure Plasma Jet", *Journal of Applied Polymer Science* , 108, 25-33

112. Wardman, R.H. and Abdrabbo, A. (2010), Effect of Plasma Treatment on the Spreading of Micro Drops Through Polylactic Acid (PLA) and Polyester (PET) Fabrics, *AUTEX Research Journal*, 10 (1), 1-7

113. Wei, Q., Liu, Y., Hon, D. and Huang, F. (2007) "Dynamic wetting behavior of plasma treated PET fibers", *Journal of Materials Processing Technology*, 94, 89-92

114. Wertheimer, M.R., Martinu, L., Klemberg-Sapieha J.E. and Czeremuszkin, G. (1999) in: *Adhesion Promotion Techniques: Technological Applications*, K. L. Mittal and A. Pizzi (Eds.), Marcel Dekker, New York, 139–173.

115. Wildman, A.B. (1954) The Microscopy of Animal Textile Fibres, Wool Industries Research Association, Great Britain

116. Wong, W., Chan, K., Kwok, W.Y., Yu, M.T. and Lai, K.S. (2000) "Surface structuring of poly(ethylene terephthalate) fibres with a UV excimer laser and low temperature plasma", *Journal of Materials Processing Technology*, 103: 225-229

117. Wood, T.D. (2009) "How to Choose Wool Clothing", REI, http://www.rei.com/expertadvice/articles/wool+clothing.html (Retrieved November 23, 2010)

118. Worsham, B.J. (2010) "Cotton Technical Guide", Cotton Incorporated, http://www.cottoninc.com/Cotton-Nonwoven-Technical-Guide/#0 (Retrieved November 23, 2010)

119. Ye, H., Sun, C.Q. and Hing, P. (2000) "Control of grain size and size effect on the dielectric constant of diamond films", *Journal of Physics D: Applied Physics*, 33, L148-L152

120. Yin, G.Z. and Jillie, D.W. (1987) "Orthogonal Design for Process Optimization and its Application in Plasma Etching," *Solid State Technology*, 28, 127–132

121. Yip, J., Chan, K., Sin, K.M. and Lau, K.S. (2006) "Formation of periodic structures by surface treatments of polyamide fiber Part II. Low temperature plasma treatment", *Applied Surface Science*, 253, 2493-2497

122. Zhang, C. and Fang, K. (2009) "Surface modification of polyester fabrics for inkjet printing with atmospheric-pressure air/Ar plasma", *Surface and Coatings Technology*, 203, 2058–2063

123. Zhu, L., Wang, C.X. and Qiu, Y.P. (2007) "Influence of the amount of absorbed moisture in nylon fibers on atmospheric pressure plasma processing", *Surface and Coatings Technology*, 201, 7453-7461

124. Zhu, L., Teng, W.H., Xu, H.L., Liu, Y., Jiang, Q.R., Wang, C.X. and Qiu, Y.P. (2008) "Effect of absorbed moisture on the atmospheric plasma etching of polyamide fibers", *Surface and Coatings Technology*, 202, 1966-1974